

**Analysis of Carotenoids Using LC-MS-MS with
Ion Mobility Spectrometry and Photoionization**

BY

LINLIN DONG

B.S., Yunnan University, Kunming, China, 1996

DISSERTATION

Submitted as partial fulfillment of the requirements
for the degree of Doctor of Philosophy in Pharmacognosy
in the Graduate College of the
University of Illinois at Chicago, 2013

Chicago, Illinois

Defense Committee:

Richard B. van Breemen, Chair and Advisor
Steven M. Swanson
Jimmy Orjala
Peter H. Gann, Pathology
Maarten C. Bosland, Pathology

To my beloved wife Shunyan & our precious kids Joanna and Ethan
for their love and support

ACKNOWLEDGEMENTS

This dissertation would not be possible without contributions, assistances, and support from a number of people.

First and foremost, I am very grateful to my advisor Professor Richard van Breemen who has a passion for guiding young scientists. Just like myself, there are always new students being attracted to join the group each year. Professor van Breemen keeps providing us the tools, environment, and guidance that we need to succeed. During my thesis research with him, I was frequently astonished by his knowledge, foresight, and optimistic attitude which will remain to make positive impact on my future career. Besides required courses and research projects at school, Professor van Breemen encourages us to broaden our professional skills through off campus internship programs. I was fortunate to benefit from both my scientific education program and pharmaceutical industrial internship experience throughout my graduate study.

I would like to thank my preliminary exam and dissertation defense committee members -- Professors Steven M. Swanson, Jimmy Orjala, Peter H. Gann, and Maarten C. Bosland -- for their valuable comments and suggestions on this dissertation, as well as their time and patience. I never forget that Professors Swanson and Orjala, the former and current Director of Graduate Studies for the Pharmacognosy program, have given me tremendous help in many aspects. Professors Gann and Bosland from the Department of Pathology imparted me with the most recent cancer research and epidemiology basics. I truly appreciate and enjoy the knowledge I have gained in those courses.

ACKNOWLEDGEMENTS (continued)

I appreciate Dr. Dejan Nikolic for being my co-mentor and friend when I started my first project focused on isoflavone analysis for the Botanical Center. I enjoyed and benefited a lot from the LC-MS course he taught and the scientific discussions we had.

I want to recognize a few senior lab members who were particular helpful when I first started in the laboratory. They are Dr. Ang Liu, Dr. Dongting Liu, Dr. Long Yuan, Dr. Hongmei Cao, Dr. Jinghu Li, Dr. Christopher Pennington, and Dr. Jeffrey Dahl.

I want to thank everybody who contributed to our lycopene dietary intervention study: the principal investigator Professor van Breemen; the human subjects study coordinator Mr. Rich Morrissy; the fellow analytical chemists Dr. Ang Liu, Dr. Jeffrey Dahl, Dr. Yang Yuan, Dr. Long Yuan, and Dr. Kevin Krock; the dietician Ms. Amanda Guide; the statistician Dr. Marlos Viana; the study pharmacist Mr. Mike Pacini.

For the ion mobility spectrometry work, I am very thankful to Dr. Henry Shion at Waters for his guidance, help, and discussions. I also want to thank Mr. Roderick Davis for his excellent user training and assistance on Synapt HDMS, and Mr. Brent Terry-Penak for his contribution in the theoretical calculation of collision cross sections.

I would like to thank Dr. Yan Wang, Dr. Carrie Crot, Dr. Alexander Schilling, and Dr. Larry Helseth from the Mass spectrometry, Metabolomics & Proteomics Facility for providing great technical support and assistance over the years.

I appreciate fellow graduate students or postdocs, Dr. Yang Yuan, Dr. Chenqi Hu, Dr. Xi Qiu, Mr. Yongchao Li, Mr. Ke Huang, Mr. Zhiyuan Sun, Dr. Jerry White, Dr. Rui

ACKNOWLEDGEMENTS (continued)

Yu, Dr. Yang Song, Dr. Lian Chen, Ms. Guannan Li, Mr. Andrew Newsome, Mr. Brian Wright, Mr. Caleb Nienow, Ms. Elizabeth Martinez, Dr. Soyoun Ahn, and Dr. Yongsoo Choi, from the van Breemen laboratory for their help, support, and discussions. I also thank Dr. Yan Pang, Dr. Jian Guo, Dr. Yi Tao, Dr. Yan Luo from the van Breemen laboratory for their friendship.

Many colleagues outside the group extended their help during my graduate study and made it pleasant and memorable. My appreciation goes to Dr. Norman R. Farnsworth & Dr. Judy L. Bolton (former and current Department Head), Dr. Guido F. Pauli (former DGS for Pharmacognosy graduate program), Dr. John F. Fitzloff & Dr. Pavel A. Petukhov (former and current DGS for Medicinal Chemistry graduate program), Mr. Dan Lantvit (my rotation mentor), Dr. Zhican Wang, Dr. Yang Tian, Dr. Chuan Bai, Dr. George Chlipala, Dr. Aleksej Kronic, Dr. Shaonong Chen, Dr. Jialin Mao, Dr. Kuan-Wei Peng, Ms. Kimberly Bean, Dr. Changhwa Hwang, Dr. Xiao Zhang, Ms. Qi Shen, Ms. Ping Yao, Ms. Arletta Harris, Ms. Mei Zhang, Mr. Dan Lu, Ms. Colleen Piersen, and Ms. Kimberly Huang. I want to thank all the faculty members, staffs, graduate students, and friends in the Department of Medicinal Chemistry and Pharmacognosy who helped me over the years. Please forgive me if I missed any of your names by accident.

I also want to acknowledge my summer intern supervisors, Dr. Jun Zhang & Dr. Hai-Hua Gong at AbbVie and Dr. Natasha Penner at Biogen Idec for providing me the unique learning experience in their laboratories.

ACKNOWLEDGEMENTS (continued)

I thank the financial support for my research projects and graduate study through National Cancer Institute (grant number: 5R01CA101052) and the teaching and research assistantship from the Department of Medicinal Chemistry and Pharmacognosy.

Finally, I would like to express my heartfelt gratitude to my family, especially my wife Shunyan and our kids, my mother Jingchi, my parents-in-law Jianzhen and Xinghai, my uncle Jiazhen and aunt Di Shen, my brother Jieyong, and my brother-in-law Shunxiang. Thank you all for your love, encouragement, and patience!

LD

TABLE OF CONTENTS

<u>CHAPTER</u>		<u>PAGE</u>
1.	INTRODUCTION	1
1.1	Prostate cancer	1
1.1.1	Risk factors for prostate cancer.....	2
1.1.2	Chemoprevention of prostate cancer	2
1.1.3	Molecular mechanisms of lycopene.....	3
1.1.4	Clinical trials	4
1.1.5	PSA	7
1.2	Analysis of carotenoids	8
1.2.1	Carotenoids	8
1.2.2	Traditional methods for carotenoid analysis.....	9
1.2.3	Ion mobility mass spectrometry (IM-MS)	10
1.2.4	Traveling wave ion mobility spectrometry	11
1.2.5	APPI interface	14
2.	QUANTITATIVE ANALYSIS OF LYCOPENE IN HUMAN SERUM AND ITS EFFECTS	18
2.1	Introduction	18
2.2	Lycopene dietary intervention study.....	19
2.2.1	Study design.....	19
2.2.2	Clinical sample analysis.....	20
2.3	Materials and methods	21
2.3.1	Chemicals.....	21
2.3.2	Sample preparation	22
2.3.3	LC-MS-MS analysis of lycopene.....	23
2.3.4	PSA measurement.....	24
2.3.5	Food recall analysis.....	25
2.3.6	Statistical analysis	25
2.4	Results and discussion	25
2.4.1	Enrollment and characteristics of study subjects	25
2.4.2	Quantitative analysis of lycopene	28
2.4.3	Lycopene response.....	31
2.4.4	Antioxidant biomarkers	38
2.4.5	Total PSA and free PSA	43
2.5	Conclusions	47
3.	COLLISION CROSS-SECTION DETERMINATION AND TANDEM MASS SPECTROMETRIC ANALYSIS OF ISOMERIC CAROTENOIDS USING ELECTROSPRAY ION MOBILITY TIME-OF-FLIGHT MASS SPECTROMETRY	49
3.1	Introduction	49
3.2	Materials and methods	51

TABLE OF CONTENTS (continued)

<u>CHAPTER</u>	<u>PAGE</u>
3.2.1	Materials 51
3.2.2	Methods..... 52
3.2.2.1	Effect of electrospray on isomerization of lycopene and β-carotene 52
3.2.2.2	Effect of collision-induced dissociation on isomerization of lycopene and β-carotene 53
3.2.2.3	LC-MS-IM-CID-Time-of-Flight (TOF) MS of lycopene and β-carotene 54
3.2.2.4	Collision cross-section measurements of lycopene and β-carotene.....54
3.2.2.5	Effect of electrospray on isomerization of lutein and zeaxanthin55
3.2.2.6	Collision cross-section measurements of lutein and zeaxanthin 56
3.2.2.7	LC-MS-IM-CID-Time-of-Flight (TOF) MS of lutein and zeaxanthin..... 57
3.3	Results and Discussion 57
3.4	Conclusions..... 87
4.	DOPANT-ASSISTED APPI MASS SPECTROMETRY OF CAROTENOIDS 88
4.1	Introduction 88
4.1.1	Direct APPI..... 89
4.1.2	Dopant-assisted APPI 90
4.1.3	Thermospray 91
4.1.4	UV lamps and photoionization 92
4.2	Materials and methods 95
4.2.1	Materials 95
4.2.2	Methods..... 95
4.2.2.1	APPI MS and APPI MS-MS of carotenoids..... 95
4.2.2.2	LC-APPI-MS-MS analysis of carotenoids..... 97
4.2.3	Data processing..... 98
4.3	Results and discussion 98
4.3.1	Positive ion APPI MS 99
4.3.2	Negative ion APPI MS..... 108
4.3.3	Negative ion APPI MS-MS 117
4.3.3.1	Carotenes..... 118
4.3.3.2	Xanthophylls..... 120
4.3.4	LC-APPI-MS-MS analysis of carotenoids..... 120
4.4	Conclusions..... 124
5.	MAIN CONCLUSIONS AND FUTURE DIRECTIONS..... 127
	CITED LITERATURE 131

TABLE OF CONTENTS (continued)

<u>CHAPTER</u>	<u>PAGE</u>
VITA.....	146

LIST OF TABLES

<u>TABLE</u>	<u>PAGE</u>
I. DEMOGRAPHIC CHARACTERISTICS OF ALL STUDY SUBJECTS BY INTERVENTION GROUPS.....	28
II. CLINICAL OUTCOMES OF THE STUDY GROUPS: 21-D LYCOPENE SUPPLEMENTATION	37
III. SERUM LEVELS OF PSA AND FREE PSA MEASURED BY ELISA KITS USING SINGLE-STEP PROTOCOLS	45
IV. COLLISION CROSS-SECTION VALUES OF GEOMETIC ISOMERS OF LYCOPENE AND β -CAROTENE.....	65
V. COLLISION CROSS-SECTION (CCS) VALUES OF GEOMETIC ISOMERS OF LUTEIN AND ZEAXANTHIN.....	79
VI. IONIZATION ENERGIES (IE) AND PROTON AFFINITIES (PA) OF SELECTED CAROTENIODS.....	93
VII. GAS PHASE ION THERMOCHEMICAL DATA OF SOME COMMON SOLVENTS, APPI DOPANTS AND ATMOSPHERIC GASES.....	94
VIII. MAJOR IONS OBSERVED IN THE POSITIVE APPI MASS SPECTRA OF INVESTIGATED CAROTENOIDS UNDER DIFFERENT DOPANT CONDITIONS.....	102
IX. MAJOR IONS OBSERVED IN THE NEGATIVE APPI MASS SPECTRA OF INVESTIGATED CAROTENOIDS UNDER DIFFERENT DOPANT CONDITIONS.....	111
X. COMPARISON OF THE SIGNAL TO NOISE RATIO OF CAROTENOID PEAKS BETWEEN POSITIVE AND NEGATIVE ION APPI.....	117

LIST OF FIGURES

<u>FIGURE</u>	<u>PAGE</u>
1. Chemical structures of selected carotenes and xanthophylls	9
2. Schematic of conventional ion mobility separation	11
3. A schematic diagram of the Synapt ion mobility ToF mass spectrometer system used during this investigation	13
4. Schematic of the Syage APPI source used on an Agilent triple quadrupole mass spectrometer during this investigation	16
5. A Bruins-type APPI source used by Applied Biosystems/MDS SCIEX	17
6. Study design of the phase II clinical intervention of lycopene in healthy men.	20
7. Flowchart of subject recruitment for high-dose lycopene study in healthy men	27
8. Negative ion APCI product ion tandem mass spectra of all- <i>trans</i> -lycopene and [¹³ C ₁₀]-all- <i>trans</i> -lycopene.	30
9. Negative ion APCI LC-MS-MS SRM chromatograms for the quantitative analysis of lycopene in a serum sample from the clinical study	31
10. Serum levels of lycopene of individual subjects at day 0 (baseline), day 21(intervention), and day 42 (wash out).	32
11. Mean differences of serum lycopene concentrations between day 0 (baseline) and day 21 (intervention) in the placebo arm and lycopene intervention arm	33
12. Urinary levels of 8-oxo-dG (normalized to creatinine) of individual subjects in the placebo group and in the lycopene (60 mg/d) supplementation group at day 0 (baseline), day 21(intervention), and day 42 (wash out).....	39
13. 8-iso-PGF _{2α} (normalized to creatinine) in urine from subjects receiving placebo or lycopene (60 mg/d) at day 0 (baseline), day 21(intervention), and day 42 (wash out)	40
14. Mean differences of urinary 8-oxo-dG concentrations between day 0 (baseline) and day 21 (intervention) in the placebo group and the lycopene (60 mg/d) intervention group.	41

LIST OF FIGURES (continued)

<u>FIGURE</u>	<u>PAGE</u>
15. Mean differences of urinary 8-isoprostaglandin-F _{2α} concentrations between day 0 (baseline) and day 21 (intervention) in the placebo arm and lycopene intervention arm (60 mg/d).....	43
16. Chemical structures of all- <i>trans</i> -lycopene, β-carotene, lutein, zeaxanthin, and their thermodynamically favored <i>cis</i> isomers.	50
17. Positive ion electrospray IM-MS drift time distributions of the M ⁺ ions of <i>m/z</i> 536.4 corresponding to <i>cis</i> (peak 1) and all- <i>trans</i> (peak 2) isomers of lycopene after infusion of (A) <i>cis/trans</i> -lycopene mixture (38/62); and (B) all- <i>trans</i> -lycopene. ...	59
18. LC-IM-MS analysis of a mixture of β-carotene isomers using a C ₃₀ carotenoid HPLC column, positive ion electrospray and ion mobility separation prior to mass spectrometric detection	60
19. C ₃₀ carotenoid column HPLC separation of lycopene geometrical isomers with on-line positive ion electrospray IM-MS analysis	61
20. Effect of electrospray desolvation gas temperature on the abundances of <i>cis</i> (peak 1) and all- <i>trans</i> isomers (peak 2) of (A) lycopene; and (B) β-carotene following infusion of the all- <i>trans</i> isomer	63
21. Relative abundances of <i>cis</i> isomers (peak 1 in Figure 20) and total (<i>cis</i> plus all- <i>trans</i>) isomers as a function of desolvation gas temperature for (A) lycopene; and (B) β-carotene.....	64
22. Ion mobility separations of poly-DL-alanine, lycopene and β-carotene under identical TWIMS conditions.....	66
23. Positive ion electrospray IM-MS-MS CID spectra of the M ⁺ ions of <i>m/z</i> 536 corresponding to (A) <i>cis</i> -lycopenes (ion mobility peak 1); and (B) all- <i>trans</i> -lycopene (ion mobility peak 2)	70
24. Positive ion electrospray IM-MS-MS with CID of (A) <i>cis</i> -β-carotenes; and (B) all- <i>trans</i> -β-carotene.	72
25. C ₃₀ reversed-phase HPLC-UV analysis of the 13- <i>cis</i> lutein levels in a lutein standard solution before and after the heated-induced isomerization process using USP Normalization Procedure for chromatography.	73

LIST OF FIGURES (continued)

<u>FIGURE</u>	<u>PAGE</u>
26. C ₃₀ reversed-phase HPLC-UV analysis of the 13- <i>cis</i> zeaxanthin levels in a zeaxanthin standard solution before and after the heated-induced isomerization process using USP Normalization Procedure for chromatography.	74
27. LC-IM-MS analysis of a mixture of lutein cis/trans isomers. (A) LC-MS chromatogram of lutein isomers; (B) 2D map showing ion mobility and LC-MS separation of lutein isomers.	76
28. LC-IM-MS analysis of a mixture of zeaxanthin isomers. (A) LC-MS chromatogram of zeaxanthin isomers; (B) 2D map showing ion mobility and LC-MS separation of zeaxanthin isomers.	76
29. Effect of electrospray desolvation gas temperature on the abundances of cis (peak 1) and all-trans isomers (peak 2) of (A) lutein; and (B) zeaxanthin following infusion of the all-trans isomer	78
30. Relative abundances of cis isomers (peak 1 in Figure 29) and total (cis plus all-trans) isomers as a function of desolvation gas temperature for (A) lutein; and (B) zeaxanthin.....	78
31. Positive ion electrospray IM-MS-MS with CID of (A) cis-luteins; and (B) all-trans-lutein	82
32. Positive ion electrospray IM-MS-MS with CID of (A) cis-zeaxanthins; and (B) all-trans-zeaxanthin.....	83
33. Positive ion APPI mass spectra of carotenoids (no dopant).....	100
34. Positive ion APPI mass spectra of xanthophylls (no dopant)	101
35. Dopant effects on α -carotene ionization during positive ion APPI mass spectrometry.....	105
36. Dopant effects on β -carotene ionization during positive ion APPI mass spectrometry.....	105
37. Dopant effects on lycopene ionization during positive ion APPI mass spectrometry.....	106
38. Dopant effects on lutein ionization during positive ion APPI mass spectrometry	106

LIST OF FIGURES (continued)

<u>FIGURE</u>	<u>PAGE</u>
39. Dopant effects on zeaxanthin ionization during positive ion APPI mass spectrometry.....	107
40. Negative ion APPI mass spectra of xanthophylls (no dopant).....	109
41. Negative ion APPI mass spectra of carotenes.....	110
42. Dopant effects on α -carotene ionization during negative ion APPI mass spectrometry.....	113
43. Dopant effects on β -carotene ionization during negative ion APPI mass spectrometry.....	113
44. Dopant effects on lycopene ionization during negative ion APPI mass spectrometry.....	114
45. Dopant effects on lutein ionization during negative ion APPI mass spectrometry.	114
46. Dopant effects on zeaxanthin ionization during negative ion APPI mass spectrometry.....	115
47. Negative ion APPI tandem mass spectra with CID of the deprotonated molecules of α -carotene (A), β -carotene (B), lycopene (C), lutein (D), and zeaxanthin (E).....	119
48. Positive ion APPI and APCI SRM chromatograms showing the detection of zeaxanthin, lycopene and β -carotene in a standard mixture at 3 μ g/mL.....	122
49. Positive ion APPI SRM chromatograms showing the detection of zeaxanthin, lycopene and β -carotene in a human serum sample.....	123
50. Negative ion APPI and APCI SRM chromatograms showing the detection of zeaxanthin, lycopene and β -carotene in a standard mixture at 3 μ g/mL.....	124

LIST OF ABBREVIATIONS

8-iso-PGF _{2α}	8-iso-prostaglandin F _{2α}
8-oxo-dG	7,8-Dihydro-8-oxo-2'-deoxyguanosine
ADT	Androgen deprivation therapy
APCI	Atmospheric pressure chemical ionization
APPI	Atmospheric pressure photoionization
BHT	Butylated hydroxytoluene
BPH	Benign prostatic hyperplasia
CB	Chlorobenzene
CCS	Collision cross section
CID	Collision-induced dissociation
CRPC	Castration-resistant prostate cancer
DMA	Differential mobility analyzer
DNA	Deoxyribonucleic acid
ECD	Electrochemical detection
EGCG	Epigallocatechin-3-gallate
ELISA	Enzyme-linked immunosorbent assay
FAB	Fast atom bombardment
FAIMS	Field asymmetric ion mobility spectrometry
FDA	US Food and Drug Administration
FIA	Flow injection analysis
GC-MS	Gas chromatography-mass spectrometry
GCRC	General Clinical Research Center

LIST OF ABBREVIATIONS (continued)

HPLC	High performance liquid chromatography
IE	Ionization energy
IMS	Ion mobility spectrometry
IM-MS	Ion mobility-mass spectrometry
IM-MS-MS	Ion mobility tandem mass spectrometry
LC-MS	Liquid chromatography-mass spectrometry
LC-MS-MS	Liquid chromatography-tandem mass spectrometry
LLOQ	Lower limit of quantification
LOD	Limit of detection
mg/d	Milligram per day
MS	Mass spectrometry
MS-MS	Tandem mass spectrometry
MTBE	Methyl- <i>tert</i> -butyl ether
m/z	Mass-to-charge ratio
NCI	National Cancer Institute
PA	Proton affinity
PCPT	Prostate Cancer Prevention Trial
PSA	Prostate specific antigen
QC	Quality control
Q-ToF	Quadrupole time-of-flight MS
ROS	Reactive oxygen species

LIST OF ABBREVIATIONS (continued)

SD	Standard deviation
SRM	Selected reaction monitoring

SUMMARY

Carotenoids are naturally occurring fat-soluble pigments found principally in bacteria and plants including edible plants. Because of their extensively conjugated carbon-carbon double bond system, carotenoids are potent antioxidants. The most abundant carotenoid and best singlet oxygen quencher found in red tomatoes is lycopene. Many studies have found that consumption of tomatoes or tomato products is associated with reduced risk of prostate cancer. However, it is inconclusive whether the protection effects are through lowering oxidative stress and reducing DNA damage in men or due to other mechanisms. Additional randomized controlled clinical trials may help address this issue.

Using lycopene as a potential dietary chemopreventive agent, a four-arm randomized, placebo-controlled, and double-blind phase II clinical intervention trial was carried out at the University of Illinois at Chicago. Unlike previous studies by our group, healthy men were recruited. A validated LC-MS-MS assay was used to analyze serum levels of lycopene for each subject. An intermediate endpoint biomarker for DNA oxidation (urinary 8-oxo-deoxyguanosine; 8-oxo-dG) and one for lipid peroxidation (urinary 8-iso-prostaglandin- $F_{2\alpha}$; 8-iso-PGF $_{2\alpha}$) were measured in the study to evaluate the change of oxidative stress in men after lycopene intervention. The prostate cancer biomarkers total prostate specific antigen (PSA) and percent-free PSA were measured in the study as indicators for prostate cancer risk.

SUMMARY (continued)

In the investigation, it was found that lycopene supplements at either 30 mg/d or 60 mg/d lycopene for 21 d were well tolerated by healthy men enrolled to the two lycopene intervention arms. Similar increases in serum levels of lycopene were observed in both treatment groups during this randomized, placebo controlled intervention study (1.63-fold vs 1.52-fold for 30 mg/d vs 60 mg/d, respectively). These results suggest that serum lycopene concentrations may have reached a plateau.

Stronger effects were observed for these two antioxidant biomarkers with the high dose intervention arm compared with its placebo control. For example, the mean of urinary 8-oxo-dG concentrations decreased from 2.486 to 2.358 ng/mg creatinine in the lycopene supplementation group (60 mg/d) with a *P* value of 0.16 compared with the placebo control. During this same period, 8-iso-PGF_{2α} concentrations dropped from 152.7 to 148.8 pg/mg creatinine in subjects receiving 60 mg/d lycopene with a *P* value of 0.07 compared with the placebo control. Although these changes remained statistically insignificant, the subtle differences may become more discernable with longer intervention or in trials with a larger sample size. Nevertheless, these results confirmed that lycopene supplementation did not show pro-oxidant effects. Previously, a significant decrease in total PSA and no change in percent free PSA were observed in serum of men on the 30 mg/d lycopene intervention arm. However, the same ELISA kits used are no longer available. Therefore, serum levels of total PSA and free PSA for the high dose arms are to be determined as corresponding assays become available.

SUMMARY (continued)

For several decades, extensive efforts have been devoted to the analysis of carotenoids using a variety of techniques including high performance liquid chromatography with UV/vis absorbance or mass spectrometric detection because of their biological significance in living organisms. Even though significant progress has been made in analyzing these isoprenoid pigments, there is a continuing demand for more efficient and more sensitive analytical methods. Technologies that have seldom been applied to carotenoid analysis including ion mobility spectrometry and photoionization mass spectrometry were explored for their potential utility in this area.

As the separation of cis and all-trans isomers of carotenoids using HPLC can be quite time-consuming (up to 90 min), a rapid gas-phase separation (msec) may be achievable using ion mobility (IM) spectrometry. In this project, the separation of cis and all-trans isomers of carotenoids, including lycopene, β -carotene, lutein, and zeaxanthin, was demonstrated using traveling wave ion mobility spectrometry with drift time separations of 1-4 ms. Because the cis isomers had collision cross-sections that were smaller than those of the corresponding all-trans isomers, they were detected first followed at a later drift time by the all-trans isomer. However, the various cis isomers were not resolved.

The use of LC-IM-tandem mass spectrometry (LC-IM-MS-MS) helped confirm that in-source isomerization of lycopene, β -carotene, lutein, and zeaxanthin occurred during positive ion electrospray. This in-source isomerization was found to be temperature dependent. Although cis/trans isomerization could not be eliminated during

SUMMARY (continued)

electrospray, this temperature dependence suggests that softer ionization conditions might minimize cis/trans isomerization in the ion source. After separation using IM, the cis and all-trans isomers of lycopene, β -carotene, lutein, and zeaxanthin were shown by MS-MS with CID to produce unique fragmentation patterns that could be used to distinguish them.

Atmospheric pressure photoionization (APPI) is a mass spectrometric ionization technique that is new in carotenoid analysis. Unlike electrospray and atmospheric pressure chemical ionization (APCI), APPI often depends on dopants to achieve good sensitivity. Since APPI can produce unique ion species, which may be used for compound characterization, the potential of APPI was explored as a complementary ionization technique to previously used techniques such as electronic impact, APCI and electrospray.

In the study, we first reported that carotenoids can be ionized during negative ion APPI, and this study was the first to report the formation of negative ions of carotenes using APPI. Dopants were essential for the formation of positive carotenoid ions as well as negative ions during APPI. Positive ion APPI produced more unique fragment ions than did negative ion mode, which can be used to distinguish carotenoid structural isomers.

Methyl-*tert*-butyl ether (MTBE) was found to be particularly effective as a dopant evaluated towards the photoionization of carotenoids during negative ion APPI. As for positive ion APPI, the dopants anisole and chlorobenzene were the most effective.

SUMMARY (continued)

Overall, the compositions of mobile phases, dopants, diluents, and their flow rates were found to have a critical impact on the overall ionization efficiency of APPI.

1. INTRODUCTION

1.1 Prostate cancer

Prostate cancer is the second leading cause of cancer death among males in the United States and is second only to skin cancer as the most common type of cancer diagnosed in men in developed countries.^[1, 2] The American Cancer Society estimates that approximately 238,590 new prostate cancer cases will be diagnosed among the United States population during 2013, while ~29,720 men will die due to this disease.^[2] Many prostate cancer patients actually die from other causes, since the progression of this disease is relatively slow. However, a decrease in the quality of life is common among prostate cancer patients due to symptoms like urinary retention and sexual dysfunction.^[3]

Treatment recommendations for prostate cancer differ by life expectancy of patients and the severity of their diseases. Active surveillance, radical prostatectomy and radiation therapy (external beam or brachytherapy) are major options for localized prostate cancer patients. In the case of metastatic or locally advanced prostate cancer, androgen deprivation therapy (ADT)^[4] such as surgical or chemical castration may also be recommended.^[5] However, prostate cancer cells can eventually become resistant to ADT and progress to a state known as castration-resistant prostate cancer (CRPC).^[6, 7] Furthermore, ADT can potentially lead to higher cardiovascular morbidity and mortality.^[5, 8]

1.1.1 Risk factors for prostate cancer

The established risk factors for prostate cancer are older age, race and family history.^[1, 9] Among these, age is the most important risk factor in prostate cancer.^[10] According to epidemiology data during 2002-2006, half of men diagnosed with prostate cancer were over 68 years of age, and men aged from 70 to 74 had the highest incidence.^[5]

Other than age, genetic factors play a role in prostate cancer. For instance, men with BRCA-2 mutations have up to 20 times greater risk for the disease compared with the general population.^[11-13] Furthermore, African American men have the highest incidence of prostate cancer, followed by white men and other racial and ethnic groups.^[5] Recent genome-wide association studies have identified multiple novel loci which account for the increased risk in prostate cancer, such as loci at chromosomal locations 8q24 and 17q21.^[14-17] Elevated risk of clinical prostate cancer in men with affected relatives was observed as early as 1956.^[18-20] It is believed that genetic factors may account for up to 10% of all prostate cancer cases with significantly more in younger men (age <55).^[21, 22] Although no preventable risk factors for prostate cancer have yet been established,^[1] epidemiologic studies suggest that the development of prostate cancer can be affected by environmental factors like diet and lifestyle.^[10]

1.1.2 Chemoprevention of prostate cancer

The term “chemoprevention” was coined by Sporn *et al.* ^[23] in 1976 and then widely adopted when referring to the use of dietary or pharmaceutical agents to prevent cancer. Since then, numerous studies have been carried out in this active area. As prostate cancer generally progresses slowly, it might be a good target for intervention and

chemoprevention.^[24] Given current unsatisfactory treatment options for prostate cancer and its non-modifiable major risk factors (age, race, family history), prevention appears to be a promising option for the majority of men.^[25, 26]

Diets containing tomatoes, green tea, cruciferous vegetables, soy, and/or red wine, might reduce prostate cancer risk, while consumption of meat, fat and dairy products might increase susceptibility.^[9, 10, 27-29] In addition, dietary chemoprevention is an attractive approach because dietary supplements can be taken orally with good compliance. Many epidemiological studies have supported the hypothesis that dietary antioxidants might be used as a relatively inexpensive means of chemoprevention of cancer.^[30, 31] In this dissertation, chemoprevention by the most abundant carotenoid found in tomatoes, lycopene, will be explored for its potential effects on prostate cancer.

1.1.3 Molecular mechanisms of lycopene

One well known mechanism of cancer initiation involves mutations and alterations of nucleic acids caused by free radical or singlet oxygen attack.^[32] Besides DNA, lipids and proteins can also be damaged by reactive oxygen species (ROS) through uncontrolled oxidation.^[33] Reducing exposure to ROS generating systems and environmental carcinogens reduces the risk of oxidative stress related carcinogenesis. Such protection might be achieved through the action of antioxidants in the diet.^[32]

Lycopene (Ψ, Ψ -carotene) is a lipophilic red pigment mainly found in plant fruits, such as tomatoes (*Lycopersicon esculentum*), watermelon, pink grapefruit, papaya, and guava.^[33-35] Lycopene has no pro-vitamin A activity due to lacking of β -ionone ring in its chemical structure (Figure 1). However, with 11 conjugated C=C and two

non-conjugated C=C in the system, lycopene is an excellent antioxidant and has been reported to be the most effective singlet oxygen quencher among carotenoids.^[36, 37]

Although the role of ROS in prostate carcinogenesis is not fully understood, Muzandu *et al.*^[38, 39] and Park and co-workers^[40] reported that lycopene could reduce DNA damage in vitro. In a different study, Liu^[41] in our laboratory found that the nuclei of the prostate cancer cells LNCaP contained approximately 81% of cellular lycopene after being treated with lycopene beadlets containing 10% lycopene in vitro. Consequently, a significant decrease in DNA oxidation product (8-oxo-dG) levels ($P < 0.001$) was observed in lycopene-treated LNCaP cells (at concentrations of $\geq 0.58 \mu\text{M}$).^[42] All these findings suggest that lycopene, as an antioxidant, can reduce oxidative stress and protect DNA.

Besides reducing oxidative stress as a ROS scavenger, a number of other molecular mechanisms have been suggested for lycopene in prostate cancer chemoprevention. These mechanisms include up-regulation of the antioxidant response element,^[24, 43] induction of cancer cell apoptosis and cell cycle arrest, inhibition of signaling pathways of growth factors as well as the metastasis of cancer cells.^[33]

1.1.4 Clinical trials

In a review by Giovannucci,^[44] 57 of 72 epidemiological studies showed that tomato-based foods and lycopene intake could reduce the risk of multiple types of cancer, including prostate cancer, breast cancer, lung cancer, stomach cancer, colorectal cancer, and so on. Tomato-rich diets and higher blood lycopene levels have been inversely related to prostate cancer risk. For example, a cohort study of 14,000 Seventh Day Adventist men found that the consumption of tomato products was significantly related to

lower prostate cancer risk, while the consumption of β -carotene rich foods was not.^[45] In a larger prospective cohort study conducted among 47,894 male health professionals including dentists, optometrists, osteopaths, podiatrists, pharmacists, and veterinarians, a relative risk in prostate cancer of 0.79 (95% confidence interval) between the high and low quintiles of lycopene intake was achieved. However, no such association was observed for intakes of other carotenoids such as β -carotene, α -carotene, lutein, and β -cryptoxanthin for the study population.^[46]

In 1999, Gann and colleagues^[47] published a nested case-control study of 578 prostate cancer patients and 1,294 matched controls using plasma samples from the Physicians' Health Study. They demonstrated an inverse association between plasma lycopene levels and prostate cancer risk, particularly in the most aggressive cancer cases. HPLC analysis was used to measure serum lycopene levels in two other case control studies, however, no significant correlation between lycopene levels and prostate cancer risk was observed.^[48, 49]

Because of some common limitations of epidemiological studies and inconsistent results in the literature, well-designed clinical intervention trials are needed to better understand the prevention of this disease. In 2001, Chen *et al.*^[50] reported a preliminary 21-day whole-foods intervention of 32 prostate cancer patients using tomato sauce at a dose equivalent to 30 mg lycopene per day. As the serum lycopene levels and prostate lycopene levels increased by 1.97-fold and 2.92-fold respectively, total serum prostate specific antigen levels^[51] and 8-oxo-dG levels in leukocytes of these men both decreased compared with their baseline concentrations. These results indicated a potential benefit of consuming tomato sauce for prostate cancer patients. Since this was a whole-foods based

study, no blinding or placebo control group was used. In a recent randomized, placebo controlled, double blind phase II clinical trial published by van Breemen *et al.*^[52], a 1.93-fold increase of plasma lycopene levels was observed for 54 BPH and prostate cancer patients randomized for 21-day 30 mg/d lycopene supplementation. Although no significant changes in 8-oxo-dG or malondialdehyde were found in prostate tissue and plasma of those patients, a declining trend for both oxidation biomarkers following lycopene intervention suggests that lycopene did not function as a pro-oxidant. In 2011, Kristal *et al.* reported a nested case-control study, which was a follow-up investigation of the Prostate Cancer Prevention Trial (PCPT). Originally, PCPT was a National Cancer Institute (NCI) funded placebo-controlled trial of finasteride for prostate cancer prevention, which began in 1993 and ended in 2003. Later, a large cohort (n=1,809) was selected among the PCPT participants to examine the associations of serum lycopene with prostate cancer risk. Although the outcomes do not support a role for lycopene in prostate cancer prevention,^[53] a fairly plausible argument made by Giovannucci^[54] suggests that the results suffered from selection bias in the study design.

In summary, due to the complexity of prostate cancer and variations in study designs, mixed results have been obtained regarding lycopene and prostate cancer risk. Although many risk factors were controlled in at least some of the clinical intervention trials, few of them involved healthy men who would benefit the most by lycopene chemoprevention. Therefore, there might be some difficulties in generalizing these findings to the general population. To address this issue, a new randomized, placebo controlled, double blind phase II clinical trial of lycopene was carried out in healthy men as a part of this dissertation. Details of this study are described in Chapter 2.

1.1.5 PSA

Prostate specific antigen (PSA) is a 33 kDa single chain glycoprotein produced by the epithelial cells of prostate. Since its discovery in the 1970s, PSA has been one of the most widely used early detection biomarkers for prostate cancer.^[55-58] The only known physiological function of PSA is to liquefy the seminal fluid. Since only low levels of PSA can be found in the blood of healthy men, elevated blood levels of PSA is often an indication of abnormalities in the prostate due to trauma or disease.^[59]

Serum PSA circulates in both noncomplexed (free PSA) and complexed forms. PSA forms complexes predominantly with α_1 -antichymotrypsin, α_1 -protease inhibitor, and α_2 -macroglobulin in serum.^[60] Generally, serum levels of total PSA (both forms) greater than 10 ng/mL or percent free PSA less than 10% indicates an increased risk of prostate cancer.^[58, 61, 62] Although men with serum total PSA levels greater than 4 ng/mL and other risk factors such as family history and enlarged prostate are often recommended by clinicians for prostate biopsy and pathological examination for possible diagnosis of prostate cancer, false positive analyses are very common. Along with serum total PSA, percent free PSA has also been widely used for prostate cancer screening or active surveillance because of its improved specificity in men with total serum PSA levels between 4 and 10 ng/mL.^[63, 64] Since it is not practical or cost-effective to use true clinical endpoints in most clinical prevention trials,^[65, 66] total PSA and percent free PSA in serum were used as the intermediate endpoint biomarkers for the lycopene intervention study described in this dissertation.

1.2 Analysis of carotenoids

1.2.1 Carotenoids

Carotenoids provide important physiological functions such as protecting plants from photodamage and providing precursors for vitamin A biosynthesis in humans.^[67] There are over 600 known carotenoids in nature,^[68] and carotenes comprise which represent the unsaturated hydrocarbon subclass. The other major subclass is the xanthophylls which are oxygenated carotenoids. The three most abundant dietary carotenes are α -carotene, β -carotene and lycopene. β -Carotene and α -carotene can be converted to retinol (vitamin A) during intestinal absorption. Although not a provitamin A carotenoid, lycopene is the most potent antioxidant among the carotenes.^[33] Lutein and zeaxanthin are major dietary xanthophylls occurring in plants and micro-organisms. Dietary intake of lutein and zeaxanthin helps prevent age-related macular degeneration.^[69]

Biosynthesized in plants as the all-trans isomers, dietary carotenoids can form multiple cis isomers when exposed to heat or light, and these cis isomers have been reported to have different bioavailabilities.^[70-73] The planar chemical structures of all-trans-lycopene, all-trans- α -carotene, all-trans- β -carotene, all-trans-lutein, and all-trans-zeaxanthin are shown in Figure 1.

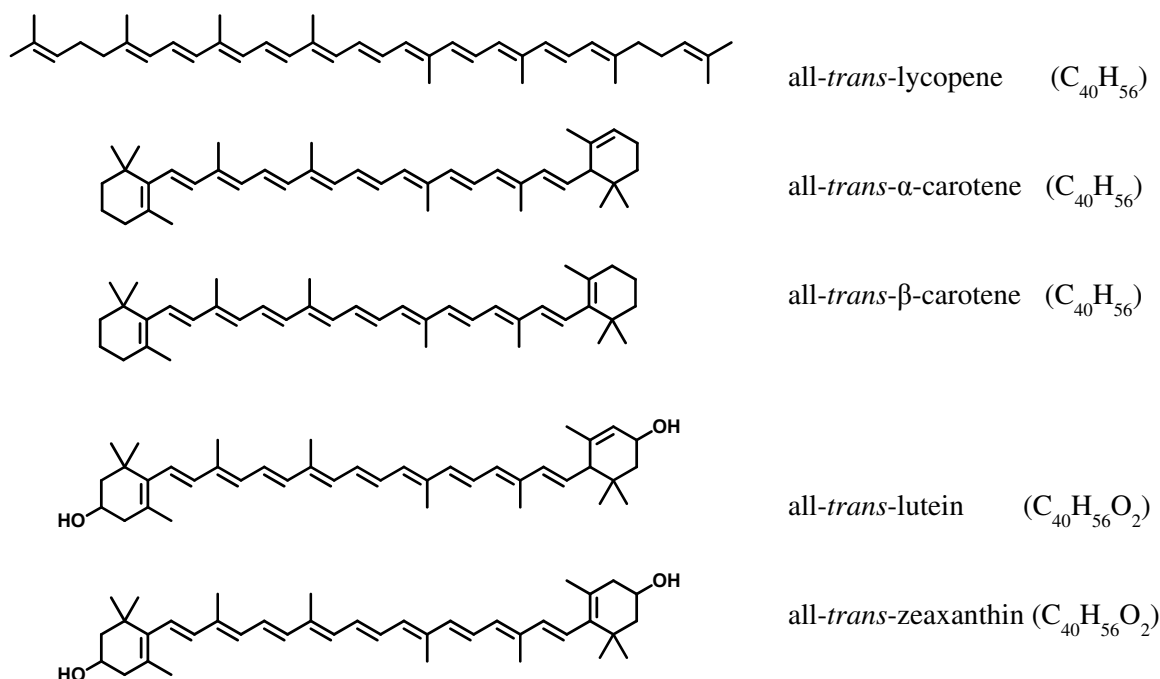


Figure 1. Chemical structures of selected carotenes and xanthophylls

1.2.2 Traditional methods for carotenoid analysis

The open-column chromatography used during the early years of carotenoid analysis have been replaced by more efficient HPLC techniques, and reversed-phase HPLC has become the most often used type of chromatography for the separation of carotenoids extracted from biological samples.^[74] The detection and quantitation of carotenoids during HPLC is usually based on their UV/vis spectral properties^[75] or their masses during LC-MS.^[76] Electrochemical detection (ECD) is another type of detection method available for HPLC analysis of carotenoids.^[77-79] Even though it is more sensitive than most common absorption spectrophotometric techniques, HPLC-ECD is less

commonly used due to very limited structure information provided and relatively narrow application range.^[80]

Although LC-MS provides good liquid based separation, sensitive detection as well as elemental composition information of carotenoids, mass spectrometry has not been able to distinguish cis/trans isomers of carotenoids. Furthermore, the time required for fully optimized reversed-phase HPLC separations of carotenoid isomers can be up to 90 min in the case of lycopene.^[81] Undoubtedly, rapidly resolving and quantifying carotenoid geometrical isomers in biological specimens with good sensitivity would facilitate research efforts directed toward the understanding of their physiological functions. Toward this goal, we hypothesized that ion mobility mass spectrometry (IM-MS) and ion mobility tandem mass spectrometry (IM-MS-MS) due to its non-chromatographic separation could overcome the issue of speed and the simultaneous application of tandem mass spectrometry could be used to distinguish geometric carotenoid isomers for the first time. Separately, we investigated the utility of atmospheric pressure photoionization (APPI) as an alternative to other atmospheric pressure ionization techniques such as electrospray and atmospheric pressure chemical ionization (APCI) for carotenoid analysis using mass spectrometry.

1.2.3 Ion mobility mass spectrometry (IM-MS)

Ion mobility spectrometry (IMS)^[82] is the gas-phase separation of ions on the basis of size and shape in an electric field. When coupled with mass spectrometry, a dimension of high speed separation can be added to mass spectrometric analysis.^[83-86] To be concise, the hyphenation of IMS and MS can be abbreviated as IM-MS.^[87] Figure 2

shows a schematic diagram of a conventional IMS drift cell. Ions of different sizes (based on mass and shape) are separated in the drift cell as smaller ones travel faster through the drift gas due to their smaller collision cross section (CCS). Since a weak and uniform static electric field is used as the driving force in during conventional IMS, the mobility or CCS of an ion can be calculated directly without further calibration. Although excellent resolution has been achieved with conventional IMS, it suffers for low sensitivity due to severe ion loss.^[88]

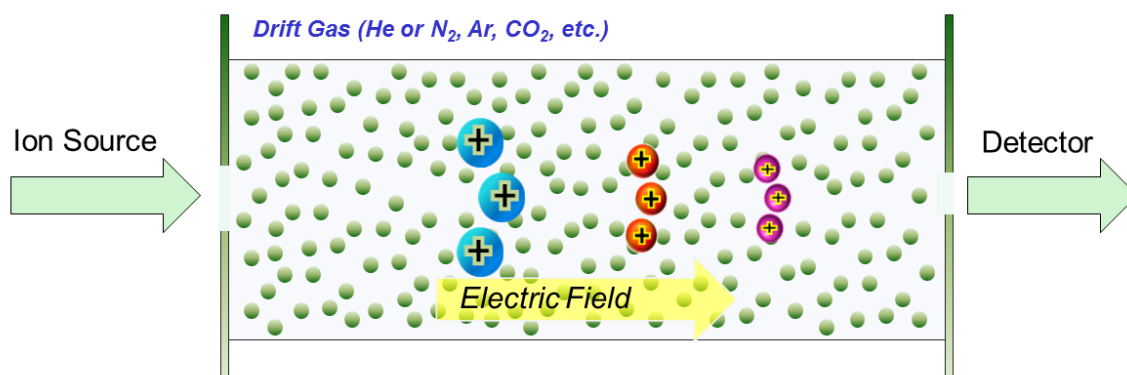


Figure 2. Schematic of conventional ion mobility separation. Larger ions are delayed due to their more extensive interaction with the drift gas compared with ions of smaller collision cross sections.

1.2.4 Traveling wave ion mobility spectrometry

In addition to conventional IMS, three other major IMS techniques have been developed including differential mobility IMS or field asymmetric IMS, traveling wave ion mobility spectrometry (TWIMS), and differential mobility analyzer. Compared with

conventional IMS (also known as drift time IMS), these alternative techniques normally have better sensitivity but lower resolution.^[88] Although all four IMS techniques are commercially available, TWIMS was selected for investigation in this dissertation as the only type of ion mobility instrument available in our laboratory, on campus or in Chicago.

The ion trajectory in a TWIMS drift cell is different from its path in a conventional IMS drift cell because a non-uniform electric field is used to drive ions through. In addition, a calibration is also required to obtain the CCS values of separated ions. A schematic diagram for the first generation of a TWIMS based hybrid Q-ToF mass spectrometer, the Synapt system made by Waters Corp., is shown in Figure 3.

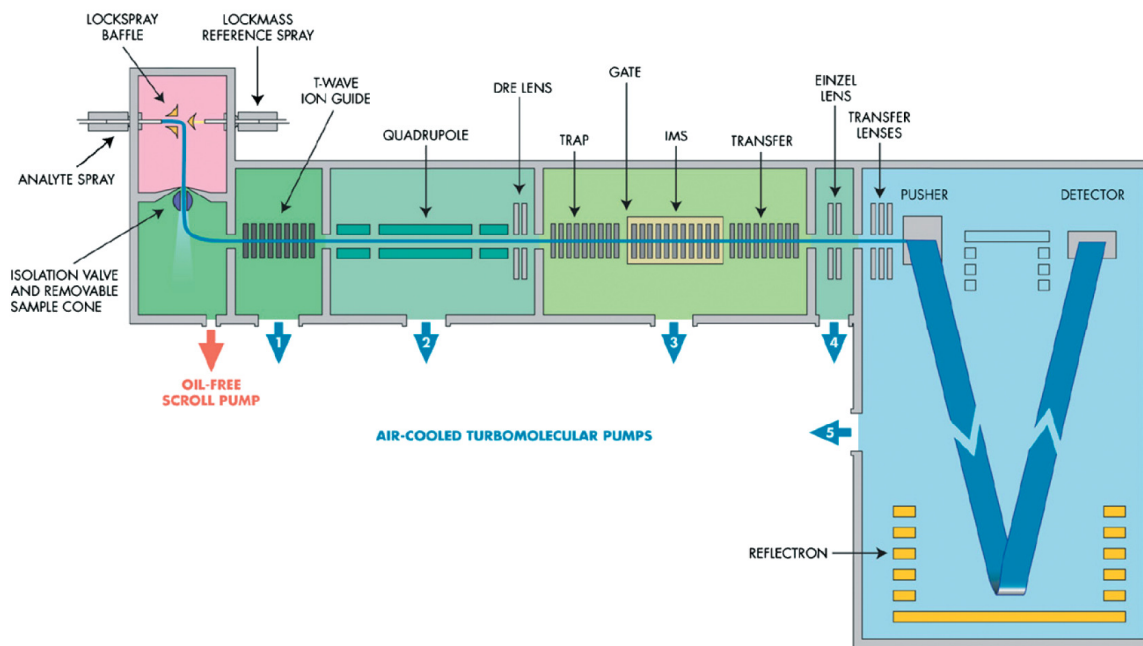


Figure 3. A schematic diagram of the Synapt ion mobility ToF mass spectrometer system used during this investigation. *Reprinted with permission from Steven D. Pringle et al., An investigation of the mobility separation of some peptide and protein ions using a new hybrid quadrupole/travelling wave IMS/oa-ToF instrument, Int J Mass Spectrom, 261(1): 1-12. Copyright (2007) Elsevier.*

The traveling wave cell of the Synapt ion mobility ToF mass spectrometer is a combination of three stacked ring ion guides (labeled as TRAP, IMS, and TRANSFER in Figure 3). The function of the trap ion guide is to accumulate ions while previous ion packet is undergoing ion mobility separation within the IMS ion guide. Separated ions are sent to the ToF analyzer by the transfer ion guide for mass determination.^[89] Alternatively, the entire traveling wave unit can also serve as a collision cell for collision-induced dissociation tandem mass spectrometry.

Historically, IM-MS is more commonly used in studies of large molecules such as proteins and peptides.^[87, 89, 90] The utility of IM-MS for small natural product studies, such as investigation of geometrical isomers of carotenoids, has not been investigated previously. Theoretical estimation suggests that a typical commercial IMS instrument could provide ~100,000 times faster separation speed than a typical HPLC separation in terms of carotenoid isomer analysis (*e.g.*, 20 ms IMS separation vs 40 min chromatographic separation). In this dissertation, travelling wave IM-MS technology was applied for the first time to the measurement and characterization of carotenoids including lycopene, β -carotene, lutein, and zeaxanthin.

1.2.5 APPI interface

APPI is the latest atmospheric pressure ionization technique widely adopted for LC-MS.^[91-93] The most common mechanism in positive ion APPI is the absorption of a high-energy photon by the analyte molecule and subsequent ejection of an electron. APPI can also produce negative ions. The process probably is that analytes capture thermal electrons generated from solvent ions, or produced by photons striking metal surfaces in the ionization source.^[94, 95] More detailed mechanisms are described in Chapter 4 of this dissertation.

The APPI source can be operated with or without a dopant. Frequently, dopant-assisted photoionization increases the ionization efficiency compared with direct photoionization by enhancing ion-molecule reactions.^[96-99] An extended conjugated polyene chain with few functional groups makes carotenoids more hydrophobic and

probably more suitable for APPI than many other natural products. Nevertheless, the use of dopants might still enhance the limits of detection and quantitation of carotenoids.

Although numerous mass spectrometry related studies of carotenoids have been published by the van Breemen lab as well as other researchers, APCI and electrospray have been the most often used ionization techniques. To date, the APPI source has not been widely applied to the analysis of carotenoids. In 2011, Rivera *et al.* published the first comprehensive evaluation of dopant-assisted positive ion APPI of 16 carotenoids, but negative ion APPI was not included.^[100] Therefore, in this dissertation, both positive ion and negative ion APPI and the utility of a variety of dopants were explored for carotenoids mass spectrometry.

Two distinct types of APPI sources have become commercially available including that described by Syage *et al.*^[101] and that of Bruins and co-workers^[102] (see Figures 4 and 5). The orthogonal APPI source of Syage is equipped with a radio frequency induced krypton UV lamp, which has greater radiant output and potentially higher ionization efficiency than conventional krypton UV lamps as used in the Bruins APPI source. However, when a dopant is used for the ionization, both APPI designs have shown comparable performance.^[103] A Syage APPI source was used in this dissertation mounted onto an Agilent 6410 triple quadrupole mass spectrometer (Figure 4).

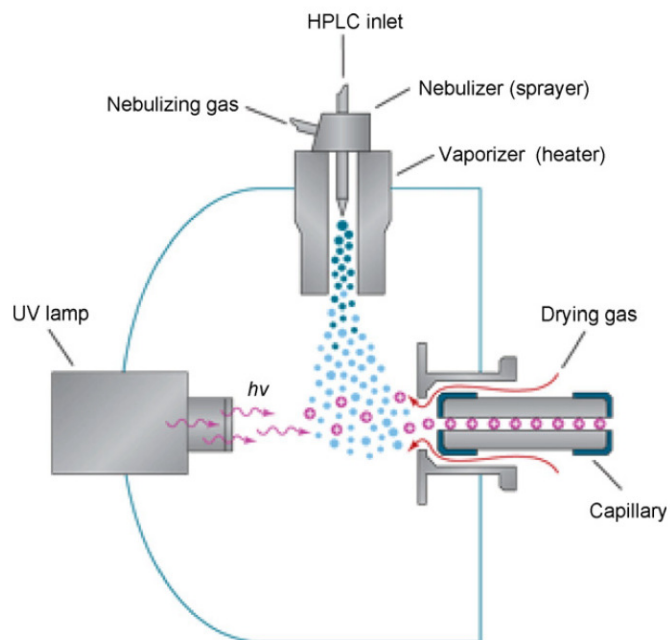


Figure 4. Schematic of the Syage APPI source used on an Agilent triple quadrupole mass spectrometer during this investigation. *Reprinted with permission from Damon B. Robb & Michael W. Blades, State-of-the-art in atmospheric pressure photoionization for LC/MS, Analytica Chimica Acta, 627(1): 34-49. Copyright (2008) Elsevier.*

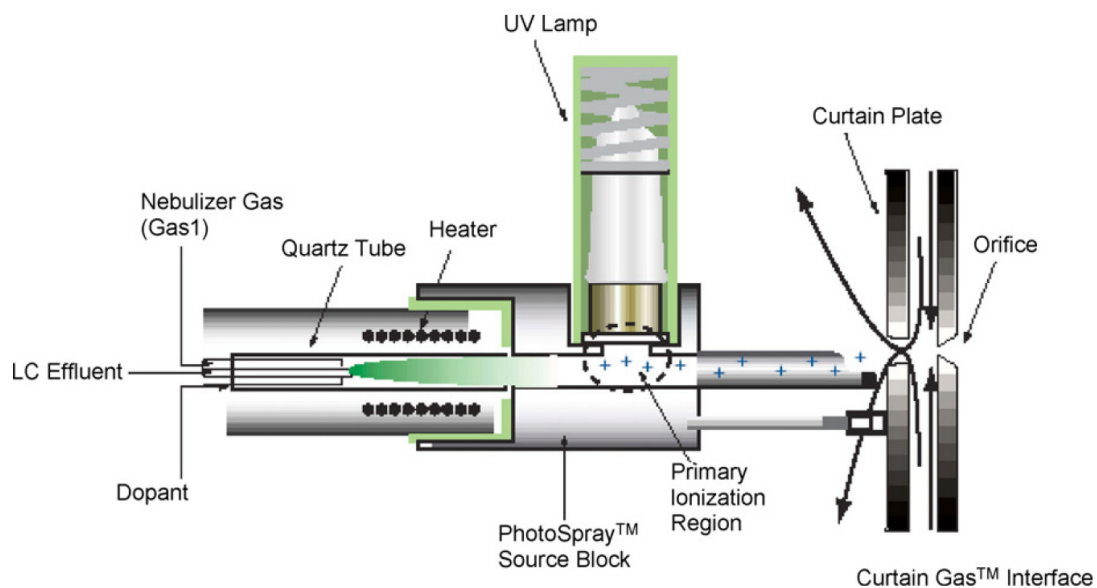


Figure 5. A Bruins-type APPI source used by Applied Biosystems/MDS SCIEX. *Reprinted with permission from Damon B. Robb & Michael W. Blades, State-of-the-art in atmospheric pressure photoionization for LC/MS, Analytica Chimica Acta, 627(1): 34-49. Copyright (2008) Elsevier.*

2. QUANTITATIVE ANALYSIS OF LYCOPENE IN HUMAN SERUM AND ITS EFFECTS

2.1 Introduction

Lycopene, the most abundant carotenoid in red tomatoes, is under investigation as a chemopreventive agent against prostate cancer.^[33, 44, 52] The consumption of tomatoes and tomato sauce has been associated with reduced risk of prostate cancer.^[104] In 1999, Gann and colleagues^[47] reported an inverse association of plasma lycopene levels and prostate cancer risk, particularly in aggressive cases of prostate cancer. Therefore, it has been hypothesized that lycopene is responsible for these protective effects. Since dietary recalls may not accurately reflect the lycopene intake of subjects and are subject to recall bias, here we used a validated LC-MS-MS assay developed in the van Breemen laboratory^[42, 105] to measure serum levels of lycopene in a randomized, placebo controlled, double-blind phase II clinical trial of lycopene in healthy men.

As discussed briefly in Chapter I, intermediate endpoint biomarkers are often used in clinical trials when the clinically meaningful endpoint (e.g., survival rates and deaths) are not accessible.^[65] Hypothesizing that lycopene functions as an antioxidant to prevent prostate cancer, intermediate endpoint biomarkers for DNA oxidation and lipid peroxidation were measured during this study to evaluate the effects of lycopene on oxidative stress in men. Urinary 8-oxo-dG was selected as a DNA oxidation marker, while urinary 8-iso-PGF₂ α was used as a marker of lipid peroxidation. Detailed information about these biomarkers is available elsewhere.^[106, 107] In addition, total PSA

and percent free PSA in the serum, which are used as indicators of prostate health, were determined.

2.2 Lycopene dietary intervention study

2.2.1 Study design

Directed by principal investigator Dr. Richard van Breemen, a four-arm randomized, placebo-controlled, and double-blind phase II clinical intervention study of lycopene dietary supplement was carried out at the University of Illinois at Chicago.^[108] The latest version of the study protocol (ID #: 2004-0217) was approved for the period May 4, 2012 - May 3, 2013 by Institutional Review Board^[109] at UIC. Both lycopene and placebo capsules used for the intervention study were provided by LycoRed (Beer-Sheva, Israel). The lycopene capsules were standardized to contain 15 mg lycopene per capsule while the placebo capsules contained only soybean oil.^[106]

In summary, 150 healthy men from the local community who met with the criteria (i.e. research subject candidates must be at least 18 years old and cannot be hospital inpatients, or allergic to tomatoes or tomato products, or have taken lycopene in supplement form within two weeks prior to enrollment) were enrolled the intervention study after each received informed consent.^[42] Demographic information concerning each subject including age, ethnicity, height, weight, health history, smoking status, alcohol consumption, current medications, vitamin and dietary supplement usage was documented at the time of enrollment. Subjects were then randomized into one of the four arms and administered capsules containing either lycopene (30 or 60 mg/d) or placebo for 21 days followed by a 21-day washout period (see Figure 6 for more details of the

treatment regime). All enrolled subjects agreed to supply blood and urine specimens on three occasions as follows: on day 0 (baseline), on day 21, and on day 42. Meanwhile, subjects were interviewed by a bionutrition manager for a 24-h diet recall during each of their General Clinical Research Center (GCRC) visits at UIC. More details for this clinical study have been reported by Dr. Ang Liu,^[42] Dr. Jeffrey Dahl^[106] and Dr. Long Yuan.^[107] A brief summary of the study protocol can also be accessed through ClinicalTrials.gov via identifier NCT00322114.

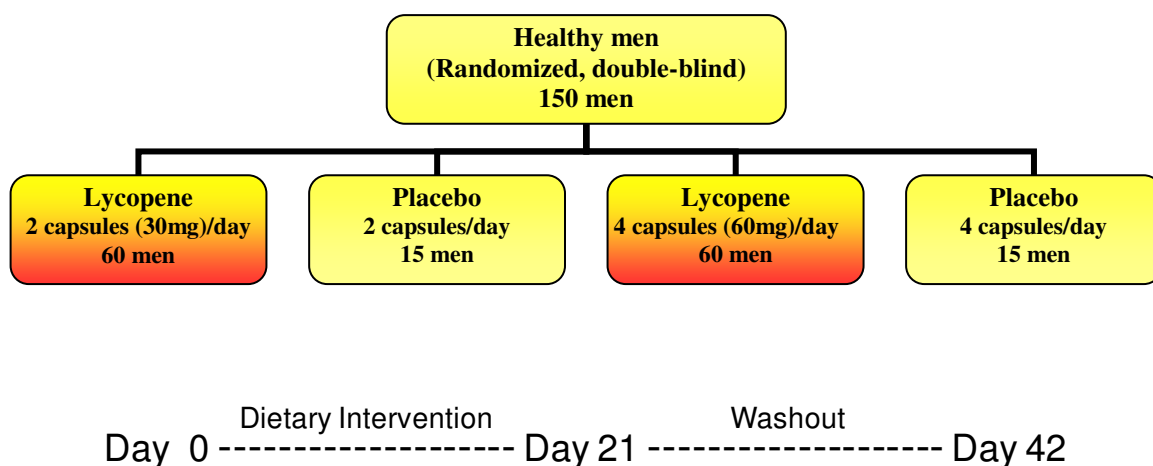


Figure 6. Study design of the phase II clinical intervention of lycopene in healthy men.

2.2.2 Clinical sample analysis

Results of the 30 mg/d lycopene dietary intervention part of this study (low dose arms) have been described previously in the dissertations of Dr. Ang Liu (lycopene and PSA),^[42] Dr. Jeffrey Dahl (8-iso-PGF_{2α})^[106] and Dr. Long Yuan (8-oxo-dG)^[107] from the van Breemen laboratory. This chapter will therefore focus on the analysis, results and

discussion of data from the two high dose arms of this study (60 mg/d lycopene and corresponding controls).

Quantitative analysis of serum levels of lycopene in the high dose study subjects was carried out using a validated LC-MS-MS assay reported previously by Fang *et al.*^[105] and Liu^[42] of the van Breemen laboratory. The serum levels of total PSA and free PSA were measured using commercially available enzyme-linked immunosorbent assay (ELISA) kits manufactured by Bio-Quant (San Diego, CA). The urinary levels of 8-oxo-dG were measured by Dr. Yang Yuan using an LC-MS-MS assay developed previously in the same laboratory.^[107] The urinary levels of creatinine were also measured by Dr. Yang Yuan using a commercially available clinical chemistry assay kit manufactured by Cayman (Ann Arbor, MI). The levels of 8-iso-PGF_{2α} in urine were determined by Dr. Jeffery Dahl and Dr. Kevin Krock using a LC-MS-MS assay developed in this laboratory.^[106, 110]

2.3 Materials and methods

2.3.1 Chemicals

All-*trans*-lycopene (≥90%), absolute ethanol (≥99.5%), and butylated hydroxytoluene (BHT) were purchased from Sigma-Aldrich (St. Louis, MO). [8,8',9,9',10,10',11,11',19,19'-¹³C₁₀]-all-*trans*-lycopene was supplied by Cambridge Isotope Laboratories (Andover, MA). Defibrinated, charcoal stripped, pooled human serum was purchased from Innovative Research (Novi, MI). HPLC-grade acetonitrile, methyl-*tert*-butyl ether (MTBE), hexane, and dichloromethane were purchased from

Fisher Scientific (Fairlawn, NJ). Water was prepared on demand using a Millipore Milli-Q water purification system (Billerica, MA).

2.3.2 Sample preparation

Lycopene stock solutions were prepared by dissolving ~1 mg of all-*trans* lycopene in 10 mL of dichloromethane. Since lycopene is sensitive to light and oxygen exposure, stock solutions were prepared under dim light then stored in amber vials at -80°C. Concentrations of lycopene stock solutions were measured using a Bio-Rad (Hercules, CA) SmartSpec™ Plus spectrophotometer and standardized based on the absorbance at 502 nm using the reported molar absorption coefficient of lycopene ($1.72 \times 10^5 \text{ L mol}^{-1} \text{ cm}^{-1}$) in hexane/CH₂Cl₂ (98:2; v/v).^[105] Separate stock solutions were used to prepare calibration standards and quality control samples. Fresh working standard solutions were prepared each day by evaporating stock solutions followed by reconstitution and dilution with acetonitrile/MTBE (1:1, v/v).

Each calibration curve consisted of a double blank sample (charcoal stripped human serum processed without surrogate standard), a zero sample (charcoal stripped human serum processed with surrogate standard), and seven non-zero samples covering the expected range. Seven calibration levels from 0.04 to 5.0 µM and quality control samples of 0.3, 1.0 and 3.0 µM were prepared by diluting the appropriate volume of working standard solutions with charcoal stripped human serum. Fresh calibration standards and quality control samples were prepared each day using freshly prepared working standard solutions.

Serum samples from the lycopene intervention study were thawed at room temperature followed by vortexing to ensure homogeneity. Two aliquots (200 µL each)

per clinical serum sample were each spiked with the surrogate standard, [$^{13}\text{C}_{10}$]-all-*trans*-lycopene (20 μL , 10 μM) after mixing with equal volumes of water. All samples were then deproteinized with 600 μL of absolute ethanol. The mixtures were extracted twice with 2.5 mL portions of hexane containing 100 mg/L BHT, followed by centrifugation for 5 min at $800 \times g$ and 4°C . The hexane extracts were collected, combined, and evaporated to dryness under a stream of nitrogen. Each residue was reconstituted in 40 μL MTBE and then 40 μL acetonitrile was added. Aliquots (10 μL) of each prepared sample were injected onto the HPLC column for LC-MS-MS analysis. Serum samples representing all time points from a particular subject were prepared and analyzed simultaneously to minimize experimental variations.

2.3.3 LC-MS-MS analysis of lycopene

LC-MS-MS was carried out using a Thermo-Finnigan TSQ Quantum triple quadrupole mass spectrometer (San Jose, CA) interfaced with a Waters Alliance 2695 HPLC System (Milford, MA). The HPLC separation was carried out using a Phenomenex (Torrance, CA) Luna C_{18} HPLC column (5 μm , 2.0×150 mm) at a flow rate of 0.4 mL/min. Lycopene was eluted as a single HPLC peak (the sum of *cis*- and all-*trans* lycopene isomers) from the column using isocratic acetonitrile/MTBE (85:15, v/v). Negative ion APCI mass spectrometry was operated at a discharge current of 17 μA with a capillary temperature of 336°C and vaporizer temperature of 329°C . The operating sheath gas (N_2) and auxiliary gas (N_2) pressures were 50 psi and 5 psi respectively. Argon collision gas was set to 1.2 torr for CID with a collision energy of 25 eV. Selected reaction monitoring (SRM) transitions of m/z 536 to m/z 467 and m/z 546 to m/z 477 were

monitored with a dwell time of 0.5 s each for all-*trans* lycopene and [$^{13}\text{C}_{10}$]-all-*trans*-lycopene (surrogate standard). The peak area ratios of the two SRM transitions were calculated using Thermo Xcalibur 2.0.7 software for the quantitation of total lycopene in the serum samples.

2.3.4 PSA measurement

Serum samples were first incubated with an anti-PSA monoclonal antibody coated on the surface of each well, and then a mouse anti-PSA antibody labeled with horseradish peroxidase (HRP) was added as the tracer. After washing off unbound enzyme-labeled antibody, an enzyme substrate, tetramethyl benzidine (TMB) was added. The absorbance of the quenched reaction solution was proportional to the concentration of PSA in the sample. For the measurement of total PSA concentration, aliquots (50 μL) of blanks, standards, or serum samples were added into the antibody coated wells in duplicates. Followed by adding 100 μL of enzyme conjugate, the mixed solutions were incubated at room temperature (18-26°C) for 60 min. Each well on the plate was washed three times with 300 μL wash buffer to remove unbounded enzyme conjugate, and then 100 μL of TMB substrate was added. After 15 min incubation at room temperature, the reaction was quenched by adding 50 μL stop solution. The absorbance was measured at 450 nm within 15 min. Total PSA concentrations in human serum were calculated from the calibration curve. The serum levels of free PSA were measured similarly, except that antibodies targeted to free PSA were used.

2.3.5 Food recall analysis

Twenty-four-hour dietary recall data for each study subject were analyzed by Ms. Amanda Guide of the GCRC using Nutrition Data System for Research software released by the University of Minnesota (Minneapolis, MN).

2.3.6 Statistical analysis

Statistical analysis was carried out using Statistical Package for Social Sciences (SPSS) software (version 16.0, SPSS, Inc, Chicago, IL). Continuous variables were presented as means \pm standard deviation (SD), and means were compared by using the independent samples t-test or Mann-Whitney test depending on the distributions of datasets subjected to comparison. The Pearson chi-square test was used for the analysis of categorical variables such as ethnicity, smoking status and alcohol assumption status. All statistical tests were 2-sided, and *P* values <0.05 were considered to be statistically significant.

2.4 Results and discussion

2.4.1 Enrollment and characteristics of study subjects

Overall, 80 out of 234 screened healthy men were admitted and randomized into the lycopene high dose intervention study (see Figure 7). Three subjects in the 60 mg/d lycopene arm and 1 subject in the 4-capsule placebo arm withdrew from the study after their first laboratory visits without any explanation. Therefore, none of these subjects were included in the sample analysis. No side effects were noted by any of the subjects.

Statistical analyses of demographic characteristics of the 76 study subjects were carried out by comparing means of the lycopene treated group vs. placebo group. As shown in Table I, the 60 mg/d lycopene treated arm and the placebo arm did not differ significantly in terms of age ($P = 0.323$), height ($P = 0.432$), weight ($P = 0.949$), or BMI ($P = 0.472$). Furthermore, no significant differences were found regarding ethnicity, smoking or consumption of alcohol between the subjects randomized to the two arms ($P > 0.28$; Table I).

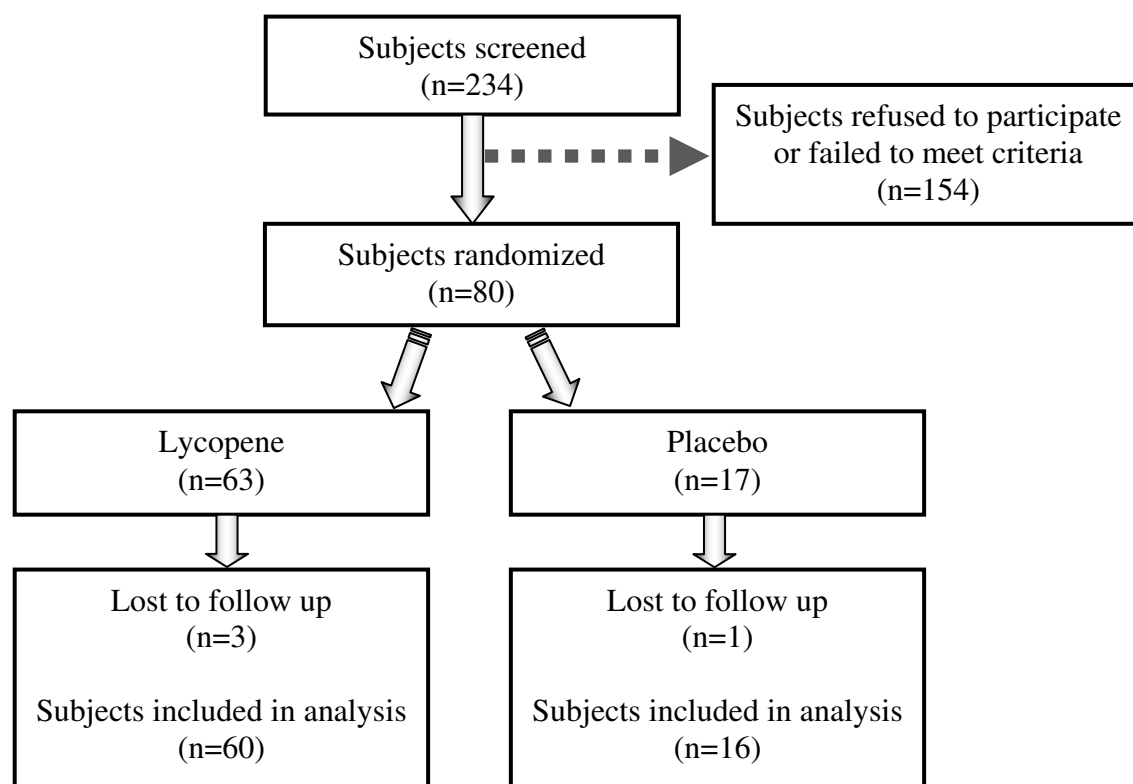


Figure 7. Flowchart of subject recruitment for high-dose lycopene study in healthy men

TABLE I
DEMOGRAPHIC CHARACTERISTICS OF ALL STUDY SUBJECTS BY
INTERVENTION GROUPS (60 MG/DAY OR PLACEBO)

Characteristic	Total (n=76)	Placebo (n=16)	Lycopene (n=60)	P
Age, y	33.8±13.8	37.8±16.3	32.8±13.0	0.323 ^a
Height, cm	177.4±7.5	176.1±7.9	177.7±7.4	0.432 ^b
Weight, kg	83.0±13.9	81.6±9.8	83.3±14.9	0.949 ^a
BMI, kg/m ²	26.3±3.9	26.3±2.6	26.3±4.2	0.472 ^a
Ethnicity, %				
NH White	67.1	75.0	65.0	0.558 ^c
Asian	23.7	25.0	23.3	
Black	1.3	0	1.7	
Other	7.9	0	10.0	
Smoking status, %				
Yes	6.6	12.5	5.0	0.282 ^c
Former/no	93.4	87.5	95.0	
Alcohol consumption, %				
Yes	78.9	75.0	80.0	0.663 ^c
Former/no	21.1	25.0	20.0	

^a P values determined by comparing demographic characteristics of study subjects in placebo group versus lycopene group using Mann-Whitney test.

^b P value determined by comparing demographic characteristics of study subjects in placebo group versus lycopene group using independent-samples t-test.

^c P values determined by comparing demographic characteristics of study subjects in placebo group versus lycopene group using Pearson Chi Square test.

2.4.2 Quantitative analysis of lycopene

The APCI product ion tandem mass spectra of lycopene and [¹³C₁₀]-all-*trans*-lycopene (used as a surrogate standard) are shown in Figure 8. As previously reported by Fang et al.,^[105] loss of a terminal isoprene group from the radical

anion of lycopene was found to be the most abundant product ion during negative ion APCI of both lycopene and its surrogate standard. The fragment ions corresponding to $[M-69-69]^-$ and $[M-69-106]^-$ formed by the elimination two terminal isoprene radicals or one isoprene radical plus one xylene molecule, respectively, were also observed, but were not used for quantitation due to their lower abundances.^[68, 111]

The SRM transitions of m/z 536 > 467 and m/z 546 > 477 were used during LC-MS-MS analysis of serum extracts to achieve optimal sensitivity and specificity for the measurement of lycopene and its surrogate standard, respectively.^[105] Since isomeric α -carotene and β -carotene contain terminal rings, they do not fragment to eliminate an isoprene group and were not detected during LC-MS-MS, even though they are abundant in human serum. An example of an LC-MS-MS analysis of a serum sample from this investigation showing the selective detection of lycopene and its surrogate standard is shown in Figure 9.

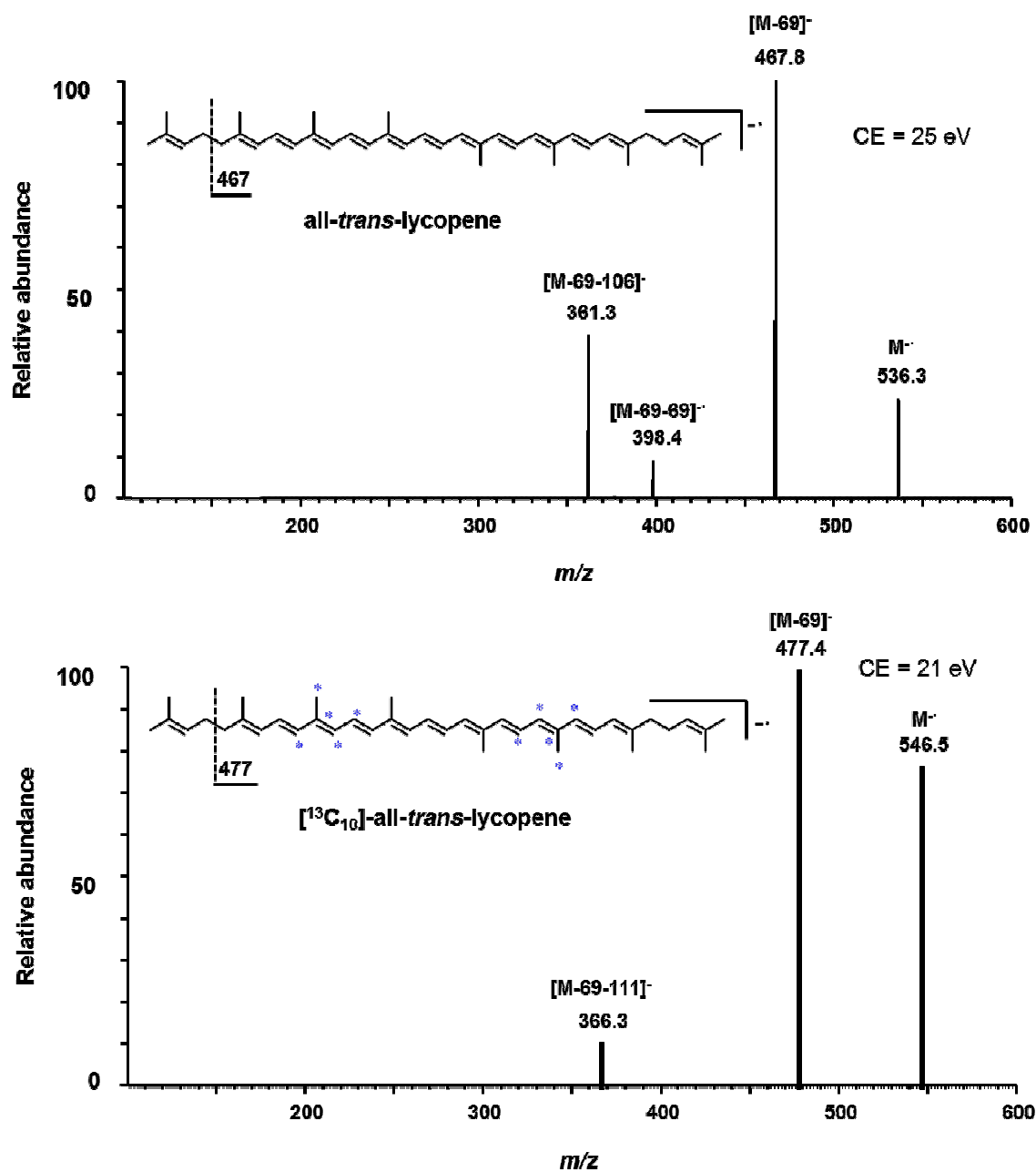


Figure 8. Negative ion APCI product ion tandem mass spectra of *all-trans*-lycopene and $[^{13}\text{C}_{10}]$ -*all-trans*-lycopene.

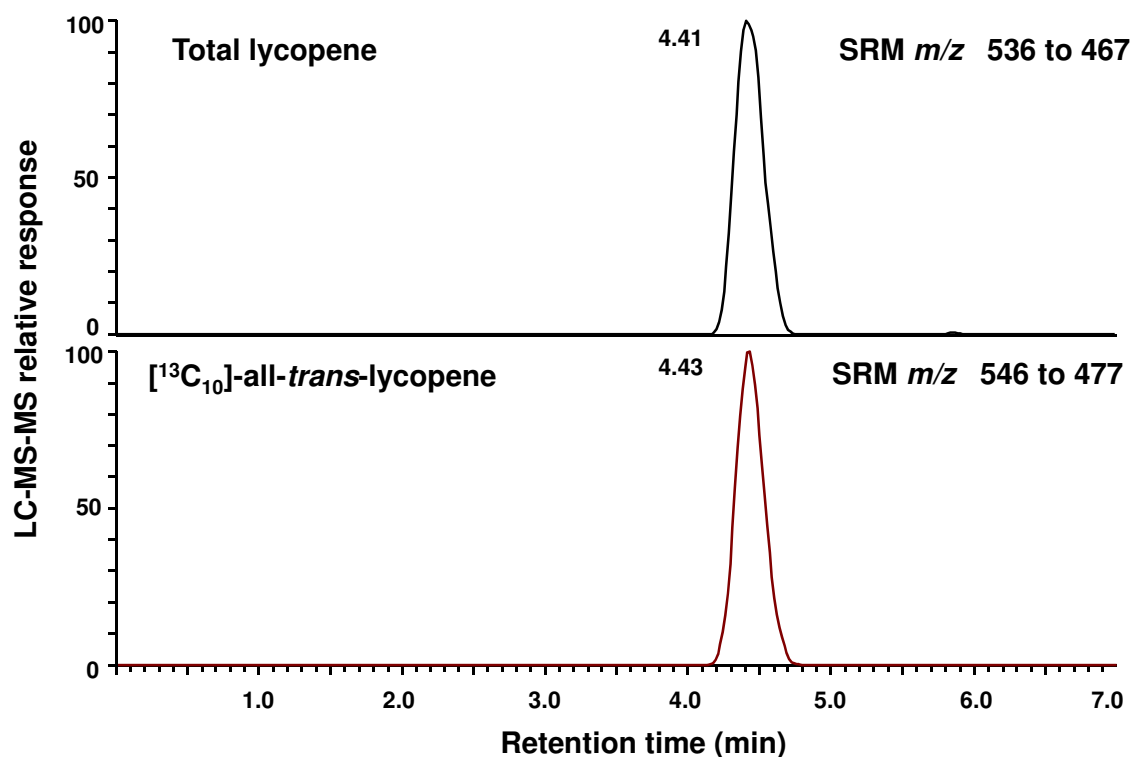


Figure 9. Negative ion APCI LC-MS-MS SRM chromatograms for the quantitative analysis of lycopene in a serum sample from the clinical study. The lycopene peak represented a serum concentration of 0.435 μM .

2.4.3 Lycopene response

The concentrations of lycopene in the serum of all subjects at day 0, day 21 and day 42 were determined using LC-MS-MS, and the results are summarized in Figure 10. A box plot of mean differences of serum lycopene concentrations for the placebo arm and lycopene intervention arm before and after 21-day intervention is shown in Figure 11. Mean serum lycopene concentration increased 1.52-fold in the 60 mg/d lycopene intervention arm from $0.753 \pm 0.347 \mu\text{mol/L}$ at day 0 to $1.147 \pm 0.432 \mu\text{mol/L}$ at day 21 (Table II). Compared with a mean difference of $-0.149 \pm 0.715 \mu\text{mol/L}$ for the placebo

group, a mean difference of $0.393 \pm 0.285 \mu\text{mol/L}$ was observed for the lycopene intervention group, which was a statistically significant increase in lycopene concentration due to supplementation ($P < 0.0001$).

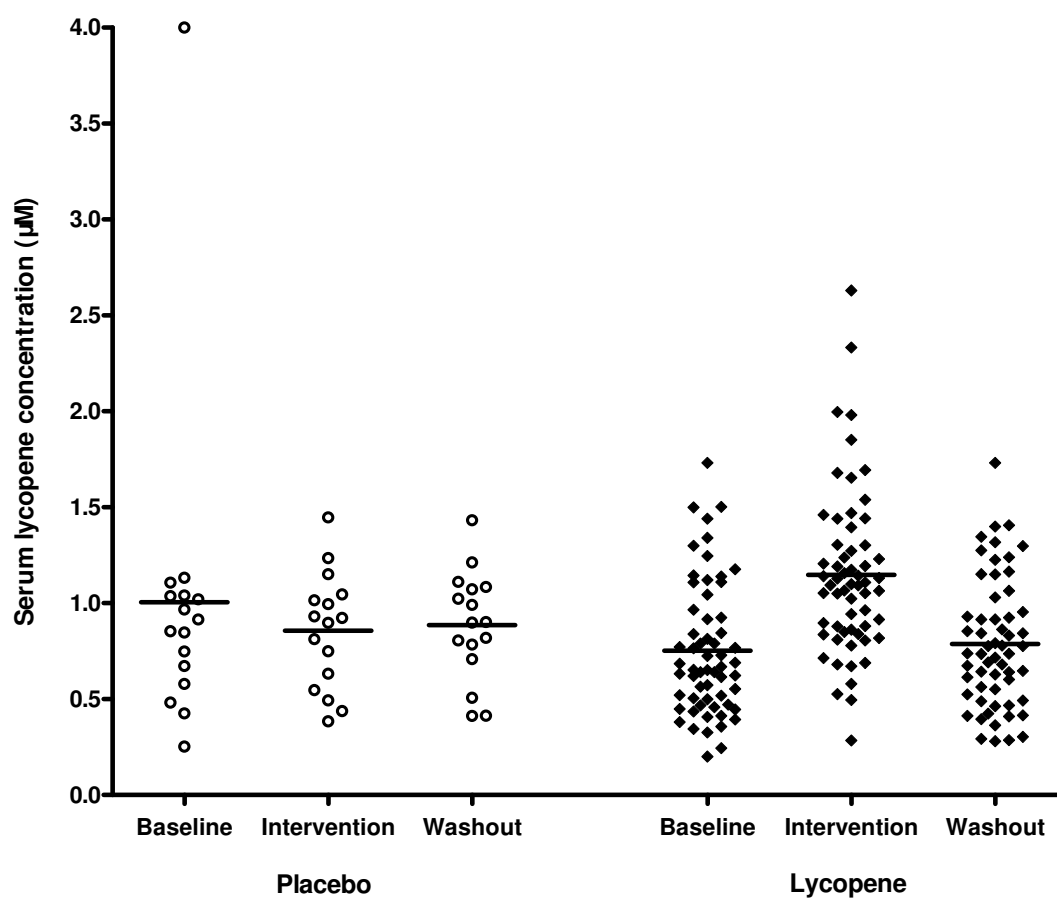


Figure 10. Serum levels of lycopene of individual subjects at day 0 (baseline), day 21(intervention), and day 42 (wash out).

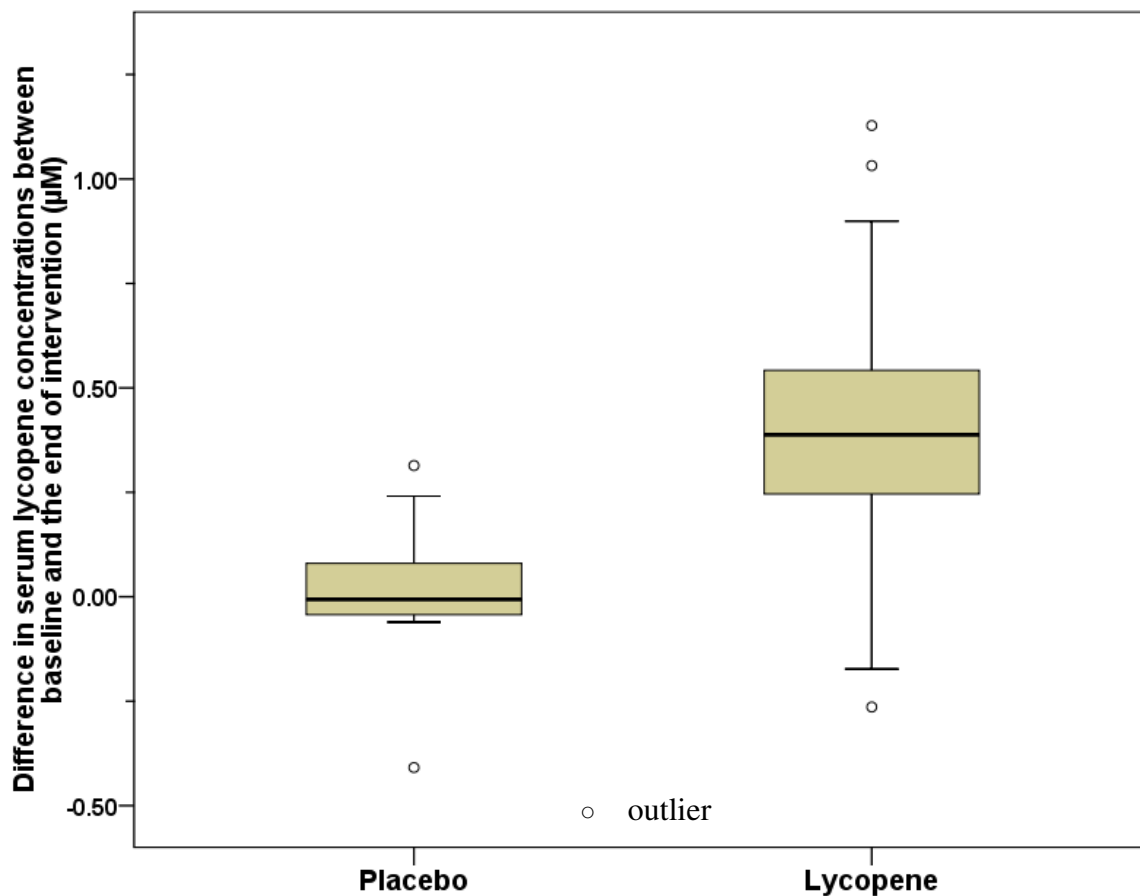


Figure 11. Mean differences of serum lycopene concentrations between day 0 (baseline) and day 21 (intervention) in the placebo arm and lycopene intervention arm.

The increase in serum lycopene due to supplementation was similar to a dietary intervention reported by Chen *et al.*^[50] using tomato sauce equivalent to 30 mg/d lycopene, which demonstrated an increase in human serum lycopene levels of 1.97-fold in 3 weeks. This magnitude of increase was also comparable to our previous study focused on African American men with prostate cancer or benign prostate hyperplasia (BPH),^[52] in which a mean plasma lycopene increased by 1.93-fold following 21-day lycopene supplementation at 30 mg/d. The serum level of lycopene obtained in healthy

men using 60 mg/d was not significantly different from that we observed previously following supplementation using 30 mg/d in healthy men, in which mean serum lycopene levels increased 1.63-fold.^[42]

Considering that the mean serum lycopene concentration for the 30 mg lycopene intervention arm of the present study was $1.483 \pm 0.685 \mu\text{mol/L}$ at day 21,^[42] and for the 60 mg lycopene arm was $1.147 \pm 0.432 \mu\text{mol/L}$ at day 21, there was clearly no positive correlation between the mean serum concentrations of lycopene and dosage levels. Although a dose-dependent increase in serum lycopene levels was reported by Kim *et al.*^[112] in their 8-week randomized controlled trial using lycopene supplementation at 6 mg/d and 15 mg/d, this finding indicates that serum levels of lycopene in men probably reached a plateau following a 3-week lycopene supplementation at the higher dosage of 30 mg/d. Our results are in good agreement with a dose-escalating trial of lycopene conducted by Clark *et al.*,^[113] which reported similar plasma levels of lycopene across 15, 30, 45, 60, 90 mg/d groups with up to 12 months of supplementation.

After the supplementation ended, it was found that the mean serum lycopene level returned to the baseline after 21-day wash out period as shown in Figure 10 ($0.753 \pm 0.347 \mu\text{mol/L}$ at baseline vs $0.788 \pm 0.336 \mu\text{mol/L}$ on day 42, $P = 0.347$, Wilcoxon test). In decades ago, Gustin *et al.*^[114] and Stahl and Sies^[115] estimated that the half-life of lycopene in human plasma was 1-3 days after a single dose. In 2011, a bioavailability study using ^{14}C labeled lycopene conducted by Ross *et al.*^[116] suggested that the elimination half-life of ^{14}C -lycopene from human plasma was 5 days. All these reports support that a 21-day intervention followed by a 21-day washout period in our study

design was appropriate and cost-effective, since majority compounds reach their steady blood levels by 4-5 half-lives in response to a change of regular dosing.^[106]

To determine if there were significant differences in diet between the treatment and placebo groups, a Mann-Whitney test was performed for their 24-hour diet recall data collected at day 0, day 21 and day 42. No significant differences were observed between the two arms with respect to consumptions of lycopene, cholesterol, total fat, total carotenoids, and total tocopherols. For the consumption of total triglycerides, a significant difference ($P = 0.049$) was only observed at the end of the wash out period (day 42), which was unlikely to affect the clinical outcomes of the 21-day intervention. Additional Mann-Whitney tests of the serum lycopene levels at baseline between smokers and non-smokers ($P = 0.253$) or between men who were alcohol drinkers or non-alcohol drinkers ($P = 0.619$) also did not reveal any significant differences.

Although subjects were instructed to maintain a normal diet, mean serum lycopene concentrations declined slightly in the placebo arm from $1.005 \pm 0.840 \mu\text{mol/L}$ (day 0) to $0.856 \pm 0.301 \mu\text{mol/L}$ (day 21). According to the 24-hour food recall analysis, average 24-h lycopene intakes were $1050 \mu\text{g}$ (day 0), $836 \mu\text{g}$ (day 21), and $943 \mu\text{g}$ (day 42) for the placebo arm, and $670 \mu\text{g}$ (day 0), $581 \mu\text{g}$ (day 21), and $518 \mu\text{g}$ (day 42) for the lycopene intervention arm respectively. As indicated by the food recall information, average lycopene consumption through diet was lower for men on both arms at their second visit (day 21) and third visit (day 42). Therefore, this decreased lycopene level in serum may be attributed the reduction of lycopene containing food consumption after enrollment.

In summary, while no significant differences were observed with respect to 24-h lycopene intake ($P = 0.514$, Mann-Whitney test) or baseline serum lycopene levels ($P = 0.185$, Mann-Whitney test) between the two arms at day 0, men who received lycopene at 60 mg per day for 3 weeks demonstrated a significant increase ($P < 0.0001$) in their mean serum lycopene concentrations (Figure 11 and Table II).

TABLE II
CLINICAL OUTCOMES OF THE STUDY GROUPS: 21-D LYCOPENE SUPPLEMENTATION AT 60 MG/DAY VS. PLACEBO

Biomarker	Placebo			Lycopene			<i>p</i>
	Baseline	End of intervention	Difference	Baseline	End of intervention	Difference	
Serum lycopene (μmol/L)	1.005±0.840 (n=16)	0.856±0.301 (n=16)	-0.149±0.715 (n=16)	0.753±0.347 (n=60)	1.147±0.432 (n=60)	0.393±0.285 (n=60)	<0.0001 ^a
Urinary 8-oxo-dG (ng/mg creatinine)	1.785±2.212 (n=16)	1.939±1.427 (n=16)	0.154±2.194 (n=16)	2.486±2.850 (n=60)	2.358±2.530 (n=60)	-0.129±2.899 (n=60)	0.16 ^a
Urinary 8-iso-PGF _{2α} (pg/mg creatinine)	140.5±120.3 (n=16)	178.9±120.7 (n=16)	38.4±109.6 (n=16)	152.7±141.7 (n=55)	148.8±96.2 (n=55)	-4.0±119.1 (n=55)	0.07 ^a

^a *P* values determined by comparing the placebo group with the lycopene group using Mann-Whitney test.

2.4.4 Antioxidant biomarkers

The urinary levels of 8-oxo-dG and 8-iso-PGF_{2α}, normalized to creatinine, were measured as indications of systemic DNA oxidation and lipid peroxidation, respectively, at day 0, day 21 and day 42 for all study subjects. The concentrations of 8-oxo-dG and 8-iso-PGF_{2α} in all urine samples are plotted in Figures 12 and 13, respectively. The Mann-Whitney test was used for the comparison of both urinary levels of 8-oxo-dG and 8-iso-PGF_{2α} between the two arms, since these data did not follow a Gaussian distribution. These comparisons are summarized in Table II.

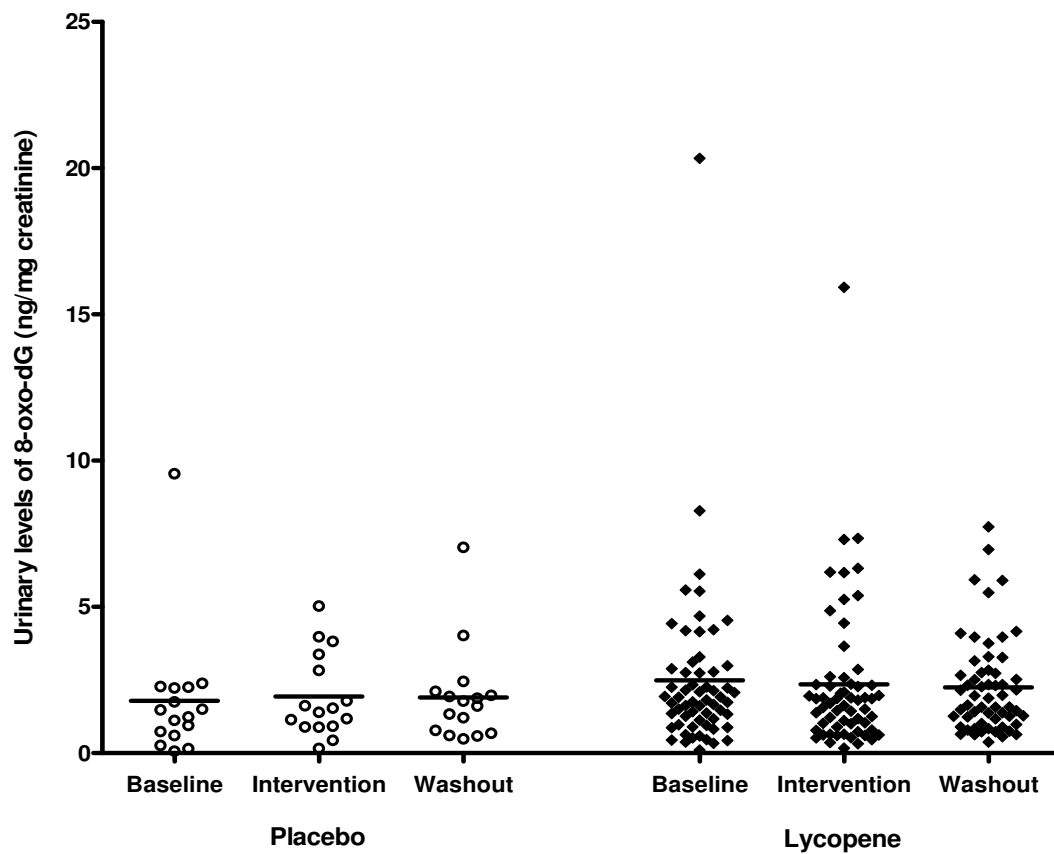


Figure 12. Urinary levels of 8-oxo-dG (normalized to creatinine) of individual subjects in the placebo group and in the lycopene (60 mg/d) supplementation group at day 0 (baseline), day 21(intervention), and day 42 (wash out).

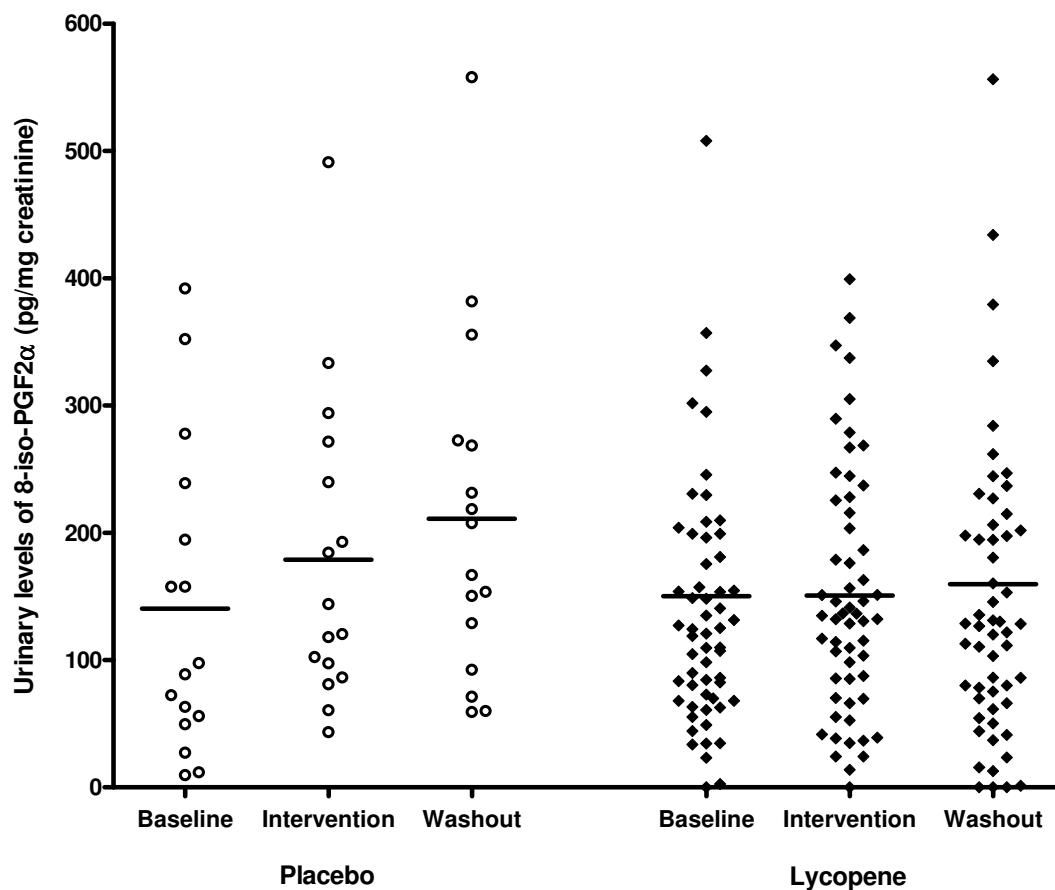


Figure 13. 8-iso-PGF_{2α} (normalized to creatinine) in urine from subjects receiving placebo or lycopene (60 mg/d) at day 0 (baseline), day 21 (intervention), and day 42 (wash out).

As shown in Table II, the mean of urinary 8-oxo-dG concentrations in the placebo arm increased slightly from 1.785 ± 2.212 ng/mg creatinine at day 0 to 1.939 ± 1.427 ng/mg creatinine at day 21. During this same period, the mean of urinary 8-oxo-dG concentrations decreased from 2.486 ± 2.850 to 2.358 ± 2.530 ng/mg creatinine in the lycopene supplementation group (60 mg/d) with a mean difference of -0.129 ± 2.899 ng/mg creatinine. Since the mean values of 8-oxo-dG increased in the control group while decreasing in the lycopene treatment group (Figure 14), there was a trend toward reduced oxidative stress as indicated by reduced DNA damage in healthy men receiving

lycopene. However, this trend did not achieve statistical significance in this small study population ($P = 0.16$, Table II).

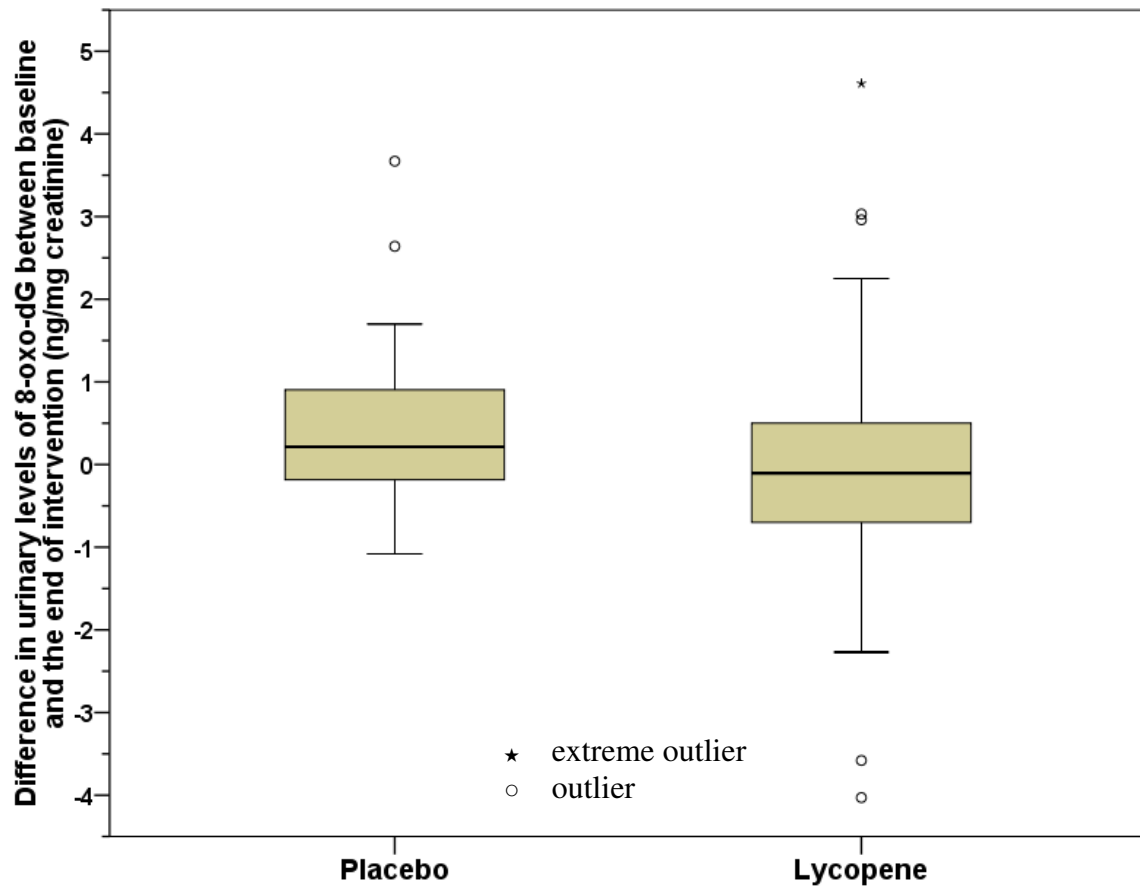


Figure 14. Mean differences of urinary 8-oxo-dG concentrations between day 0 (baseline) and day 21 (intervention) in the placebo group and the lycopene (60 mg/d) intervention group.

A biomarker of lipid peroxidation, 8-iso-PGF_{2α} concentrations dropped from 152.7 ± 141.7 pg/mg creatinine to 148.8 ± 96.2 pg/mg creatinine (-4.0 ± 119.1 pg/mg creatinine) in subjects receiving 60 mg/d lycopene for 21 days. During the same 21-day period, urinary 8-iso-PGF_{2α} increased in the control group (38.4 ± 141.7 pg/mg creatinine). Although these differences in urinary 8-iso-PGF_{2α} levels showed a strong trend suggesting that lycopene supplementation helps prevent lipid peroxidation in vivo (Figure 15), the concentrations between the two arms were not quite significant ($P = 0.07$, Table II).

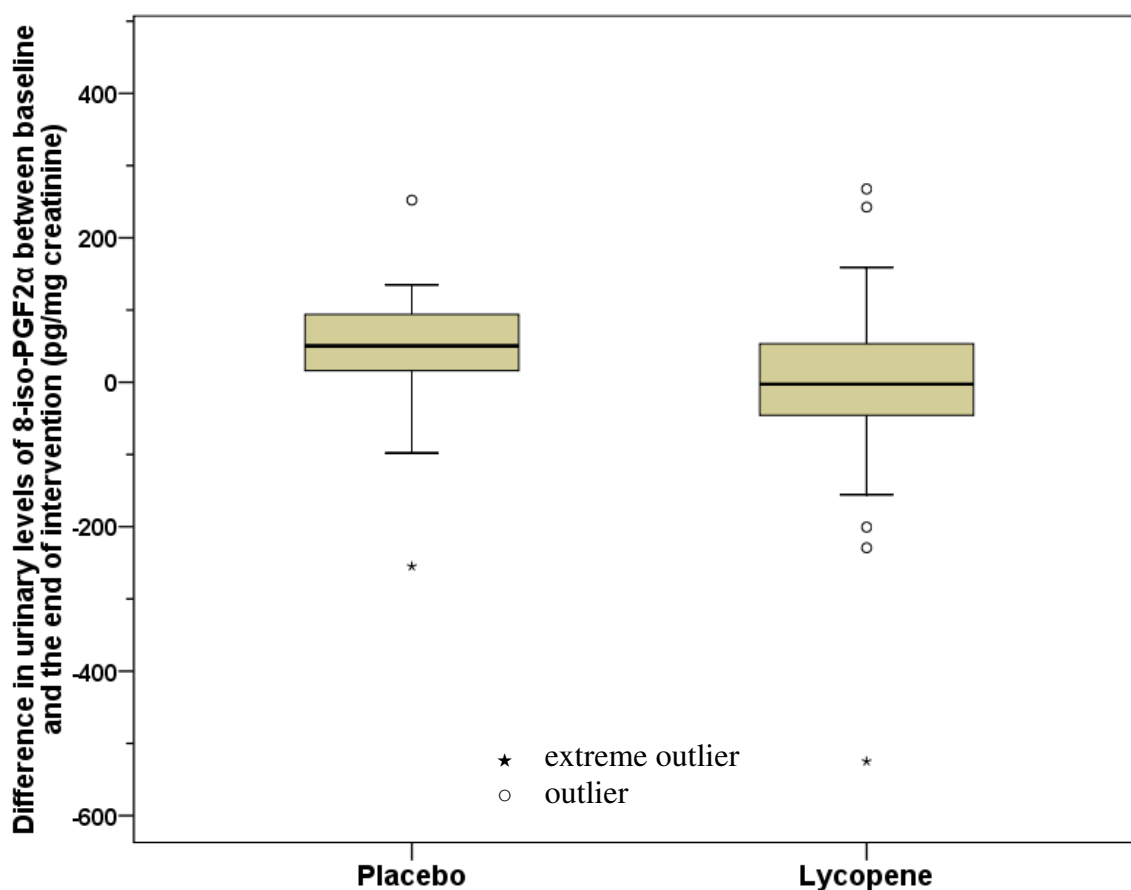


Figure 15. Mean differences of urinary 8-isoprostaglandin-F_{2α} concentrations between day 0 (baseline) and day 21 (intervention) in the placebo arm and lycopene intervention arm (60 mg/d).

2.4.5 Total PSA and free PSA

Serum levels of total PSA and free PSA in men of high dose arms (60 mg/d or placebo) were measured using two types of ELISA kits by strict adherence to the supplied protocols summarized in section 2.3.4. The results for all high dose study samples analyzed are listed in Table III. It was found that 53 out of 226 (23.5%) total

PSA measurements and 155 out of 226 (68.5%) free PSA measurements were unsuccessful (<LLOQ).

In comparison with our successful measurements made on low dose study samples (30 mg/d or placebo) previously, a few critical changes made to the new batches of ELISA kits probably contributed to the decreased sensitivity. Firstly, the enzyme-linked antibodies (anti-PSA or anti-free PSA antibodies) have been reformulated (technical details were not disclosed). Secondly, the initial 60-min incubation step of coated antibodies (solid-phase antibodies) with PSA or free PSA in human serum along with subsequent washes has been combined with the second incubation step for enzyme-linked antibodies.^[42] Although the assay times were significantly shortened from previous 140 min (2-step incubation) to less than 80 min (single-step incubation), the new protocols were more vulnerable to nonspecific reactions.^[117] For instance, less PSA or free PSA in the samples are available to react with solid-phase antibodies due to the nonspecific binding with enzyme conjugates in the incubation. Since the current format of total PSA or free PSA ELISA kits did not produce reliable measurements for significant portions of the study samples, no conclusion can be made due to the lack of necessary statistical power. Therefore, the entire analysis needs to be repeated with a validated alternative assay when possible.

TABLE III
SERUM LEVELS OF PSA AND FREE PSA MEASURED BY ELISA USING
SINGLE-STEP PROTOCOLS (60 MG/DAY OR PLACEBO)

Subject	Day 0 PSA (ng/mL)	Day 21 PSA (ng/mL)	Day 42 PSA (ng/mL)	Day 0 free PSA (ng/mL)	Day 21 free PSA (ng/mL)	Day 42 free PSA (ng/mL)
1	0.137	0.314	0.294	<LLOQ ^a	0.140	<LLOQ
2	0.255	0.510	0.294	0.105	0.133	0.140
3	0.104	0.104	0.278	<LLOQ	<LLOQ	<LLOQ
4	0.686	<LLOQ	<LLOQ	<LLOQ	<LLOQ	<LLOQ
5	0.157	0.137	<LLOQ	<LLOQ	<LLOQ	<LLOQ
6	1.500	1.463	1.452	0.363	0.347	0.347
7	0.822	0.933	0.867	<LLOQ	<LLOQ	<LLOQ
8	<LLOQ	<LLOQ	<LLOQ	<LLOQ	<LLOQ	<LLOQ
9	0.533	0.222	<LLOQ	<LLOQ	<LLOQ	<LLOQ
10	0.661	0.678	0.209	<LLOQ	<LLOQ	<LLOQ
11	3.253	3.793	4.108	0.193	0.203	0.178
12	<LLOQ	<LLOQ	<LLOQ	<LLOQ	<LLOQ	<LLOQ
13	0.356	0.600	0.311	<LLOQ	<LLOQ	<LLOQ
14	0.178	0.244	0.244	<LLOQ	<LLOQ	<LLOQ
15	<LLOQ	0.324	<LLOQ	<LLOQ	<LLOQ	<LLOQ
16	<LLOQ	0.405	0.108	<LLOQ	<LLOQ	<LLOQ
17	0.176	0.275	0.275	<LLOQ	<LLOQ	<LLOQ
18	1.463	1.329	1.214	0.201	0.195	0.212
19	1.539	1.838	1.781	0.158	0.194	0.192
20	0.430	0.404	0.447	0.181	0.179	0.166
21	2.092	2.278	2.718	0.415	0.390	0.376
22	1.156	0.933	0.844	1.353	1.108	1.058
23	0.529	<LLOQ	0.118	<LLOQ	<LLOQ	<LLOQ
24	1.971	1.979	2.063	0.414	0.389	0.390
25	0.139	<LLOQ	<LLOQ	<LLOQ	<LLOQ	<LLOQ
26	0.243	0.216	0.189	<LLOQ	<LLOQ	<LLOQ
27	0.118	<LLOQ	<LLOQ	<LLOQ	<LLOQ	<LLOQ
28	0.506	0.506	1.149	<LLOQ	<LLOQ	<LLOQ
29	0.176	0.412	0.235	<LLOQ	<LLOQ	<LLOQ
30	<LLOQ	0.330	<LLOQ	<LLOQ	<LLOQ	<LLOQ
31	<LLOQ	<LLOQ	<LLOQ	<LLOQ	<LLOQ	<LLOQ
32	0.345	0.138	0.161	<LLOQ	<LLOQ	0.168
33	0.333	0.178	0.267	<LLOQ	<LLOQ	<LLOQ
34	<LLOQ	<LLOQ	<LLOQ	<LLOQ	<LLOQ	<LLOQ
35	1.443	1.219	1.346	0.116	<LLOQ	0.109
36	0.270	0.243	0.162	<LLOQ	<LLOQ	<LLOQ
37	0.644	0.200	0.356	<LLOQ	<LLOQ	<LLOQ
38	0.289	0.133	<LLOQ	<LLOQ	<LLOQ	<LLOQ

TABLE III (continued)
 SERUM LEVELS OF PSA AND FREE PSA MEASURED BY ELISA USING
 SINGLE-STEP PROTOCOLS (60 MG/DAY OR PLACEBO)

Subject	Day 0 PSA (ng/mL)	Day 21 PSA (ng/mL)	Day 42 PSA (ng/mL)	Day 0 free PSA (ng/mL)	Day 21 free PSA (ng/mL)	Day 42 free PSA (ng/mL)
39	<LLOQ	0.405	0.135	<LLOQ	<LLOQ	<LLOQ
40	0.627	0.570	0.605	0.428	0.358	0.299
41	0.690	0.782	0.713	<LLOQ	<LLOQ	<LLOQ
42	0.531	0.605	0.399	<LLOQ	<LLOQ	<LLOQ
43	1.586	1.169	1.260	0.567	0.566	0.587
44	0.333	0.471	0.333	0.133	0.147	0.168
45	<LLOQ	<LLOQ	0.422	<LLOQ	<LLOQ	<LLOQ
46	0.330	0.296	0.104	0.118	0.299	<LLOQ
47	<LLOQ	<LLOQ	0.296	<LLOQ	0.139	<LLOQ
48	3.294	3.588	3.559	0.218	0.223	0.202
49	0.373	0.451	0.510	0.210	0.161	0.154
50	0.104	<LLOQ	0.139	<LLOQ	<LLOQ	<LLOQ
51	4.617	5.408	1.513	0.447	0.382	0.140
52	<LLOQ	0.444	0.222	<LLOQ	<LLOQ	<LLOQ
53	0.289	0.222	<LLOQ	0.161	<LLOQ	<LLOQ
54	1.544	1.504	1.474	0.200	0.174	0.145
55	<LLOQ	<LLOQ	0.118	<LLOQ	<LLOQ	<LLOQ
56	<LLOQ	0.368	N/A ^b	<LLOQ	<LLOQ	N/A
57	<LLOQ	0.174	0.296	<LLOQ	<LLOQ	<LLOQ
58	1.059	0.196	<LLOQ	<LLOQ	<LLOQ	<LLOQ
59	0.667	0.161	0.230	<LLOQ	<LLOQ	<LLOQ
60	<LLOQ	<LLOQ	0.297	<LLOQ	<LLOQ	<LLOQ
61	<LLOQ	<LLOQ	<LLOQ	<LLOQ	<LLOQ	<LLOQ
62	0.139	0.122	<LLOQ	0.118	0.112	<LLOQ
63	<LLOQ	<LLOQ	<LLOQ	<LLOQ	<LLOQ	<LLOQ
64	1.399	1.579	1.149	0.168	0.162	0.122
65	0.378	0.356	<LLOQ	<LLOQ	<LLOQ	<LLOQ
66	1.135	1.135	1.622	<LLOQ	0.105	0.105
67	0.405	0.378	1.324	<LLOQ	<LLOQ	<LLOQ
68	0.874	0.529	0.552	<LLOQ	0.117	<LLOQ
69	0.174	0.191	0.383	<LLOQ	<LLOQ	0.112
70	1.719	1.561	1.469	0.142	0.254	0.208
71	0.598	1.172	N/A	<LLOQ	0.128	N/A
72	0.243	0.378	0.270	<LLOQ	<LLOQ	<LLOQ
73	0.400	1.902	0.822	<LLOQ	0.135	<LLOQ
74	0.255	0.137	0.137	<LLOQ	<LLOQ	0.196
75	0.811	<LLOQ	0.189	<LLOQ	<LLOQ	<LLOQ
76	<LLOQ	<LLOQ	0.270	<LLOQ	<LLOQ	<LLOQ

^a Below the lower limit of quantitation (LLOQ = 0.1 ng/mL).

^b N/A: not available. Subject did not supply blood sample on day 42.

2.5 Conclusions

Randomized controlled trials are the gold standard for evaluating potential therapeutic agents as well as chemopreventive agents. Based on searches of the National Cancer Institute database (<http://www.cancer.gov/clinicaltrials/search>) and National Institutes of Health database (<http://www.clinicaltrials.gov/ct2/search/advanced>) as of Feb, 2013, this prostate cancer prevention trial has been the largest controlled randomized clinical trial to test lycopene. This investigation had the several advantages over previous lycopene trials. First, unlike lycopene or tomato product trials based on food-frequency questionnaires, which are indirect estimates of lycopene levels, this study used a validated LC-MS-MS assay to determine lycopene concentrations in human serum at baseline as well as after supplementation. Second, healthy men instead of men with existing prostate cancer or BPH were recruited for this unique clinical trial, so that evidence of lycopene antioxidant activity is directly relevant for prostate cancer chemoprevention.

In the study, 60 mg/d lycopene supplementation was well tolerated by healthy men, since no side effects were reported. Supplementation with 60 mg/d lycopene for 21 days increased serum concentration 1.52-fold, which was almost identical and definitely not more than the 1.63-fold increase in serum lycopene that we observed in the 30 mg/d arm of this study. This lack of dose-response observed in this study and reported in the literature suggests that serum lycopene concentrations may reach a plateau at a dosage of 30 mg/d and that higher dosages cannot raise serum levels any further.

No significant changes were observed in the urinary levels of the DNA oxidation biomarker 8-oxo-dG and the lipid peroxidation biomarker 8-iso-PGF_{2α} in another arm of our study as a result of lycopene supplementation at 30 mg/d.^[106] However, stronger antioxidant effects were observed in the 60 mg/d lycopene group compared with the 30 mg/d supplementation group. Although these changes remained statistically insignificant, the subtle differences may become more detectable with longer intervention period or trials with larger study populations. In any case, these results confirm that lycopene at the high dose of 60 mg/d does not act as a pro-oxidant.

Serum PSA is being used as a biomarker for prostate cancer screening. Significant decreases of total PSA following 30 mg/d lycopene supplementation was reported by our group^[42] as well as by others. Although we had intended to utilize total PSA and percent free PSA as our intermediate endpoint for the 60 mg/d lycopene study group, the measurements of total PSA and free PSA in serum from this part of the study were unsuccessful due to the insensitivity of currently available ELISA kits. As appropriate assay kits become available, these analyses will be repeated as another measure of lycopene prostate cancer chemoprevention.

3. COLLISION CROSS-SECTION DETERMINATION AND TANDEM MASS SPECTROMETRIC ANALYSIS OF ISOMERIC CAROTENOIDS USING ELECTROSPRAY ION MOBILITY TIME-OF-FLIGHT MASS SPECTROMETRY

3.1 Introduction

Carotenoids consist of carotenes and xanthophylls, which are botanical pigments and antioxidants that may or may not have provitamin A activity.^[118-120] There are more than 600 carotenoids discovered in nature.^[68] Among the most abundant dietary carotenes, β -carotene can be converted to retinol (vitamin A) during intestinal absorption, and lycopene is under investigation as a prostate cancer prevention agent.^[118-120] Oxidized forms of α -carotene and β -carotene, respectively, lutein and zeaxanthin are major dietary xanthophylls.^[121] Although neither of these xanthophylls has provitamin A activity, consumption of lutein and zeaxanthin has been linked to the prevention of age-related macular degeneration.^[69]

Biosynthesized in plants as the all-trans isomers, dietary carotenoids can form multiple cis isomers when exposed to heat or light, and these isomers have been reported to have different bioavailabilities.^[70-72] The planar chemical structures of all-trans-lycopene, all-trans- β -carotene, all-trans-lutein, all-trans-zeaxanthin, and four of their thermodynamically favored cis isomers are shown in Figure 16.

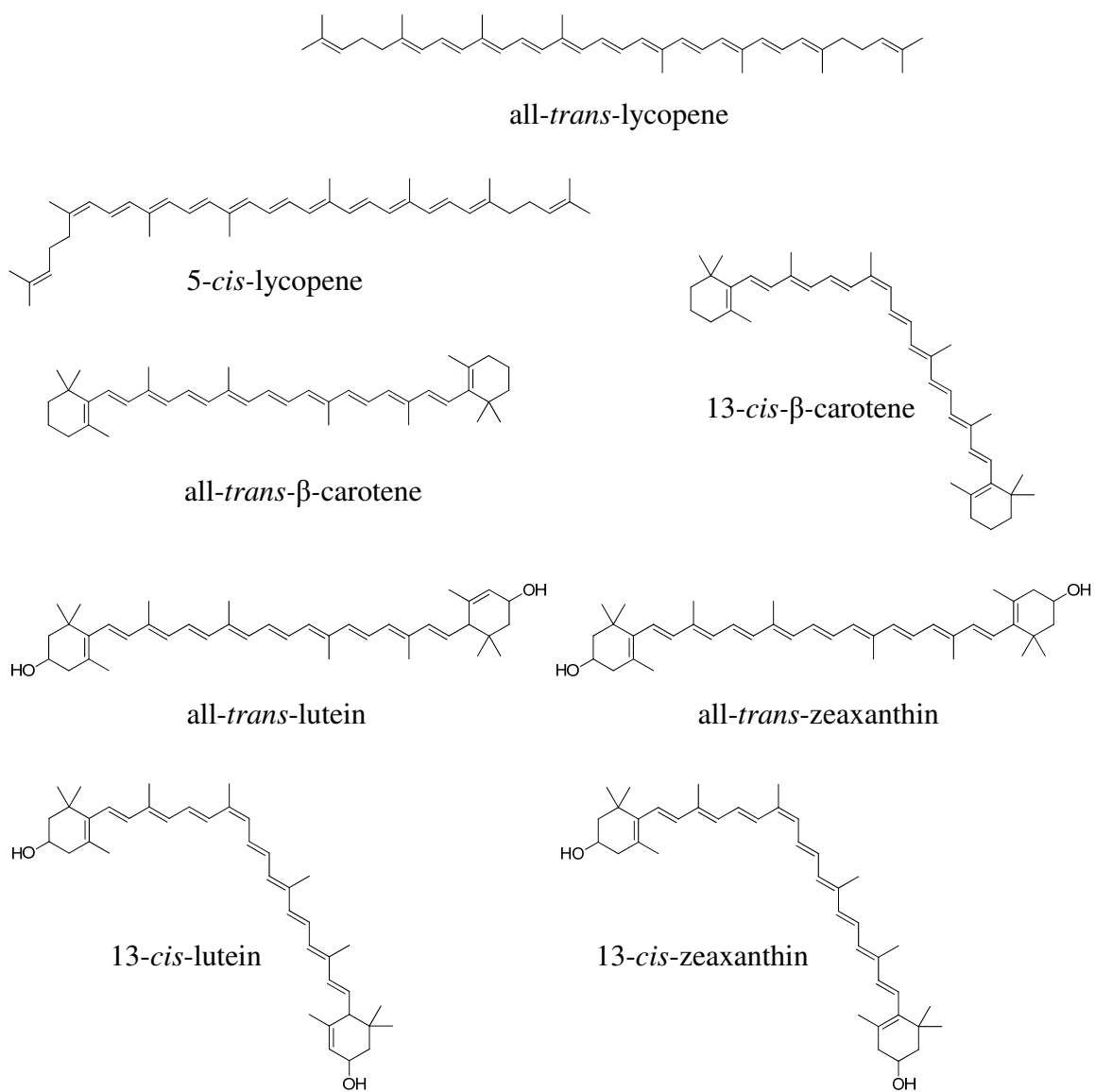


Figure 16. Chemical structures of all-*trans*-lycopene, β -carotene, lutein, zeaxanthin, and their thermodynamically favored *cis* isomers.

Since carotenoids are too thermally labile to be analyzed using GC-MS,^[122-125] HPLC and LC-MS analyses using special C₃₀ stationary phases have become routine for the separation and analysis of their various cis and trans isomers.^[76, 105, 126-130] Effective at resolving geometric isomers of dietary carotenoids in biomedical matrices, carotenoid separations using C₃₀ columns can require up to 90 min per analysis.^[81] Since faster alternatives to chromatography would be most helpful for the analysis of carotenoid isomers in biomedical samples, the feasibility of using IM-MS for this purpose was investigated.

Ion mobility spectrometry is the gas-phase separation of ions in an electric field on the basis of size and shape. When coupled with mass spectrometry, a dimension of high speed separation can be added to mass spectrometric analysis.^[83-85] Because of thermal instability, carotenoids might isomerize during the ionization process. Therefore, the possibility of in-source cis/trans isomerization of carotenoids was also investigated during this study. Geometric isomers of natural products including cis/trans carotenoids have been reported to produce identical tandem mass spectra during collision-induced dissociation and product ion analysis.^[108, 124, 131-133] With the gas phase separation of traveling wave ion mobility on a quadrupole time-of-flight mass spectrometer, we were able to revisit the tandem mass spectrometry of cis/trans carotenoids.

3.2 Materials and methods

3.2.1 Materials

All-*trans* lycopene, all-*trans*- β -carotene and poly-DL-alanine were purchased from Sigma-Aldrich (St. Louis, MO). The isomeric purity of each carotene standard was verified using reversed-phase LC-MS-MS with a YMC (Wilmington, NC) C₃₀ carotenoid

column (4.6×250 mm, 3 μ m) as reported previously.^[105] Working solutions of lycopene and β -carotene were prepared immediately before use from solid standards to minimize isomerization and degradation. Mixtures of cis and trans isomers of each carotene were prepared by dissolving the all-trans forms in methylene chloride in a sealed vial and allowing isomerization to occur during exposure to fluorescent lighting for 24 h.

All-*trans*-lutein and all-*trans*-zeaxanthin were obtained from Carotenature (Lupsingen, Switzerland). Mixture of cis and trans isomers of each of these xanthophylls were prepared through heat-induced isomerization as described in section 3.2.2.5. Methanol, acetonitrile, MTBE, and formic acid (all HPLC grade) and methylene chloride (ACS reagent grade) were purchased from Thermo Fisher (Hanover Park, IL). Deionized water was prepared using a Millipore (Bedford, MA) Milli-Q purification system.

3.2.2 Methods

3.2.2.1 Effect of electrospray on isomerization of lycopene and β -carotene

Positive ion electrospray ion mobility time-of-flight mass spectrometry was carried out using a Waters Synapt HDMS quadrupole time-of-flight hybrid mass spectrometer (Manchester, UK) equipped with TWIMS. All-*trans* lycopene or all-*trans* β -carotene (20 μ g/mL in acetonitrile/MTBE, 1:1, v/v) or mixtures of the respective cis/trans isomers were infused into the ion source at a flow rate of 10 μ L/min. Optimum positive-ion electrospray and ion mobility separation conditions included the following: capillary voltage, 4.0 kV; sampling cone voltage, 26.0 V; extraction cone voltage, 4.0 V; ion source temperature, 100 $^{\circ}$ C; cone gas flow rate, 20 L/h; desolvation gas flow rate, 500 L/h; trap collision energy, 6.0 V; transfer collision energy, 4.0 V; trap gas flow rate,

5.0 mL/min; ion mobility gas flow rate, 20.0 mL/min (~0.45 mBar); wave velocity, 300 m/s; and wave height, ramping from 5.0 V to 12.0 V. The effect of desolvation gas temperature was investigated from 50 to 300 °C with increments of 50 °C. The duty cycle of the time-of-flight mass analyzer was optimized for the analysis of carotenes of m/z 536.4 during data acquisition to maximize signal intensity throughout the range of desolvation gas temperatures. Data were acquired using Waters MassLynx (V4.1) and processed using Waters Driftscope (V2.1) software.

3.2.2.2 Effect of collision-induced dissociation on isomerization of lycopene and β -carotene

All-*trans* lycopene or all-*trans* β -carotene (20 μ g/mL in acetonitrile/MTBE, 1:1, v/v) were infused into the electrospray ion source at 10 μ L/min along with 100 μ L/min methanol as a make-up solvent. The ionization parameters were identical to those described in section 3.2.2.1 except that a capillary voltage of 5 kV and a desolvation gas temperature of 500 °C were applied. The ion mobility conditions included a nitrogen flow of 23 mL/min at ~0.51 mBar, a wave velocity of 300 m/s and a ramping of wave height from 7.0 V to 12.0 V. Positive ion collision-induced dissociation (CID) product ion tandem mass spectra were recorded for molecular ions of the *cis*- and all-*trans*-carotenes of m/z 536.4 exiting from the ion mobility cell. Argon was used as the collision gas at energies of 20, 25, 27.5, 30, 32.5, 35, 37.5, 40, 42.5, or 45 V.

3.2.2.3 LC-MS-IM-CID-Time-of-Flight (TOF) MS of lycopene and β -carotene

A Waters (Milford, MA) 2695 HPLC was interfaced to the Synapt mass spectrometer system, and chromatographic separation of all-*trans* lycopene or all-*trans* β -carotene and their corresponding *cis*-isomers was carried out using a C₃₀ carotenoid column (2.1×250 mm, 3 μ m) with a 45 min step gradient from methanol to MTBE at a flow rate of 0.30 mL/min as follows: 0 min, 65% methanol; 30 min, 40% methanol; and at 35.1 min, 65% methanol. A 20 μ L aliquot of a mixture of lycopene and β -carotene *cis/trans* isomers containing ~95 μ g/mL lycopene and ~50 μ g/mL β -carotene in acetonitrile/MTBE (1:1, v/v) was injected onto the column. With the use of positive ion electrospray ionization, ions of m/z 536.4 were selected and separated by using TWIMS, and CID was carried out in the transfer collision cell at 35 V for lycopene and 40 V for β -carotene. Product ion tandem mass spectra of the molecular ions of lycopene or β -carotene were recorded as well as their HPLC retention times and ion mobility drift times.

3.2.2.4 Collision cross-section measurements of lycopene and β -carotene

The collision cross-sections of lycopene and β -carotene were experimentally determined using the Synapt mass spectrometer system based on the method of Williams *et al.*,^[134] except that poly-DL-alanine was used for calibration instead of tryptic hemoglobin peptides. Poly-DL-alanine (1 mg/mL) was prepared in acetonitrile/0.1% aqueous formic acid (1:1, v/v) and infused into the ion source at 10 μ L/min with 100 μ L/min methanol as a make-up solvent. The electrospray ion source conditions were identical to those used for the CID measurements described above. With the use of the calibration solution, the ion mobility separation parameters were optimized at IMS gas

flow rates of 20 mL/min or 23 mL/min. The optimized ion mobility separation parameters at an IMS gas flow rate of 20 mL/min included a wave velocity of 300 m/s and a ramping wave height from 5.5 V to 12.0 V. For the 23 mL/min IMS gas flow rate, optimized operating conditions included a ramping wave height from 7.0 V to 12.0 V and a wave velocity of 300 m/s. All-*trans* lycopene and all-*trans* β -carotene (20 μ g/mL in acetonitrile/MTBE, 1:1, v/v) were each infused and analyzed using the optimized conditions. A programmable dynamic range enhancement lens was used for the response adjustment of poly-DL-alanine when necessary. Based on the collision cross-section values of poly-DL-alanine molecules in the literature,^[135] TWIMS calibration curves were plotted for each IMS gas pressure and wave height combination, and the collision cross-sections of lycopene and β -carotene isomers were determined using Driftscope software.

The theoretical collision cross-section values of all *trans*-lycopene, 5-*cis*-lycopene, all *trans*- β -carotene, and 13-*cis*- β -carotene were determined using the Tripos (St. Louis, MO) molecular modeling program Sybyl-X (ver. 1.1.1). The minimum and maximum diameters of each molecule were determined at different molecular orientations, and the mean of these values was determined to estimate each collision cross-section.

3.2.2.5 Effect of electrospray on isomerization of lutein and zeaxanthin

All-*trans* lutein or all-*trans* zeaxanthin (20 μ g/mL in acetonitrile/MTBE, 1:1, v/v) were infused into the ion source at a flow rate of 10 μ L/min. Optimum positive-ion electrospray and ion mobility separation conditions included the following: capillary voltage, 4.0 kV; sampling cone voltage, 25.0 V; extraction cone voltage, 4.0 V; ion

source temperature, 100 °C; cone gas flow rate, 20 L/h; desolvation gas flow rate, 500 L/h; trap collision energy, 6.0 V; transfer collision energy, 4.0 V; trap gas flow rate, 1.5 mL/min; ion mobility gas flow rate, 32.0 mL/min (~0.66 mBar); wave velocity, 300 m/s; and wave height, ramping from 6.0 V to 22.0 V. The effect of desolvation gas temperature was investigated from 50 to 300 °C with increments of 50 °C. The duty cycle of the time-of-flight mass analyzer was optimized for the analysis of xanthophylls of m/z 568.4 during data acquisition to maximize signal intensity throughout the range of desolvation gas temperatures.

3.2.2.6 Collision cross-section measurements of lutein and zeaxanthin

The collision cross-sections of lutein and zeaxanthin were experimentally determined using the method described in section 3.2.2.4. However, the ion mobility separation parameters were optimized at IMS gas flow rates of 32 mL/min for lutein and zeaxanthin. The optimized ion mobility separation parameters at an IMS gas flow rate of 32 mL/min included a wave velocity of 300 m/s and a ramping wave height from 7.0 V to 20.0 V. All-*trans*-lutein and all-*trans*-zeaxanthin (5 µg/mL in acetonitrile/MTBE, 1:1, v/v) were each infused to the ion source at 10 µL/min with 100 µL/min methanol as the make-up solvent and analyzed using the optimized conditions with poly-DL-alanine serving as the calibrant. The theoretical collision cross-section values of all-*trans*-lutein, 13-*cis*-lutein, all- *trans*-zeaxanthin, and 13-*cis*-zeaxanthin were estimated as described in section 3.2.2.4.

3.2.2.7 LC-MS-IM-CID-Time-of-Flight (TOF) MS of lutein and zeaxanthin

To prepare adequate amount of *cis*-lutein and *cis*-zeaxanthin for LC-MS-IM-CID-TOFMS experiments, 200 µg all-*trans*-lutein or all-*trans*-zeaxanthin was dissolved in 2 mL MTBE/methanol (1:9, v/v) and isomerized at 80 °C for 1 h using a heating block. Each of these *cis*/*trans* isomeric mixtures was injected onto the YMC C₃₀ column (2.1 x 250 mm, 3 µm) for pre-separation prior to the IM-MS analysis using the Synapt mass spectrometer system. Chromatographic separation of all-*trans*-lutein or all-*trans*-zeaxanthin and their corresponding *cis*-isomers was achieved in 15 min using 0.30 mL/min isocratic MTBE/methanol (15:85; v/v) containing 17 mM ammonium acetate as the mobile phase.^[136] The levels of major *cis* and *trans* isomers of the xanthophylls were determined using HPLC-UV analysis of zeaxanthin at 450 nm and lutein at 444 nm.^[137]

Optimum positive-ion electrospray and ion mobility separation conditions for lutein and zeaxanthin included the following: capillary voltage, 4.0 kV; sampling cone voltage, 25.0 V; extraction cone voltage, 4.0 V; ion source temperature, 110 °C; desolvation gas temperature, 500 °C; cone gas flow rate, 20 L/h; desolvation gas flow rate, 500 L/h; trap collision energy, 6.0 V; transfer collision energy, 40 V; trap gas flow rate, 5.0 mL/min; ion mobility gas flow rate, 32.0 mL/min (~0.66 mBar); wave velocity, 300 m/s; and wave height, ramping from 7.0 V to 15.0.

3.3 Results and Discussion

The isomeric purities of the all-*trans*-lycopene and all-*trans*-β-carotene standards in freshly prepared solutions were ≥92% as indicated by HPLC with mass spectrometric

detection of the molecular ions of m/z 536.4, which comprised the base peak of each mass spectrum. The light-isomerized carotenoid solutions were analyzed using LC-MS, and the cis/all-trans ratios were 62%/38% and 14%/86% for lycopene and β -carotene, respectively. The isomeric carotene mixtures were infused into the electrospray ion source to facilitate tuning of the ion mobility separation conditions. IMS flow rates ranging from 5-28 mL/min were investigated for analysis of lycopene and β -carotene, and the best results were obtained at 20 mL/min. The optimum wave velocity was 300 m/s, although variations in the wave velocity produced small changes in carotene isomer separation during IM-MS. The height of the traveling wave had the most impact on the ion mobility separation of carotene isomers, and ramping the wave height from 5 V to 12 V produced the best ion mobility separations.

As shown in Figure 17A, two lycopene peaks were observed during IM-MS with drift times differing by 3.6 ms for the isomers of m/z 536.4. Presumably, the first peak consisted of a mixture of cis isomers, and the linear all-trans isomer was detected as the second peak. To confirm which peak corresponded to the all-trans isomer, a fresh solution of all-*trans* lycopene was infused into the electrospray ion source. Instead of one peak corresponding to the all-trans isomer, two peaks were observed in the same ratio and with the same drift times as those observed for the isomeric lycopene mixture (Figure 17B). Similar results were obtained for the cis and trans isomers of β -carotene. This suggested that in-source isomerization of carotenes was occurring prior to ion mobility separation.

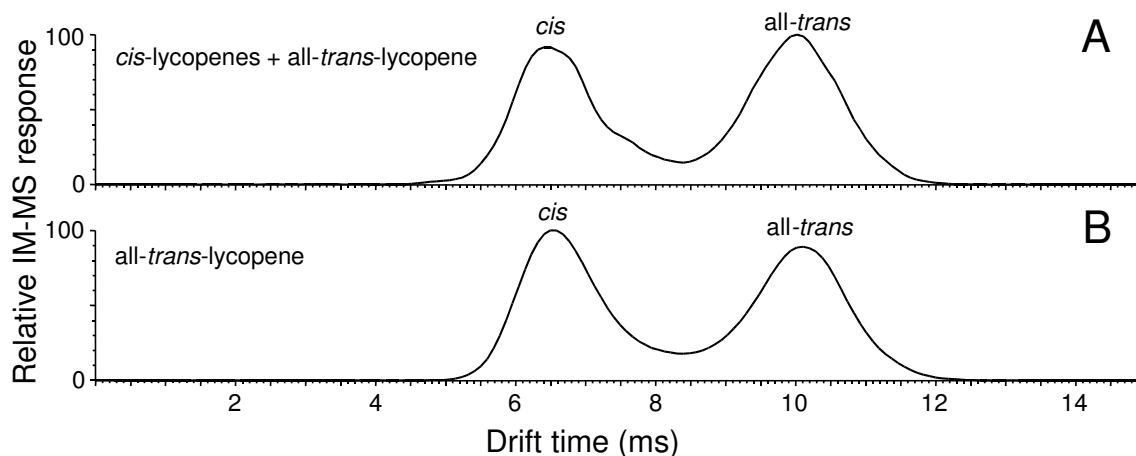


Figure 17. Positive ion electrospray IM-MS drift time distributions of the M^+ ions of m/z 536.4 corresponding to *cis* (peak 1) and *all-trans* (peak 2) isomers of lycopene after infusion of (A) *cis/trans*-lycopene mixture (38/62); and (B) *all-trans*-lycopene. Note that isomerization occurred during electrospray so that the same *cis/trans* isomer ratio was observed for each lycopene sample. Reprinted with permission from Linlin Dong *et al.*^[138] Copyright (2010) American Chemical Society.

To make certain that isomerically pure *cis*-lycopenes and *cis*- β -carotenes were entering the ion source, C_{30} chromatographic separation of the *cis/trans* isomeric mixtures was carried out on-line with IM-MS (LC-IM-MS), and the ion mobility drift time spectra were recorded for various *cis*-isomers as well as the *all-trans* isomers of lycopene and β -carotene. The molecular ions of m/z 536.4 for each chromatographically resolved carotene isomer were analyzed using LC-IM-MS, and two peaks were observed for each carotene (Figures 18 and 19). These peaks were in the same *cis/trans* ratios as had been observed during infusion of mixtures of *cis* and *trans* isomers of β -carotene (Figure 18) or lycopene (Figure 19). Regardless of the *cis/trans* ratio of lycopene or β -carotene entering

the electrospray ion source, a constant ratio of isomers was formed in the source and detected using IM-MS.

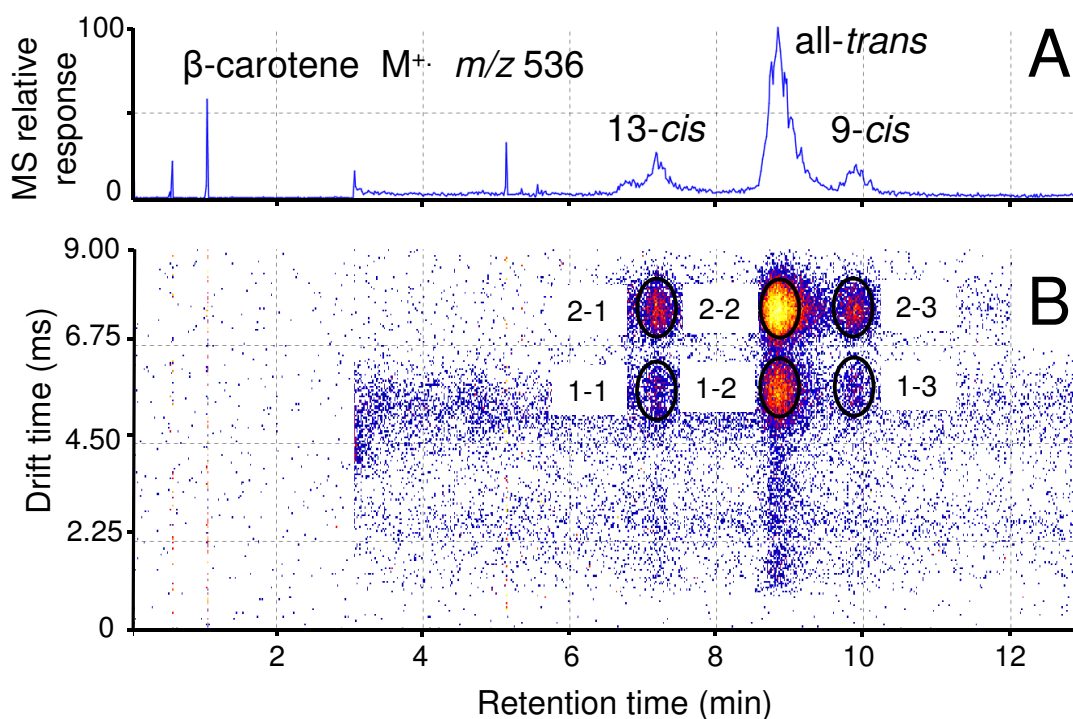


Figure 18. LC-IM-MS analysis of a mixture of β -carotene isomers using a C_{30} carotenoid HPLC column, positive ion electrospray and ion mobility separation prior to mass spectrometric detection. (A) LC-MS chromatogram showing β -carotene molecular ions of m/z 536.4 for each geometric isomer; (B) 2D map showing ion mobility drift time (y) vs. HPLC retention time (x). Ion mobility separation of molecular ions formed from 13-*cis*- β -carotene (retention time 7.2 min), 9-*cis*- β -carotene (retention time 9.9 min) and all-*trans*- β -carotene (retention time 8.8 min) indicated that all three species had isomerized in the ion source to form similar ratios of *cis*- β -carotenes (1-1, 1-2, 1-3) and all-*trans*- β -carotene (2-1, 2-2, 2-3). Reprinted with permission from Linlin Dong et al.^[138] Copyright (2010) American Chemical Society.

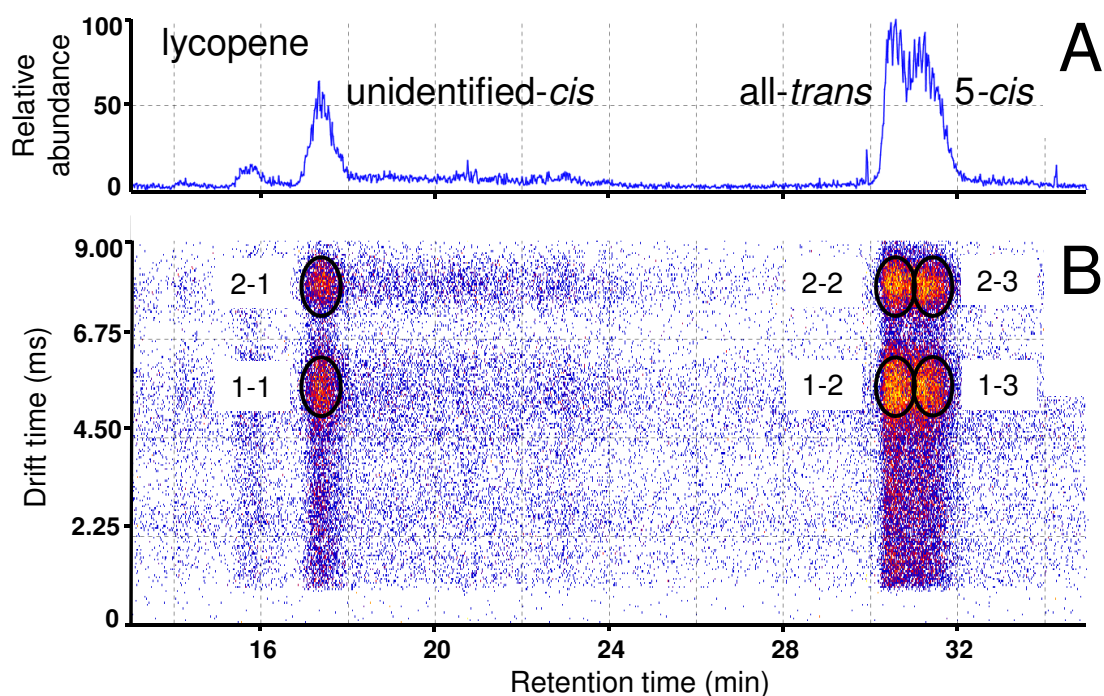


Figure 19. C_{30} carotenoid column HPLC separation of lycopene geometrical isomers with on-line positive ion electrospray IM-MS analysis. (A) LC-MS chromatogram showing detection of molecular ions of lycopene geometrical isomers of m/z 536.4; (B) 2D map showing ion mobility drift time (y) vs. HPLC retention time (x). Ion mobility separation of molecular ions formed from *cis*-lycopenes (HPLC retention times of 17.3 min and 31.2 min) and all-*trans*-lycopene (HPLC retention time of 30.5 min) indicated that all three species had isomerized in the ion source to form similar ratios of *cis*-lycopenes (1-1, 1-2, 1-3) and all-*trans*-lycopene (2-1, 2-2, 2-3). Reprinted with permission from Linlin Dong *et al.* ^[138] Copyright (2010) American Chemical Society.

Cis/trans isomerization of carotenoids is known to occur easily upon exposure to heat or light,^[76, 123, 124, 130] but the process of molecular ion formation during electrospray might also contribute to cis/trans isomerization, especially since abstraction of a π -electron is likely to occur. Thermal isomerization to an equilibrium of cis/trans carotene isomers in the electrospray source might explain, at least in part, the mixture of isomers of m/z 536.4 for lycopene or β -carotene detected using IM-MS and LC-IM-MS

regardless of the isomeric purity of the compound entering the ion source. To test this thermal isomerization hypothesis, the temperature of the desolvation gas used during electrospray was varied from 50 °C to 300 °C during sample infusion (note that desolvation gas temperatures below 50 °C or above 300 °C did not produce stable electrospray), and the relative amounts of cis and all-trans isomers were determined at each temperature using IM-MS. As shown by the drift time distributions in Figure 20 and the graphs in Figure 21, the relative abundance of the first ion mobility peak compared with the second peak increased as the temperature in the ion source was increased. This observation is consistent with the hypothesis that the first peak in each drift time spectrum (Figures 17-20) corresponds to the higher energy cis isomers, and the second IM-MS peak is the thermodynamically more stable all-trans isomer ^[72, 139].

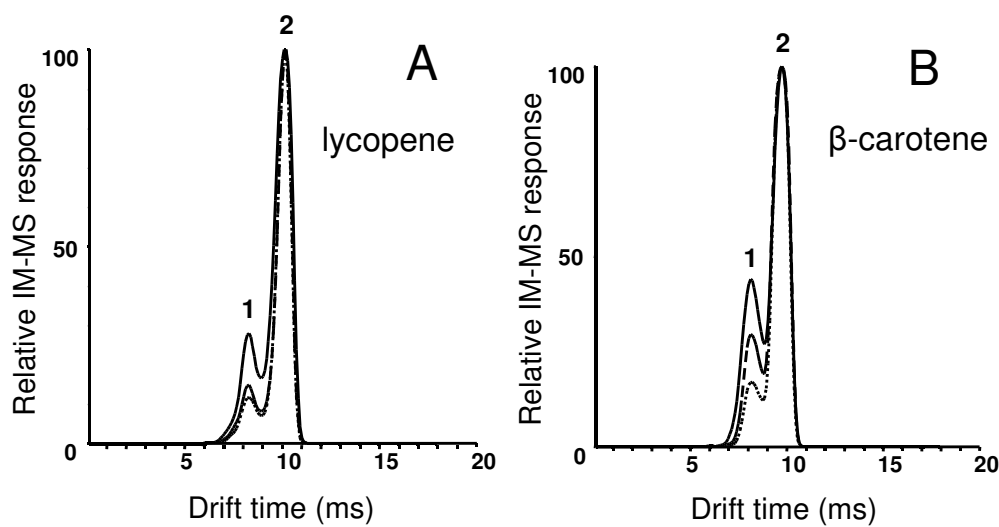


Figure 20. Effect of electro spray desolvation gas temperature on the abundances of cis (peak 1) and all-trans isomers (peak 2) of (A) lycopene; and (B) β -carotene following infusion of the all-trans isomer. Drift time spectra were acquired using positive ion electro spray mass spectrometry with detection of the molecular ions of m/z 536.4. (100 °C, dotted line; 200 °C, dashed line; 300 °C, solid line) *Reprinted with permission from Linlin Dong et al.* ^[138] Copyright (2010) American Chemical Society.

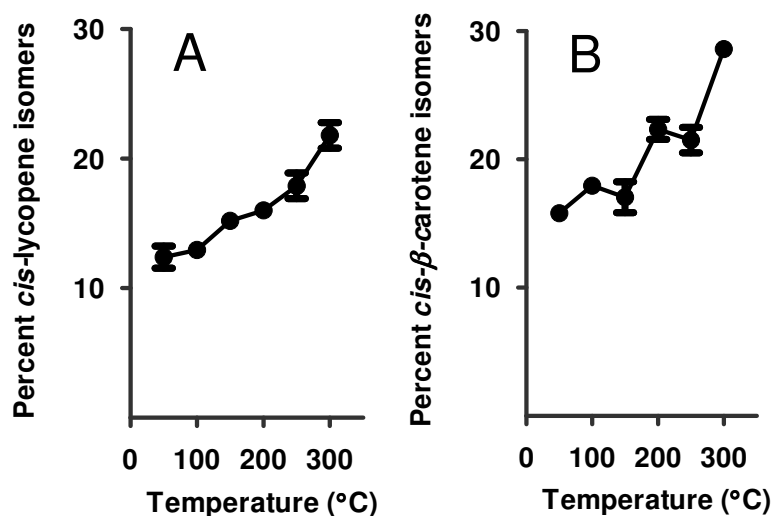


Figure 21. Relative abundances of cis isomers (peak 1 in Figure 20) and total (cis plus all-trans) isomers as a function of desolvation gas temperature for (A) lycopene; and (B) β -carotene. Reprinted with permission from Linlin Dong et al.^[138] Copyright (2010) American Chemical Society.

The collision cross-section, which characterizes the shape and conformation of a molecule in the gas phase, is proportional to the mobility of an ion during IM-MS.^[85, 140, 141] Two TWIMS calibration curves were generated by using Driftscope software for each IMS gas pressure and wave height combination. The calibration curves were $y = 192.65x^{0.6796}$ ($r^2=1.000$) and $y = 189.33x^{0.6890}$ ($r^2=1.000$) at IMS gas flow rates of 20 and 23 mL/min, respectively. The collision cross-section values of the cis and all-trans isomers of lycopene and β -carotene were determined using the standard curves, and the results are summarized in Table IV. Theoretical collision cross-sections were calculated for the all-trans isomers and some of the most abundant cis isomers of lycopene and β -carotene, and these results are shown in Table IV. Representative drift time spectra of lycopene and β -carotene using poly-DL-alanine as the calibrant are shown in Figure 22.

TABLE IV
COLLISION CROSS-SECTION (CCS) VALUES OF GEOMETIC ISOMERS OF
LYCOPENE AND β -CAROTENE

Compound	IMS gas flow (mL/min)	Experimental CCS ^a (\pm S.D.), Å ²		Theoretical CCS, Å ²	
Lycopene	20	cis ^b	180.2 \pm 1.1	5- <i>cis</i>	232
		all-trans ^c	236.2 \pm 0.9	all- <i>trans</i>	268
	23	cis ^b	179.0 \pm 0.1		
		all-trans ^c	235.4 \pm 0.4		
β -Carotene	20	cis ^b	180.7 \pm 2.3	13- <i>cis</i>	125
		all-trans ^c	224.7 \pm 0.1	all- <i>trans</i>	239
	23	cis ^b	177.8 \pm 3.5		
		all-trans ^c	224.4 \pm 0.8		

^a The classical equation for CCS calculation was applied in Driftscope software with modifications as described by Williams *et al.* [134].

$$\Omega = [(18\pi)^{0.5}/16] [ze/(k_bT)^{0.5}](1/m_{ion} + 1/m_{gas})^{0.5} (NK)^{-1}$$

Ω : the CCS of an analyte ion;

z : the number of charges on the analyte ion;

e : the charge on an electron;

k_b : Boltzmann constant;

T : temperature (K);

m_{ion} : molecular mass of the analyte ion;

m_{gas} : molecular mass of the IMS gas;

N : the number density of the IMS gas;

K : the mobility of analyte ion.

^b First IM-MS peak, shorter drift time (mixture of cis isomers)

^c Second IM-MS peak, longer drift time (all-trans isomer)

Reprinted with permission from Linlin Dong et al. [138] Copyright (2010) American Chemical Society.

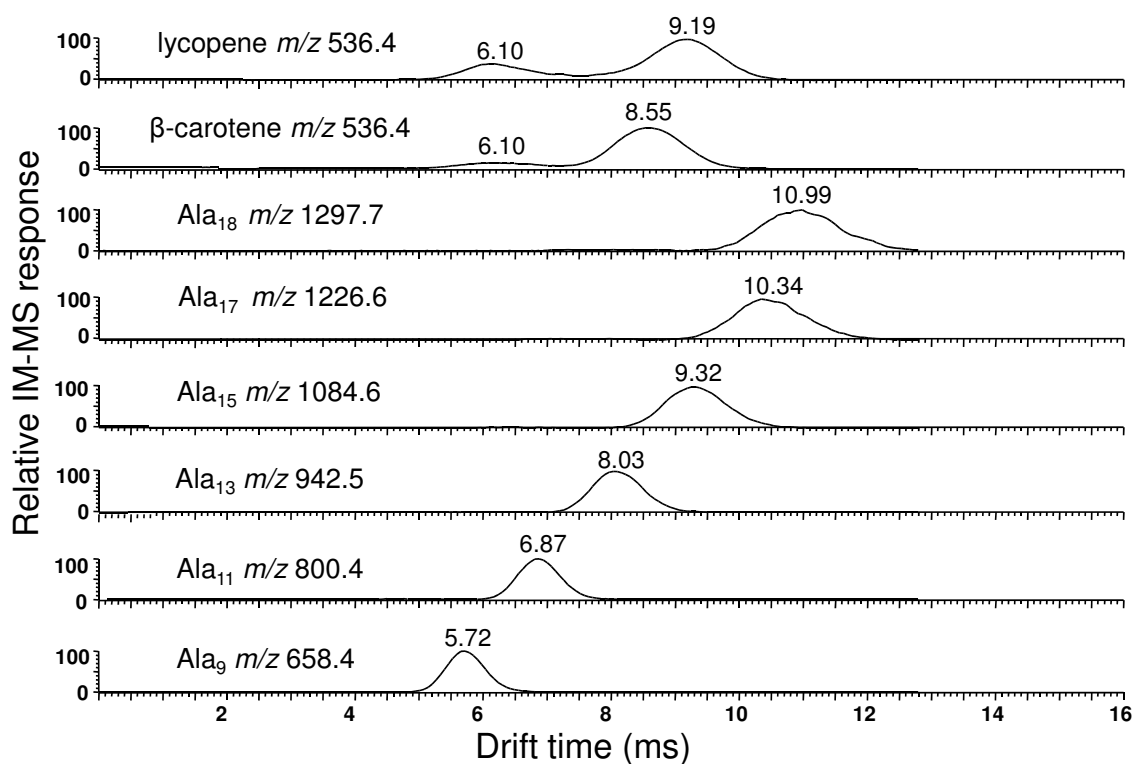


Figure 22. Ion mobility separations of poly-DL-alanine, lycopene and β -carotene under identical TWIMS conditions. The IMS gas flow rate was 23 mL/min. (Ala_n = poly-DL-alanine with n residues). Reprinted with permission from Linlin Dong et al.^[138] Copyright (2010) American Chemical Society.

As indicated in Table IV, the lycopene isomers showed larger collision cross-sections than did the corresponding β -carotene peaks. Since lycopene and β -carotene are structural isomers, this difference was probably due to the acyclic, elongated structure of lycopene compared to the cyclic, β -ionone rings of β -carotene (Figure 16). The more compact cis isomers of each carotene probably produced the first peak during IM-MS, and the all-trans isomer should have a longer drift time corresponding to the second peak. The measured collision cross-section of the cis isomers and the all-trans isomer of lycopene were 180 \AA^2 and 236 \AA^2 , respectively. For β -carotene, the measured collision cross-sections of the cis and all-trans isomers were 181 \AA^2 and 225 \AA^2 , respectively. The IMS gas flow rate of 23 mL/min produced slightly smaller collision cross-section values for both sets of isomers than did the 20 mL/min flow rate suggesting that carotenes become more compact as the IMS gas flow rate and pressure increases.

The theoretical collision cross-section values of lycopene and β -carotene were similar in magnitude to the measured values (Table IV). As expected, the β -carotene values were smaller than the corresponding lycopene values due to the presence of β -ionone rings in β -carotene, and the cis isomers had smaller collision cross-section values than did the corresponding all-trans isomers. For example, the theoretical collision cross-section of all-*trans*- β -carotene was 239 \AA^2 compared with the larger value of 268 \AA^2 for the acyclic all-*trans*-lycopene. Although IM-MS measurements could be made only on mixtures of cis isomers, theoretical collision cross-section values could be calculated for specific cis isomers. As an example of a carotene with a cis double bond located near one terminus, the collision cross-section of 5-*cis*-lycopene (Figure 16) was

determined to be 232 \AA^2 which was slightly smaller than that of all-*trans*-lycopene (Table IV). In contrast, the collision cross-section of 13-*cis*- β -carotene was only 125 \AA^2 compared with the all-*trans* isomer value of 239 \AA^2 due to the central location of the *cis* double bond in this isomer (Figure 16).

Previously, we reported that the product ion tandem mass spectra of *cis* and all-*trans* isomers of a particular carotenoid were identical, either because CID cannot produce distinguishing fragmentation of *cis/trans* isomers or because isomerization occurred during ionization, CID or at both steps of the analysis.^[124] Since IMS can separate *cis* and *trans* carotene ions after the ionization process, the use of IM-MS-MS provided an opportunity to determine if carotene geometrical isomers can be distinguished based on their fragmentation patterns produced during CID. The positive ion electrospray IM-MS-MS spectra of the *cis* and all-*trans* isomers of lycopene are shown in Figure 23. Although both geometrical isomers formed product ions of identical masses, the relative abundances of these ions varied considerably. All-*trans*-lycopene (drift time 8.0 ms) fragmented much more extensively than did the *cis*-lycopene isomers (drift time 5.5 ms). The base peak in the tandem mass spectrum of all-*trans*-lycopene corresponded to an ion of m/z 69 which was formed by the loss of a terminal isoprene group (measured m/z 69.0706, theoretical m/z 69.0704; C_5H_9 ΔM 2.9 ppm), whereas the base peak of the *cis* isomers was the molecular ion of m/z 536 (measured m/z 536.4405, theoretical m/z 536.4382; $\text{C}_{40}\text{H}_{56}$ ΔM 4.3 ppm). An abundant ion of m/z 69 was observed in the tandem mass spectrum of *cis*-lycopenes at a relative abundance of 76% (measured m/z 69.0706, theoretical m/z 69.0704; C_5H_9 ΔM 2.9 ppm), and the molecular ion of

all-*trans*-lycopene was observed at a relative abundance of only 4% (measured m/z 536.4405, theoretical m/z 536.4382; $C_{40}H_{56}$ ΔM 4.3 ppm).

Another feature that distinguished the IM-MS-MS spectra of geometrical isomers of lycopene was the product ion of m/z 467 (measured m/z 467.3663, theoretical m/z 467.3678; $C_{35}H_{47}$ ΔM -3.2 ppm), formed by the elimination of a terminal isoprene moiety,^[142] which was observed at a relative abundance of 91% in the tandem mass spectrum of the *cis* isomers but at only 17% abundance in the tandem mass spectrum of all-*trans*-lycopene (Figure 23). The ion of m/z 444 which corresponds to the elimination of toluene^[142] was observed in the tandem mass spectrum of all-*trans*-lycopene (measured m/z 444.3765, theoretical m/z 444.3756; $C_{33}H_{48}$ ΔM 2.0 ppm) but not in the tandem mass spectrum of the *cis*-lycopenes. Ions of m/z 521 (measured m/z 521.4144, theoretical m/z 521.4147; $C_{39}H_{53}$ ΔM -0.6 ppm) and m/z 493 (measured m/z 493.3883, theoretical m/z 493.3834; $C_{37}H_{48}$ ΔM 9.9 ppm) which correspond to losses of methyl and propyl radicals, respectively, were observed only in the tandem mass spectrum of the *cis*-lycopene isomers.

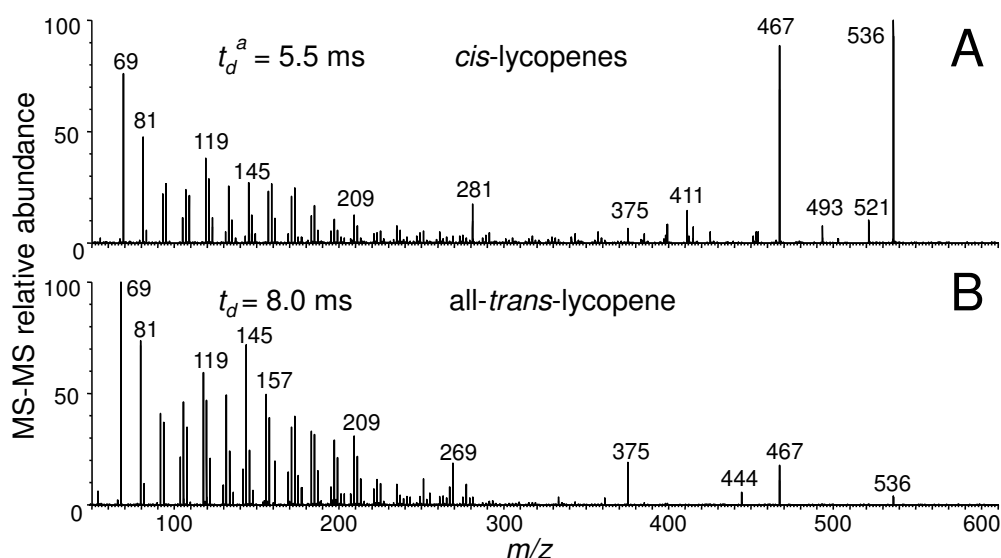


Figure 23. Positive ion electrospray IM-MS-MS CID spectra of the M^+ ions of m/z 536 corresponding to (A) *cis*-lycopenes (ion mobility peak 1); and (B) *all-trans*-lycopenes (ion mobility peak 2). ^a t_d = drift time. Reprinted with permission from Linlin Dong et al.^[138] Copyright (2010) American Chemical Society.

The *cis* and *all-trans* isomers of lycopene may be distinguished during IM-MS-MS based on their different drift times (*all-trans*-lycopenes showed the longest drift time) and by the relative abundances of fragment ions of m/z 467, m/z 521 and m/z 493 (*cis*-lycopenes) and m/z 444 (*all-trans*-lycopenes). The M^+ ions of *cis*-lycopenes fragment during collision-induced dissociation to form product ions of m/z 521 and m/z 493 whereas *all-trans*-lycopenes either does not form these ions or produces them at much lower relative abundances. Furthermore, *cis*-lycopenes fragment during MS-MS to form an abundant ion of m/z 467 (91%) whereas the ion of m/z 467 in the tandem mass spectrum of *all-trans*-lycopenes is detected at more than 5-fold lower abundance (17%).

Therefore, the detection of ions of m/z 521 and m/z 493 and an abundant ion of m/z 467 in the IM-MS-MS spectrum of lycopene is characteristic of *cis*-lycopenes. The absence of ions of m/z 521 and m/z 493 in the IM-MS-MS spectrum of lycopene along with the detection of an ion of m/z 444, which is absent from the product ion tandem mass spectrum of *cis*-lycopene, would be characteristic of all-*trans*-lycopene.

To determine if the *cis* and all-*trans* isomers of β -carotene could be distinguished using IM-MS-MS, the positive ion tandem mass spectra of β -carotene isomers were obtained and are shown in Figure 24. The base peak of the tandem mass spectrum of all-*trans*- β -carotene was observed at m/z 444 and corresponded to the loss of toluene (measured m/z 444.3756, theoretical m/z 444.3756; $C_{33}H_{48}$ ΔM 0 ppm). Since the ion of m/z 444 was observed at a relative abundance of only 11% in the tandem mass spectrum of the β -carotene *cis* isomers, the relative abundance of this ion may be used to distinguish the *cis* and all-*trans* β -carotene isomers. The base peak of the tandem mass spectrum of the *cis*- β -carotenes was the molecular ion of m/z 536 (measured m/z 536.4378, theoretical m/z 536.4382; $C_{40}H_{56}$ ΔM -0.7 ppm). Although the *cis* isomers of β -carotene did not fragment as extensively as did all-*trans*- β -carotene, the ion of m/z 521 formed by the loss of a methyl radical (measured m/z 521.4119, theoretical m/z 521.4147; $C_{39}H_{53}$ ΔM -5.4 ppm) was more abundant in the tandem mass spectrum of the *cis*- β -carotenes. In the IM-MS-MS analyses of the lycopene and β -carotene isomers, the ion of m/z 444 was more abundant in the tandem mass spectra of the all-*trans* isomers, and the ion of m/z 521 was more abundant in the tandem mass spectra of the *cis* isomers.

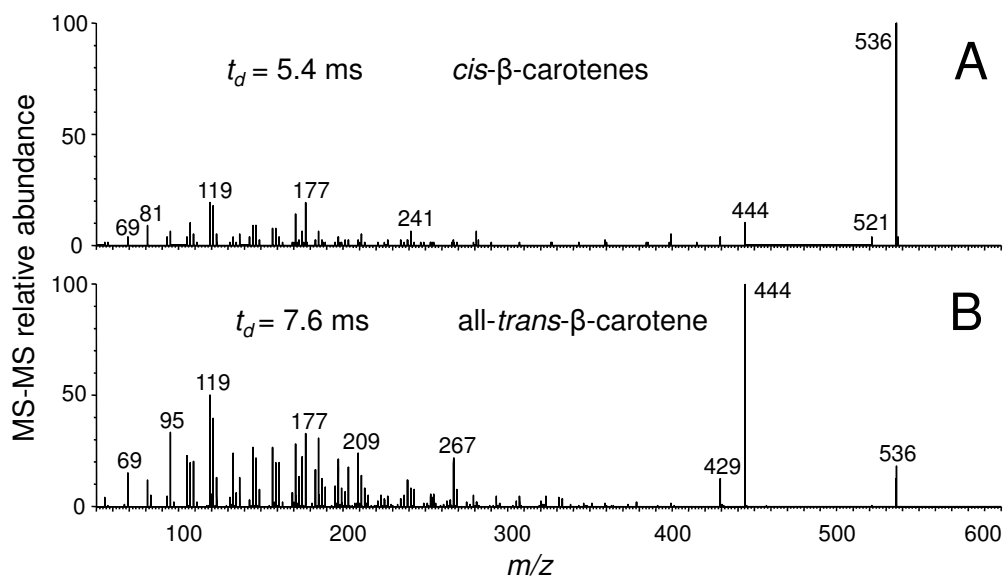


Figure 24. Positive ion electrospray IM-MS-MS with CID of (A) *cis*- β -carotenes; and (B) *all-trans*- β -carotene. Note the relative abundances of m/z 444 and m/z 536 in the tandem mass spectra which distinguish the *cis* isomers from the *all-trans*- β -carotene. Reprinted with permission from Linlin Dong et al.^[138] Copyright (2010) American Chemical Society.

A similar series of LC-MS-IM-CID-TOFMS experiments were carried out to determine whether xanthophylls also isomerize during electrospray and can be separated and distinguished based on their drift times and tandem mass spectra. Firstly, heat-induced isomerization was employed to generate *cis* isomers from *all-trans*-lutein and *all-trans*-zeaxanthin. As shown in Figures 25 and 26, *cis* isomers, especially the 13-*cis* isomer of lutein and zeaxanthin, were formed during thermal treatment. By using USP Normalization Procedure for chromatography, it was found that the level of 13-*cis*-zeaxanthin increased from 1.0% to 13.1%, whereas the level of 13-*cis*-lutein increased from 0.5% to only 3.8% during thermal isomerization (Figures 25 and 26). Substantially greater proportion of 13-*cis*-zeaxanthin was formed during the heat treatment compared to the amount of 13-*cis*-lutein produced (12.1% vs 3.3%). One possible

explanation for this difference is that the fully conjugated 13-*cis* zeaxanthin is more stable and less susceptible to reverse isomerization than *cis*-luteins.

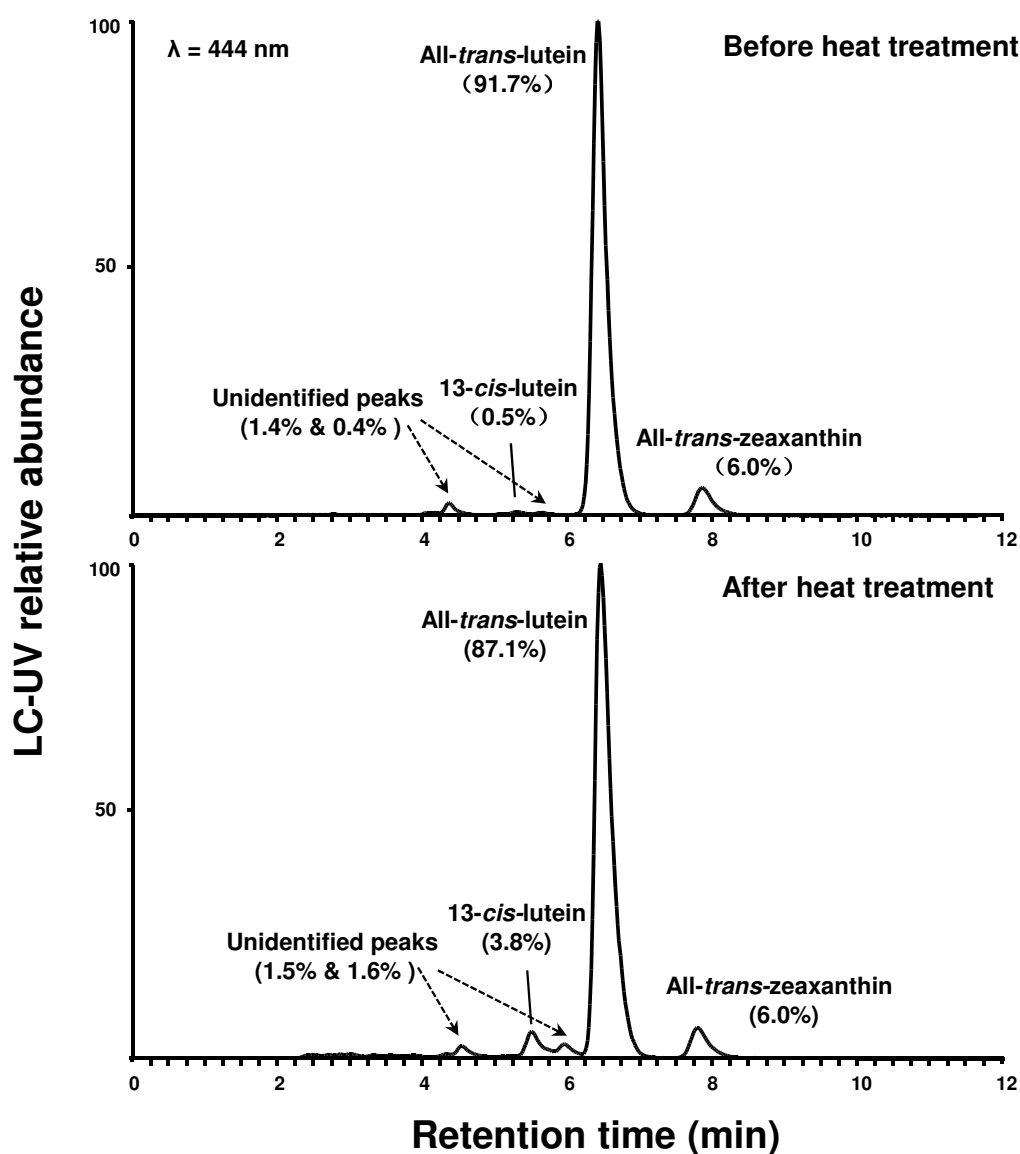


Figure 25. C₃₀ reversed-phase HPLC-UV analysis of the 13-*cis* lutein levels in a lutein standard solution before and after the heated-induced isomerization process using USP Normalization Procedure for chromatography.

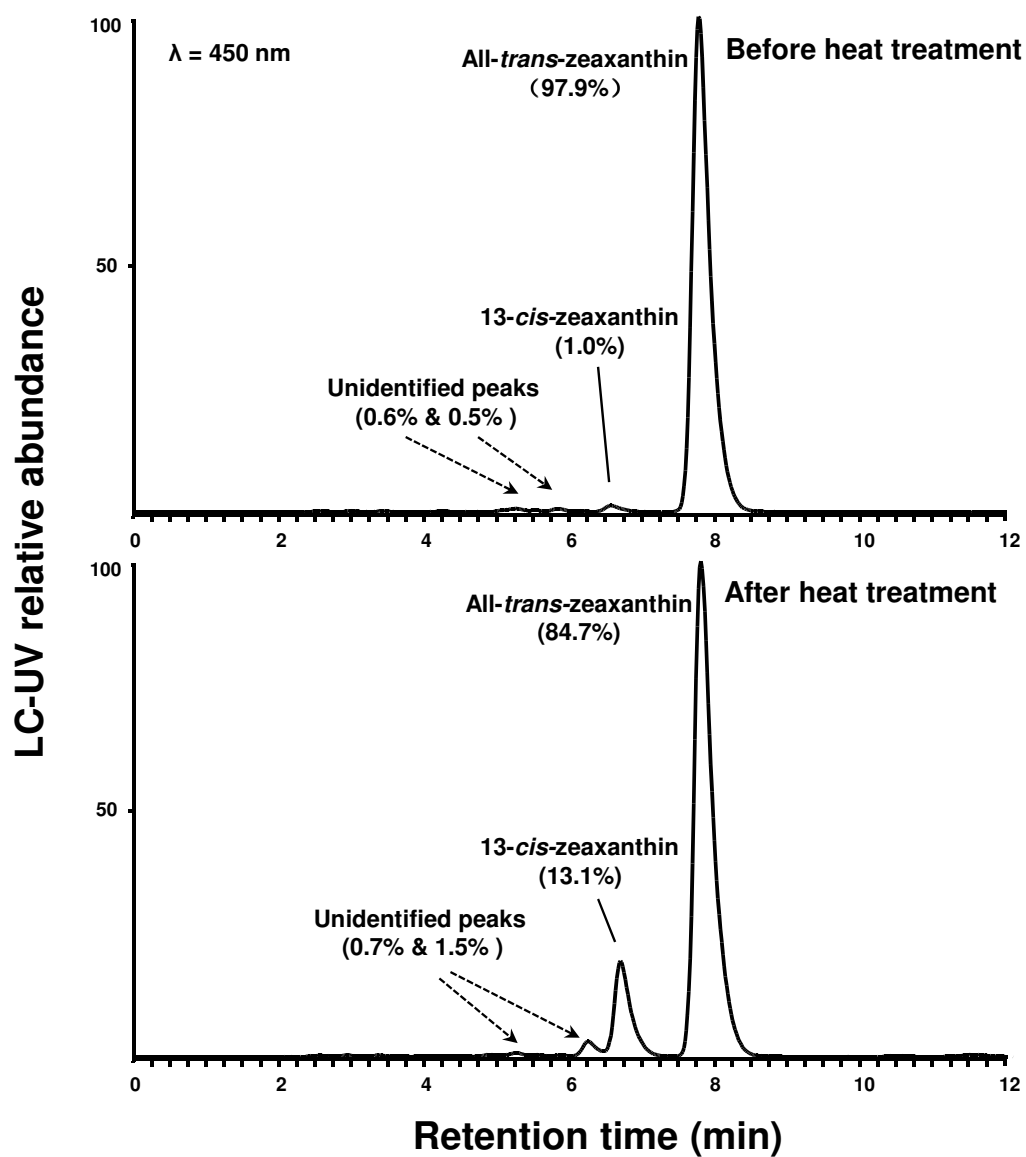


Figure 26. C_{30} reversed-phase HPLC-UV analysis of the 13-*cis* zeaxanthin levels in a zeaxanthin standard solution before and after the heated-induced isomerization process using USP Normalization Procedure for chromatography.

C₃₀ chromatographic separations of the cis/trans isomeric mixtures of lutein and zeaxanthin were then carried out online during IM-MS as shown in Figures 27 and 28, respectively. One concern to this particular study was that the synthesized zeaxanthin sample was pure, but the lutein sample isolated from plants still containing 6.0% all-*trans*-zeaxanthin (Figures 25 and 27). Assuming approximately 12% all-*trans*-zeaxanthin could be converted to 13-*cis*-zeaxanthin during the thermal treatment, the lutein sample would probably contain 0.72% 13-*cis*-zeaxanthin after the isomerization. Although 13-*cis*-zeaxanthin (Figure 26, retention time 6.6 min) cannot be resolved from all-*trans*-lutein (Figure 25, retention time 6.5 min, 87.1%) chromatographically using this particular method, it only counts for 0.008% of the all-*trans*-lutein peak. Therefore, it may be speculated that trace amount 13-*cis*-zeaxanthin in the heat processed lutein sample will not complicate the following analysis using IM-MS. During ion mobility MS, two peaks were partially resolved at 8.9 ms and 12.4 ms which represented separation of cis/trans isomers of lutein (Figure 27B) and at 9.1 ms and 12.6 ms for zeaxanthin (Figure 28B), respectively. Since these peaks were observed in the same cis/trans ratio for 13-*cis*-lutein (1-1 vs 2-1), all-*trans*-lutein (1-2 vs 2-2), 13-*cis*-zeaxanthin (1-3 vs 2-3), and all-*trans*-zeaxanthin (1-4 vs 2-4), in-source isomerization of lutein and zeaxanthin also occurred during positive ion electrospray as observed previously for lycopene and β -carotene.^[138]

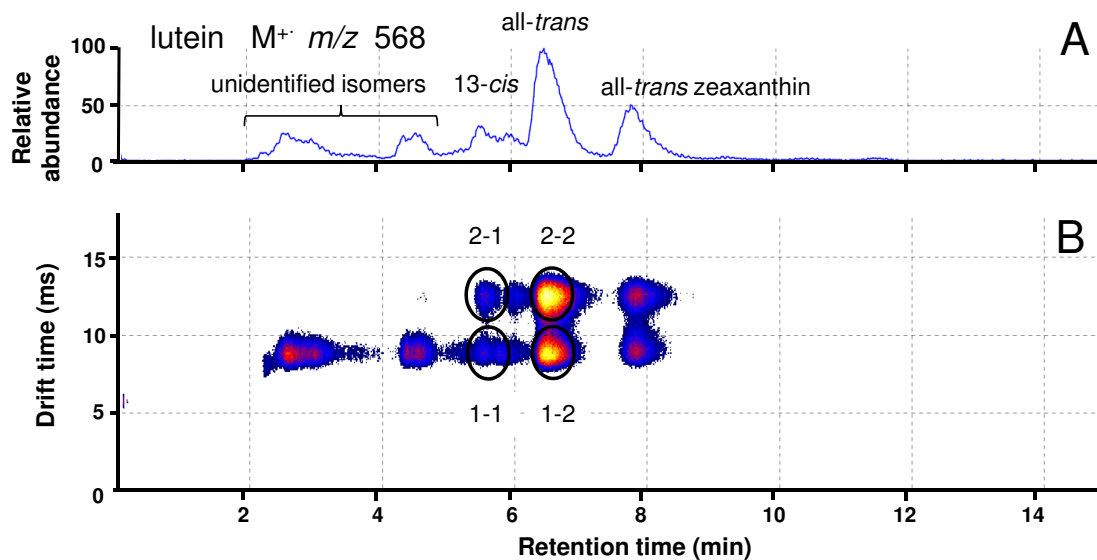


Figure 27. LC-IM-MS analysis of a mixture of lutein cis/trans isomers (note that this lutein sample contained 6.0% all-*trans*-zeaxanthin; retention time 7.8 min). (A) LC-MS chromatogram of lutein isomers; (B) 2D map showing ion mobility and LC-MS separation of lutein isomers.

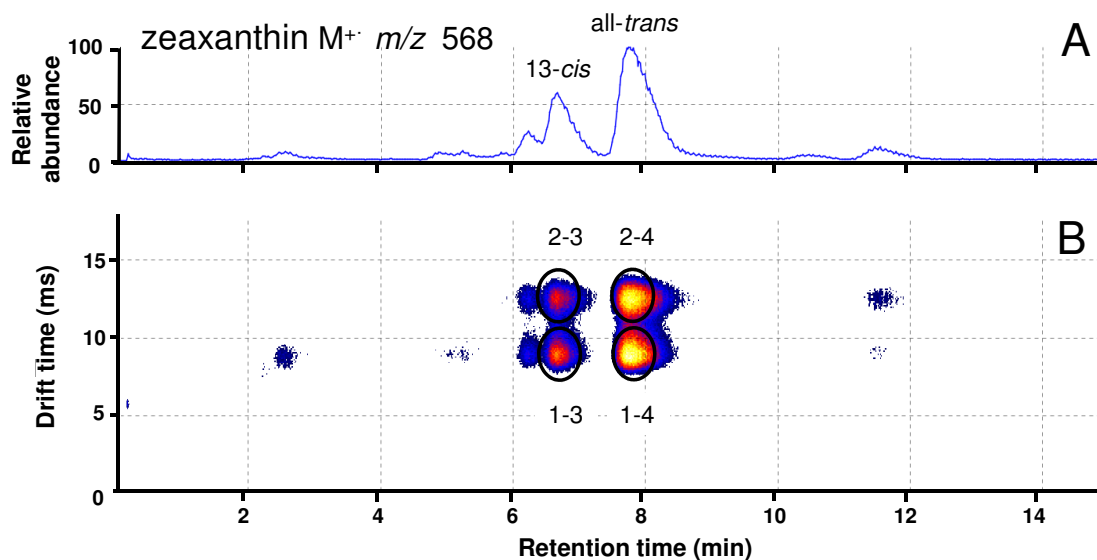


Figure 28. LC-IM-MS analysis of a mixture of zeaxanthin isomers. (A) LC-MS chromatogram of zeaxanthin isomers; (B) 2D map showing ion mobility and LC-MS separation of zeaxanthin isomers.

To test the thermal isomerization hypothesis on xanthophylls, the temperature of the desolvation gas used during electrospray was varied from 50 °C to 300 °C during sample infusion (note that desolvation gas temperatures below 50 °C or above 300 °C did not produce stable electrospray), and the relative amounts of cis and all-trans isomers were determined at each temperature using IM-MS. As shown by the drift time distributions in Figure 29 and the graphs in Figure 30, the relative abundance of the first ion mobility peak compared with the second peak increased as the temperature in the ion source was increased. This observation is consistent with the hypothesis that the first peak in each drift time spectrum (Figures 27-29) corresponds to the higher energy cis isomers, and the second IM-MS peak is the thermodynamically more stable all-trans isomer^[72, 139].

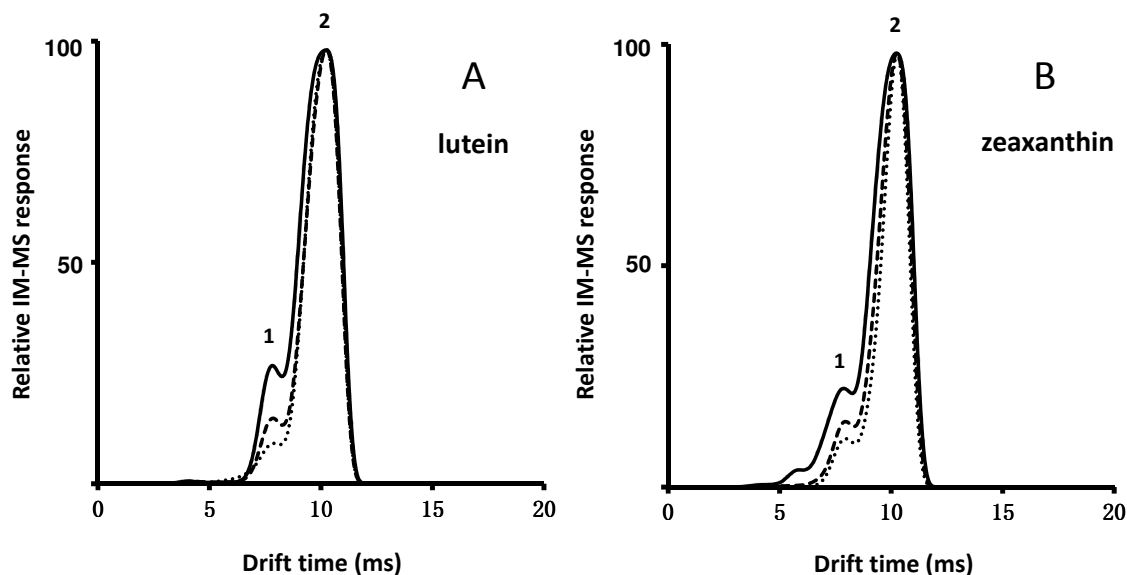


Figure 29. Effect of electrospray desolvation gas temperature on the abundances of *cis* (peak 1) and all-*trans* isomers (peak 2) of (A) lutein; and (B) zeaxanthin following infusion of the all-*trans* isomer. Drift time spectra were acquired using positive ion electrospray mass spectrometry with detection of the molecular ions of m/z 568.4. (50 °C, dotted line; 150 °C, dashed line; 300 °C, solid line)

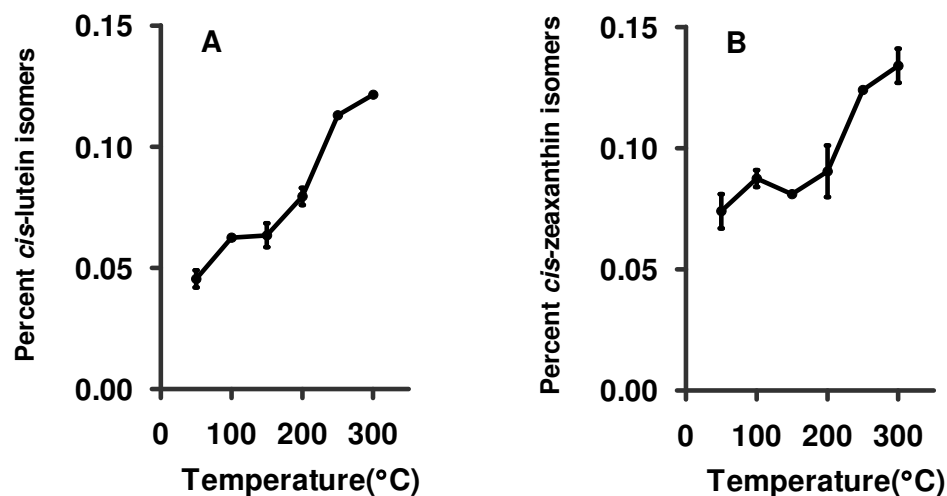


Figure 30. Relative abundances of *cis* isomers (peak 1 in Figure 29) and total (*cis* plus all-*trans*) isomers as a function of desolvation gas temperature for (A) lutein; and (B) zeaxanthin.

As suggested by our previous study of carotenes, the ion mobility peaks with shorter drift times probably corresponded to *cis* isomers (Figure 27B and Figure 28B, 1-1, 1-2, 1-3, 1-4) because of their more compact structures, while the mobility peaks with longer drift times corresponded to all-*trans*-lutein or all-*trans*-zeaxanthin (Figure 27B and Figure 28B, 2-1, 2-2, 2-3, 2-4). The CCS values of lutein and zeaxanthin isomers were determined using the method described in section 3.2.2.4. A poly-DL-alanine based calibration curve for lutein and zeaxanthin isomers at IMS gas flow rate of 32 mL/min was $y = 160.6x^{0.9394}$ ($r^2=0.9992$). The experimental CCS values of the *cis* and all-*trans* isomers of lutein and zeaxanthin are summarized in Table V. Similarly, theoretical CCSs were calculated for the all-*trans* and 13-*cis* isomers of lutein and zeaxanthin (Figure 16), and these results are listed in Table V.

TABLE V
COLLISION CROSS-SECTION (CCS) VALUES OF GEOMETIC ISOMERS OF
LUTEIN AND ZEAXANTHIN

Compound	IMS gas flow (mL/min)	Experimental CCS ^a (\pm S.D.), Å ²	Theoretical CCS, Å ²
lutein	32	<i>cis</i> ^a	178.4 \pm 1.2
		all- <i>trans</i> ^b	230.7 \pm 0.0
zeaxanthin	32	<i>cis</i> ^a	178.4 \pm 1.2
		all- <i>trans</i> ^b	232.5 \pm 0.0

^a First IM-MS peak, shorter drift time (mixture of *cis* isomers)

^b Second IM-MS peak, longer drift time (all-*trans* isomer)

Lutein and zeaxanthin are structural isomers, the only difference between them is that lutein has one α -ionone ring and one β -ionone rather than two β -ionone rings as in zeaxanthin (Figure 16). As shown in Table V, the lutein isomers showed almost identical CCSs to the corresponding zeaxanthin peaks. Likewise, the more compact cis isomers of each xanthophyll probably produced the first peak during IM-MS, and the all-trans isomer should have a longer drift time corresponding to the second peak. The measured CCS values of the cis isomers and the all-trans isomer of lutein were 178 \AA^2 and 230 \AA^2 , respectively. For zeaxanthin, the measured CCSs of the cis and all-trans isomers were 178 \AA^2 and 232 \AA^2 , respectively. An IMS gas flow rate of 32 mL/min produced smaller CCS values for all-trans isomers than their corresponding theoretical CCS values suggesting that the elongated all-trans xanthophylls may become more compact as the IMS gas pressure increases. As expected, the theoretical CCS values of 13-cis or all-trans isomers of lutein and zeaxanthin are comparable, since they only differ by one C=C location in their structures. In addition, 13-cis isomers have relatively smaller theoretical CCS values than the corresponding all-trans-lutein and zeaxanthin due to their central location of the cis double bonds (Figure 16).

Since IM-MS could at least partially separate cis and all-trans isomers of lutein and zeaxanthin, IM-tandem mass spectrometry was carried out to determine if these geometric isomers produced different fragmentation patterns. As shown in Figures 31 and 32, cis isomers of lutein and zeaxanthin formed fewer different fragment ions than did all-trans-lutein and all-trans-zeaxanthin, probably because the charge and radical electron were localized to the oxygen atoms that differentiate xanthophylls from the hydrocarbon carotenes. Thus, charge-directed fragmentation occurred primarily near the oxygen atoms

to form fewer but abundant fragment ions. The ion of m/z 550 (measured m/z 550.4195, theoretical m/z 550.4175; $C_{40}H_{54}O$ ΔM 3.6 ppm) formed by the loss of water was the most abundant product ion in the tandem mass spectra of the *cis* isomers of both lutein and zeaxanthin (Figures 31A and 32A, respectively). The $[M-H_2O]^+$ ion ranged from 37% to 42 % in relative abundance and was second in abundance only to the base peak of m/z 568 of the *cis*-xanthophylls. In contrast, the ion of m/z 550 was much less abundant (less than 10%) in the product ion tandem mass spectra of all-*trans*-lutein and all-*trans*-zeaxanthin (Figures 31B and 32B, respectively). Therefore, the *cis* isomers of lutein and zeaxanthin could be distinguished from their all-*trans* isomers by the high abundance of the $[M-H_2O]^+$ ions of m/z 550.

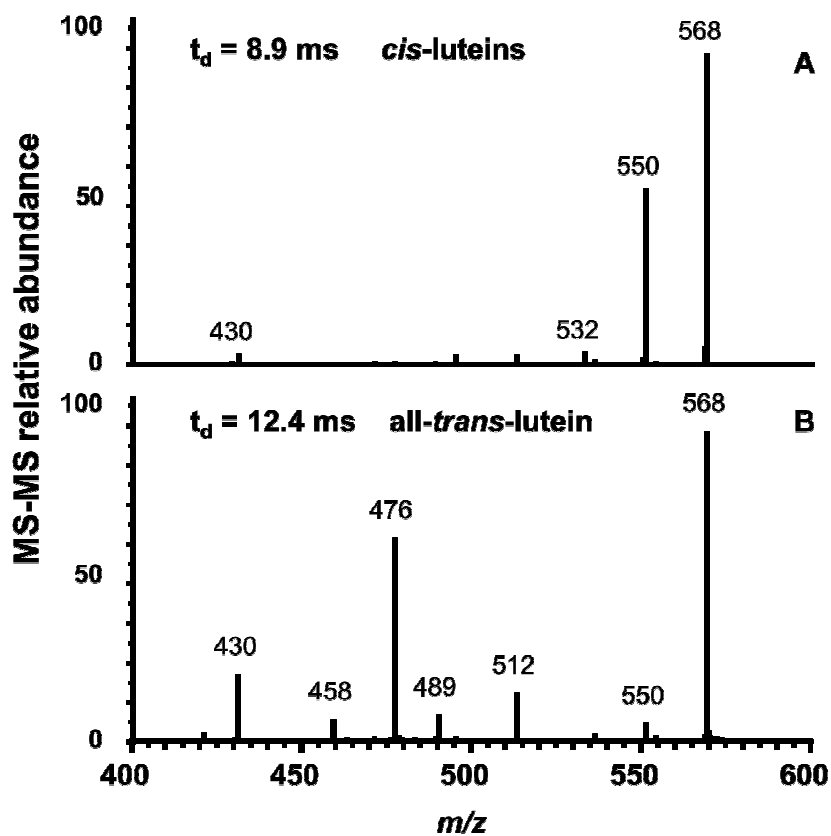


Figure 31. Positive ion electrospray IM-MS-MS with CID of (A) *cis*-luteins; and (B) *all-trans*-lutein. Note the relative abundances of m/z 476 and m/z 550 in the tandem mass spectra which distinguish the *cis* isomers from the *all-trans*-lutein.

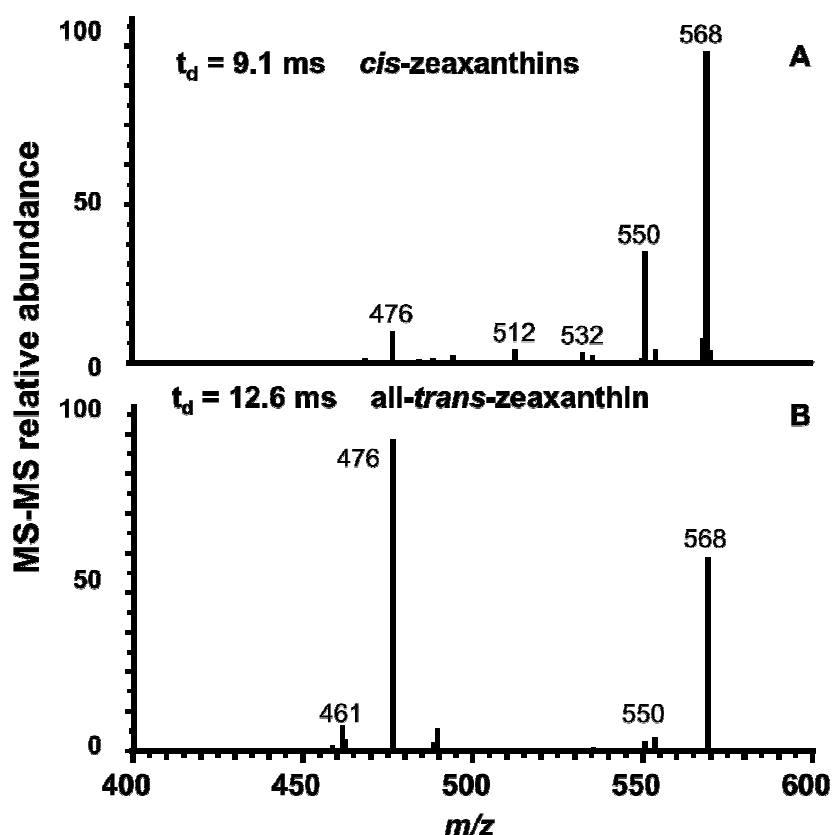


Figure 32. Positive ion electrospray IM-MS-MS with CID of (A) *cis*-zeaxanthins; and (B) *all-trans*-zeaxanthin. Note the relative abundances of m/z 476 and m/z 550 in the tandem mass spectra which distinguish the *cis* isomers from the *all-trans*-zeaxanthin.

Another product ion that distinguished the *cis* from the *trans* isomers of lutein and zeaxanthin was observed at m/z 476 (Figures 31 and 32). The ion of m/z 476 corresponds to elimination of toluene (measured m/z 476.3651, theoretical m/z 476.3654; $C_{33}H_{48}O_2$ ΔM -0.6 ppm) and was observed as the most abundant product ion formed from the molecular ion of m/z 568 for both *all-trans*-lutein (54% relative abundance) and *all-trans*-zeaxanthin (base peak).

The product ion of m/z 430 observed in Figure 31 is unique to lutein and was formed by the elimination of the α -ionone ring^[68] (measured m/z 430.3231, theoretical m/z 430.3236; $C_{31}H_{42}O$ ΔM -1.1 ppm). The ion of m/z 430 was several folds more abundant in the product ion tandem mass spectra of all-*trans*-lutein (relative abundance 30%) than in the MS-MS spectrum of *cis*-luteins (less than 5%). Since zeaxanthin does not contain an α -ionone ring, it cannot fragment to form a retro-Diels-Alder ion product of m/z 430. Therefore, the presence of the ion of m/z 430 may be used to distinguish lutein from its isomer zeaxanthin.

In the IM-MS-MS analyses of the lutein and zeaxanthin isomers, the ion of m/z 476 was significantly more abundant in the tandem mass spectra of the all-*trans* isomers (Figures 31B and 32B, respectively), and ions at m/z 550 (measured m/z 550.4145, theoretical m/z 550.4175; $C_{40}H_{54}O$ ΔM -5.4 ppm) and 532 produced (measured m/z 532.4055, theoretical m/z 532.4069; $C_{40}H_{52}$ ΔM -2.6 ppm) due to the loss of up to two molecules of water were more abundant in the tandem mass spectra of the *cis* isomers (Figures 31A and 32A, respectively). The base peak of the tandem mass spectrum of all-*trans*-zeaxanthin was observed at m/z 476 and corresponded to the loss of toluene. This characteristic was similar to the ion of m/z 444 observed in the tandem mass spectrum of all-*trans*- β -carotene (its carotene partner), which was also produced through the loss of toluene from the polyene chain and formed a base peak (Figure 24B). Lower relative abundances (~50%) of product ion m/z 476 were observed for all-*trans*-lutein. This may be due to supplementary fragmentation pathways favored by this α -ionone ring containing xanthophylls. For instance, another fragment, m/z 430 had a relative abundance up to 30% in the tandem mass spectrum of all-*trans*-lutein (Figures 31B).

Significantly lower peaks at m/z 476 in both *cis* isomers of lutein and zeaxanthin suggest that steric conflicts may exist in *cis* forms and prevent the rearrangement of the polyene chain. Thus, the sequential loss of water molecules became the major fragmentation pathways for the *cis* isomers. With approximately 50% relative abundance, the ion of m/z 550 was the most abundant product ion for *cis* xanthophylls (Figures 31A and 32A).

Like lycopene and β -carotene, *cis* and all-*trans* isomers of lutein and zeaxanthin may be distinguished during IM-MS-MS based on their different drift times (the all-*trans* isomers showed the longest drift times) and by the relative abundances of fragment ions of m/z 568, m/z 550 and m/z 532 (*cis*-isomers) and m/z 476 (all-*trans* isomers). The M^{+} ions of *cis*-luteins and *cis*-zeaxanthins fragment during CID to form product ions of m/z 550 and m/z 532 whereas the all-*trans* isomers either do not form these ions or produces them at much lower relative abundances. The M^{+} ions of all-*trans*-lutein and all-*trans*-zeaxanthins fragment during CID to form product ions of m/z 476 and m/z 430 (lutein only) whereas the *cis* isomers produce them at much lower relative abundances. The product ion of m/z 430 is unique to lutein since it is produced by the retro-Diels-Alder reaction on the α -ionone ring of lutein as reported by van Breemen *et al.*^[68] In summary, abundant ions of m/z 550 in the IM-MS-MS spectra of lutein and zeaxanthin are characteristic of their *cis*-isomers whereas m/z 476 are characteristic of their all-*trans* forms. Additionally, an increased relative abundance in the ion of m/z 430 may also discriminate all-*trans*-lutein from its *cis* forms.

Although different carotenoids can be distinguished based on their tandem mass spectra,^[142] both *cis* and *trans* isomers of the same carotenoid have consistently produced

identical tandem mass spectra during MS/MS or LC-MS-MS due to isomerization that occurs during the ionization process. Even though electrospray is one of the softest ionization techniques, these data show that cis/trans isomerization of carotenoids still occurs during this ionization process. This in-source isomerization phenomenon probably explains why MS and MS/MS produce identical responses for all-trans and various cis isomers of retinoic acid^[143] and specific carotenoids.^[105] When carrying out quantitative analysis, HPLC with absorbance detection responds differently to cis and trans isomers of carotenoids and retinoic acid, and therefore, separate standard curves are required for each geometric isomer. However, isomerization in the ion source appears to simplify quantitative analysis of these compounds when using LC-MS or LC-MS-MS, since one standard curve would be suitable for all geometric isomers of a particular compound.

When carotenoids are analyzed using IM-MS-MS, our data indicate that the cis and trans isomers may be resolved and that they produce unique tandem mass spectra that may be used to distinguish the all-trans isomer from the cis isomers. Although HPLC may be used to separate geometric isomers of carotenoids, ionization techniques such as FAB^[142] and electrospray isomerize these compounds. Since the time course for ionization is probably ~0.1 s (assuming ~10 mL/s nebulizing gas and solvent vapor in a 1 cm² spray, the flow rate would be ~10 cm/s; and for a 1 cm path length, ~0.1 s would be required for sample to travel from the electrospray emitter to the sampling cone of the mass spectrometer), carotenoid isomerization might be complete by the time ions are extracted from the ion source and tandem mass spectra obtained. However, IM-MS-MS requires only milliseconds for separation of isomers, fragmentation during CID and analysis, which is sufficient to preserve cis/trans isomeric information. Until carotenoid ionization

can be achieved without cis/trans isomerization, the slow process of HPLC separation will still be necessary as part of the analysis of carotenoid cis/trans isomers in biomedical and biological samples.

3.4 Conclusions

The separation of cis and all-trans isomers of carotenoids was demonstrated using TWIMS with drift time separations of 1-4 ms. Because the cis isomers had collision cross-sections that were smaller than those of the corresponding all-trans isomers, they were detected first followed at a later drift time by the all-trans isomer. However, the various cis isomers could not be resolved due to the low resolving power of this particular ion mobility instrument.

The use of LC-IM-MS-MS helped confirm that in-source isomerization of lycopene, β -carotene, lutein, and zeaxanthin occurred during positive ion electrospray. Although cis/trans isomerization could not be eliminated during electrospray, this temperature dependence in the ionization of carotenes and xanthophylls suggests that softer ionization conditions can minimize cis/trans isomerization in the ion source. After separation using IMS, the cis and all-trans isomers of lycopene, β -carotene, lutein, and zeaxanthin were shown by MS-MS with CID to produce unique fragmentation patterns that could be used to distinguish them. Until cis/trans isomerization of carotenoids can be eliminated in the ion source, the slow process of HPLC separation of geometrical isomers of carotenoids in biomedical samples will still be necessary for some applications.

4. DOPANT-ASSISTED APPI MASS SPECTROMETRY OF CAROTENOIDS

4.1 Introduction

The identification and quantitative analysis of carotenoids can be challenging due to their instability in the presence of light, heat and oxygen. In biological samples such as human serum and tissue, carotenoids are often present at low concentrations and in the presence of potentially interfering compounds. Since carotenoids are unstable at the high temperatures used for gas chromatography, HPLC is usually used for their separation, and UV/vis absorbance and/or mass spectrometry is used for the detection and characterization.^[124] In particular, the application of LC-MS and LC-MS-MS to the analysis of carotenoids offers the advantages of high sensitivity and superior selectivity that are essential for the identification and quantitation of carotenoids. Among the ionization techniques compatible with LC-MS, the most successful for carotenoid studies have been electrospray^[126] and APCI.^[123] Although carotenes and xanthophylls form molecular ions or protonated molecules during positive ion electrospray, the hydrocarbon carotenes do not ionize when using negative ion electrospray. However, APCI forms abundant positively or negatively charged molecular ions or protonated and deprotonated molecules of both carotenes and xanthophylls.

In 2000, another soft ionization technique, APPI was introduced as a new interface for LC-MS by Bruins and co-workers^[102] and Syage *et al.*^[101] Since then, APPI has been reported to enhance mass spectrometric response compared with electrospray and APCI for several classes of compounds, such as lipids,^[144, 145] estrogens,^[146] polycyclic aromatic hydrocarbons,^[147] and selected drugs.^[96, 148] As reviewed by Robb and Blades,^[149] the

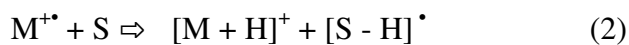
most important ionization modes during APPI are direct APPI, dopant-assisted APPI, and thermospray.

4.1.1 Direct APPI

The fundamental process in positive ion APPI is the absorption of a high-energy photon by a molecule and subsequent ejection of an electron. No photoionizable solvents or dopants other than a carrier solvent are required. As shown in Equation (1), an analyte (M) with ionization energy (IE) lower than the energy ($h\nu$) of a photon can be directly ionized during APPI:



In direct APPI, ejection of an electron from the analyte molecule forms a molecular radical cation $M^{+\bullet}$. The analyte radical cation can then be detected as $M^{+\bullet}$ or it can abstract a hydrogen atom from a solvent molecule (S) to form a stable protonated molecule,^[150, 151] $[M+H]^+$, a process which is represented in Equation (2):



APPI can also produce negative ions, $M^{\bullet-}$. Analytes of high electron affinity can capture thermal electrons formed from ionization of solvent molecules or electrons produced by photons striking metal surfaces in the APPI source,^[94, 95, 149] The formation of radical anions by electron capture is described by Equation (3):

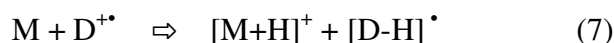
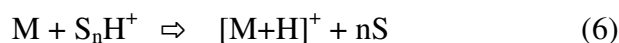
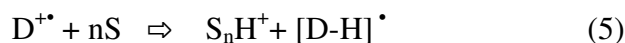


4.1.2 Dopant-assisted APPI

Robb *et al.* ^[102] was the first to describe the application of dopants to overcome low sensitivity issues during LC-APPI-MS. Except for replacing corona needles with vacuum UV lamps for the ionization process, APPI sources basically replicate their APCI counterparts. ^[102, 149] In general, dopants are molecules with ionization energies < 10 eV which can be directly photoionized by intense UV light. When the analyte molecules do not absorb UV light efficiently enough for direct photoionization, then the addition of dopant (D) molecules facilitates the formation of dopant ions that may then ionize the analytes through subsequent ion-molecule reactions. Equations (4)-(8) represent the major ion-molecule reaction pathways during dopant-assisted positive ion APPI. ^[149, 152] Dopant ionization is initiated by photons, usually generated by a krypton lamp, as indicated in Equation (4):



Subsequent ionization of the analyte (M) might proceed through proton transfer involving solvent (S), as described by the following Equations (5)-(7):



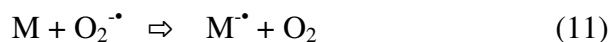
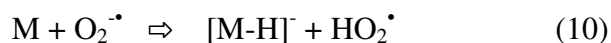
Alternatively, ionization of the analyte might occur through charge exchange, as described by Equation (8):



Similar proton transfer and charge exchange mechanisms also occur during dopant-assisted negative ion APPI. However, oxygen in the ion source plays a critical role in negative ion APPI by capturing electrons ejected by dopants (Equation 4) as described in Equation (9).^[149, 152]



Then, analytes can either be deprotonated by reaction with the newly formed superoxide ions as shown in Equation (10) or simply ionized through charge exchange as shown in Equation (11).



4.1.3 Thermospray

Thermospray releases analyte ions already present in the liquid phase into gas phase by vaporizing droplets from the inlet. It was first noticed in APPI sources when the UV lamp was off.^[149] Although thermospray was found to be useful for certain compounds, generally it is only responsible for a minor portion of ions detected during APPI due to its limited transmission efficiency to the mass analyzer.

4.1.4 UV lamps and photoionization

Xenon ($h\nu=8.4$ eV), krypton ($h\nu=10.0$ and 10.6 eV), and argon ($h\nu=11.2$ eV) vacuum UV lamps are commonly used as photon sources for APPI. Among these, krypton lamps are the most widely used UV light sources for APPI because its photon energy levels are ideal for efficient ionization of most analytes without ionizing most commonly used solvents or gases present in the ion source.^[99, 148, 153]

Methyl-*tert*-butyl ether (MTBE) has an IE of 9.24 eV, which is lower than the regular APPI krypton lamp photon energy of 10 eV (see Tables VI and VII for the gas-phase ion thermochemical data of analytes, dopants, and solvents). Although often used in mobile phases for carotenoid separations, MTBE has not been reported previously as an APPI dopant.^[153] In this dissertation, MTBE was evaluated as a novel dopant for carotenoid analysis and compared with several popular dopants (Table VII) for both positive ion and negative ion APPI.

TABLE VI

IONIZATION ENERGIES (IE) AND PROTON AFFINITIES (PA) OF
SELECTED CAROTENIIDS

Compound	IE (eV)	PA (kJ/mol)	Reference
α -carotene	6.80	-	[154]
β -carotene	6.73	925.0	[154-156]
Lycopene	6.69	-	[154]
Lutein	7.88	443.8	[157]
Zeaxanthin	7.86	540.1	[157]

TABLE VII
GAS PHASE ION THERMOCHEMICAL DATA OF SOME COMMON
SOLVENTS, APPI DOPANTS AND ATMOSPHERIC GASES

Lamp	Compound	IE^a (eV)	PA^b (kJ/mol)	Reference
	Nitrogen	15.58	493.9	[156, 158]
	Water	12.62	690.7	[156, 158]
	Acetonitrile	12.20	779.2	[158]
	Oxygen	12.07	422.8	[156, 158]
	Chloroform	11.37	-	[97]
	Dichloromethane	11.33	-	[97]
	Formic acid	11.33	742.0	[94, 156]
Ar: 11.2 eV	Methanol	10.84	754.3	[158]
	Acetic acid	10.65	783.7	[94, 156]
	Ethanol	10.48	776.9	[97, 156]
	Isopropanol	10.17	793.0	[158]
	n-Hexane	10.13	-	[97, 158]
Kr: 10.0 eV	Acetone^c	9.70	812.1	[156, 158]
	Tetrahydrofuran	9.40	822.1	[97, 158]
	Pyridine	9.26	929.3	[156, 158]
	MTBE	9.24	841.6	[97, 159]
	Benzene	9.24	750.5	[156, 158]
	Chlorobenzene	9.07	753.1	[156, 158]
	Furan	8.88	803.7	[156, 158]
	Toluene	8.83	784.0	[158]
Xe: 8.4 eV	Anisole	8.20	840.1	[97, 156]
	Triethylamine	7.53	982.4	[156, 158]

^a IE = ionization energy

^b PA = proton affinity

^c Bold-face indicates dopants evaluated during this investigation.

4.2 Materials and methods

4.2.1 Materials

All-*trans*-lycopene ($\geq 90\%$), all-*trans*- α -carotene ($\geq 90\%$), and all-*trans*- β -carotene ($\geq 97\%$) were purchased from Sigma-Aldrich (St. Louis, MO), while all-*trans*-lutein ($\geq 96\%$) and all-*trans*-zeaxanthin ($\geq 97\%$) were obtained from Carotenature (Lupsingen, Switzerland). HPLC grade *n*-hexane, methanol, acetonitrile, acetone, and MTBE were purchased from Thermo Fisher (Hanover Park, IL). Other HPLC-grade solvents, including tetrahydrofuran (THF), chlorobenzene, toluene, and anisole were purchased from Sigma-Aldrich (Milwaukee, WI or Allentown, PA).

4.2.2 Methods

4.2.2.1 APPI MS and APPI MS-MS of carotenoids

Positive ion and negative ion APPI mass spectra and product ion tandem mass spectra were obtained using an Agilent 6410 triple quadrupole mass spectrometer (Palo Alto, CA) equipped with an APPI source (krypton UV lamp) and an Agilent 1200 integrated HPLC system. A dual channel syringe pump used for APPI dopant addition was manufactured by Harvard Apparatus (South Natick, MA).

Each carotene standard (1 mg), including all-*trans*-lycopene, α -carotene and β -carotene was dissolved in 5 mL *n*-hexane in order to obtain a stock solution of 200 $\mu\text{g/mL}$. Aliquots (500 μL) of each carotene stock solution were evaporated to dryness under a gentle nitrogen stream. The residue of each carotene stock solution was reconstituted in 10 mL methanol to obtain a working standard solution of 10 $\mu\text{g/mL}$, which

was used for flow-injection analysis (FIA) with mass spectrometric detection. Xanthophyll standards (1 mg each), including all-*trans*-lutein and all-*trans*-zeaxanthin, were prepared in methanol to a final concentration of 10 µg/mL using the same procedure described above. Indirect, dim light and amber vials were used during the sample preparation process to minimize possible degradation and isomerization of the carotenoids.

Methanol was used as the mobile phase for FIA at a flow rate of 200 µL/min methanol. To evaluate the efficiency of the various dopant for carotenoid photoionization, each dopant was continuously infused into the APPI ion source at 3 different make-up flow rates, 20, 40, or 80 µL/min (corresponding to dopant addition ratios of 1:10, 2:10, or 4:10) through a T connector to the main flow using a syringe pump. Aliquots (5 µL) of each working standard solution were injected 5 times using FIA under the optimized mass spectrometry conditions at each dopant addition ratio. The autosampler was maintained at 15 °C using a thermostat module, which below room temperature to minimize degradation but high enough to prevent carotenoid precipitation from methanol.

The Agilent 6410 triple quadrupole mass spectrometer was operated in positive ion or negative ion APPI mode. The APPI source conditions recommended by the manufacturer were used as a starting point for method optimization. The optimized APPI source conditions were as follows: gas temperature 300 ° C, vaporizer temperature 350 ° C, drying gas flow 4 L/min, nebulizer gas pressure 60 psi, and capillary voltage 3000 V (positive ion mode) or 3500 V (negative ion mode). No significant improvements in ionization efficiencies were obtained by modulating these optimized parameters. Fragmentor values had significant impact on signal intensities. The optimized fragmentor

values for carotenoids were 110 V for positive ion APPI and 160 V for negative ion APPI.

Mass spectra and product ion tandem mass spectra carotenoid precursor ions were recorded over the range m/z 100 to m/z 600. Since extensive tandem mass spectra of some precursor ions derived from the 5 carotenoids had been reported previously by van Breemen *et al.*,^[68] only novel species or those that were uncommon during FAB, electrospray, and APCI were selected for collision-induced dissociation (CID) and product ion tandem mass spectrometric analysis.

4.2.2.2 LC-APPI-MS-MS analysis of carotenoids

A standard mixture of all-*trans*-lycopene, all-*trans*- β -carotene and all-*trans*-zeaxanthin were chromatographically separated using a Phenomenex (Torrance, CA) Luna C₁₈ HPLC column (5 μ m, 2.0 \times 150 mm) and analyzed by positive ion and negative ion APPI tandem mass spectrometry. MTBE was used as mobile phase B as well as the dopant for photoionization while mobile phase A was methanol. An 8 min linear gradient from 5 to 30% MTBE in 1.5 min, 30 to 40% MTBE in 6.5 min, followed by re-equilibration at the initial condition for 5 min before the next injection. The flow rate was set at 0.3 mL/min. In addition, a human serum sample was also prepared and analyzed using the positive ion APPI LC-MS-MS method described here.

As a comparison, the Agilent 6410 triple quadrupole system was then switched to a Multimode interface and operated at positive ion and negative ion APCI to analyze the standard mixture under the same chromatographic conditions. The optimized APCI source conditions were as follows: gas temperature 325 ° C, vaporizer temperature 250

° C, drying gas flow 5 L/min, nebulizer gas pressure 20 psi, corona current 4 μ A and capillary voltage 2500 V (both positive ion and negative ion modes). Fragmentor values applied were identical to those used during APPI.

4.2.3 Data processing

From the positive ion and negative ion APPI mass spectra of each carotenoid, the most abundant precursor ion peak per carotenoid standard was extracted and integrated using Agilent Mass Hunter workstation software (version B.01.03). The average peak areas of 5 replicates were used for comparison across different dopants.

4.3 Results and discussion

Although water (IE = 12.62 eV), acetonitrile (IE = 12.20 eV) and methanol (IE = 10.84 eV) are the most frequently used mobile phase solvents for reversed-phase HPLC, carotenoids are not water soluble. Therefore, water was not used as mobile phase or diluent in these carotenoid APPI studies. Although acetonitrile and methanol are not efficiently ionized by krypton lamp generated photons of 10.0 eV and 10.6 eV, methanol may form trace amounts of the dimer $[\text{CH}_3\text{OH}]_2^+$ (IE of 9.74 eV) and acetonitrile may form several species including dimers during irradiation by a krypton lamp.^[160, 161] Compared with the solvent acetonitrile, methanol tends to give better responses for analytes than acetonitrile during APPI because of its lower IE and lower PA,^[148, 149, 161, 162] so methanol was selected as the mobile phase and diluent in this investigation.

4.3.1 Positive ion APPI MS

As indicated in Table VI, all the carotenes and xanthophylls investigated during this study have IE values (rang 6.69-7.88 eV) lower than the energy of the photons produced by a krypton lamp. Therefore, direct APPI of these carotenoids was anticipated to occur without the addition of dopants. As shown in Figures 33-34 and Table VIII, the carotenes but not the xanthophylls formed molecular ions, M^+ , of up to only 15.2% relative abundance. All the carotenoids tested formed protonated molecules, which were the base peaks in all of the positive ion APPI mass spectra except for that of lutein. Both lutein and zeaxanthin formed protonated molecules that fragmented in the ion source to eliminate a molecule of water, $[MH-H_2O]^+$, and this ion was the base peak in the mass spectrum of lutein.

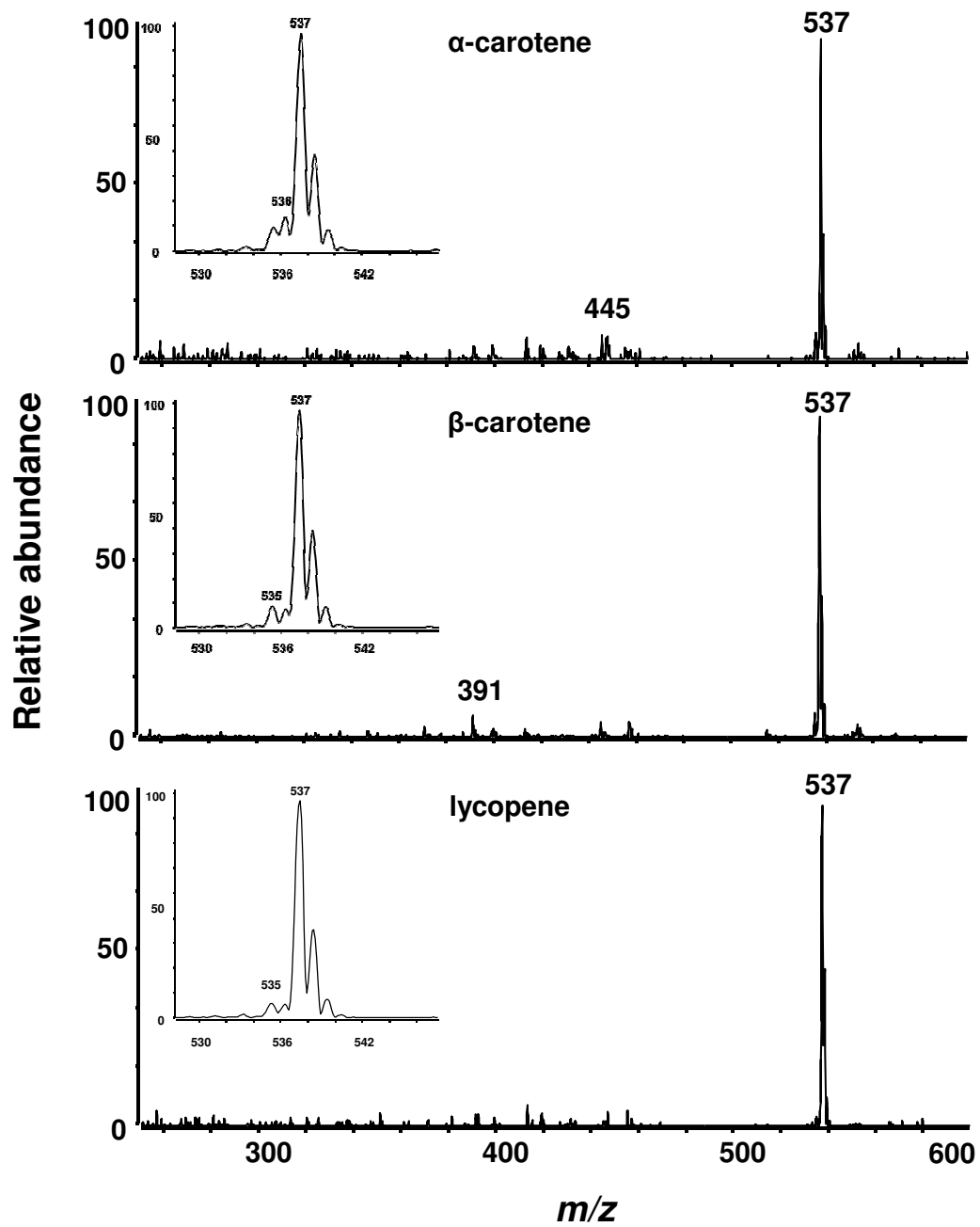


Figure 33. Positive ion APPI mass spectra of carotenes (no dopant)

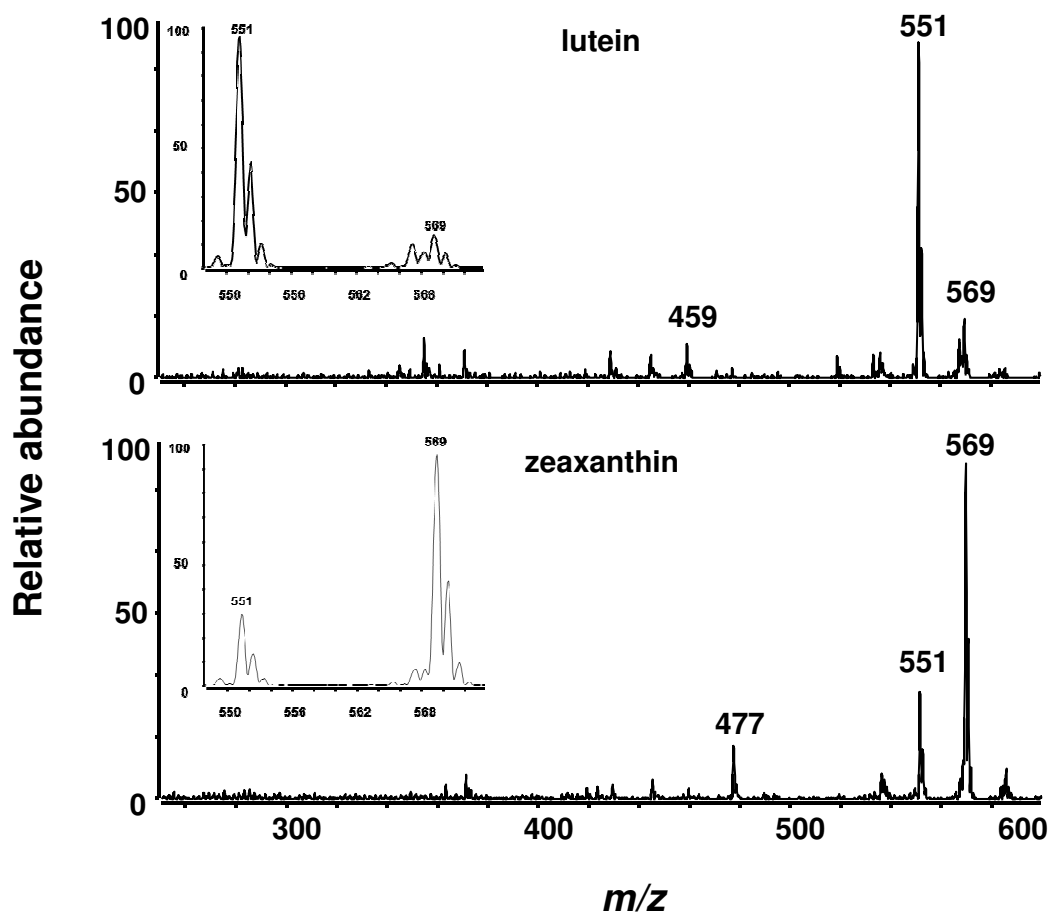


Figure 34. Positive ion APPI mass spectra of xanthophylls (no dapant)

Since protonated molecules were more abundant than molecular ions for all of the carotenoids, methanol probably functioned as a proton donor through the two-step reaction sequence described in Equations (1) and (2) and as proposed by Syage.^[150] Briefly, carotenoids formed molecular cations through direct photoionization (Equation 1) followed by a hydrogen transfer from the solvent, methanol, to form protonated molecules (Equation 2).

TABLE VIII
MAJOR IONS OBSERVED IN THE POSITIVE APPI MASS SPECTRA OF INVESTIGATED CAROTENOIDS UNDER
DIFFERENT DOPANT CONDITIONS

Carotenoid	Formula	Ion	DOPANT						
			Methanol	MTBE	THF	Acetone	Toluene	Anisole	Chlorobenzene
α -carotene	$C_{40}H_{56}$	M^{+}	536.4(15.2) ^a	536.4(7.0)	536.4(32.4)	536.4(23.4)	536.4(37.2)	536.4(100)	536.4(100)
		$[M+H]^{+}$	537.4(100)^b	537.4(100)	537.4(100)	537.4(100)	537.4(100)	537.4(59.4)	537.4(86.8)
β -carotene	$C_{40}H_{56}$	M^{+}	536.4(8.4)	536.4(8.1)	536.4(18.6)	536.4(9.2)	536.4(27.7)	536.4(100)	536.4(100)
		$[M+H]^{+}$	537.4(100)	537.4(100)	537.4(100)	537.4(100)	537.4(100)	537.4(60.3)	537.4(86.8)
Lycopene	$C_{40}H_{56}$	M^{+}	536.4(6.3)	536.4(5.8)	536.4(5.3)	536.4(9.1)	536.4(21.6)	536.4(100)	536.4(100)
		$[M+H]^{+}$	537.4(100)	537.4(100)	537.4(100)	537.4(100)	537.4(100)	537.4(56.8)	537.4(97.9)
Lutein	$C_{40}H_{56}O_2$	M^{+}	ND ^c	ND	ND	ND	ND	568.4(100)	568.4(100)
		$[M+H]^{+}$	569.4(13.9)	569.4(11.9)	569.4(13.2)	569.4(11.8)	569.4(14.9)	ND	ND
		$[MH-H_2O]^{+}$	551.4(100)	551.4(100)	551.4(100)	551.4(100)	551.4(100)	551.4(76.4)	551.4(61.9)
Zeaxanthin	$C_{40}H_{56}O_2$	M^{+}	ND	ND	ND	ND	ND	568.4(100)	568.4(100)
		$[M+H]^{+}$	569.4(100)	569.4(100)	569.4(100)	569.4(100)	569.4(100)	ND	ND
		$[MH-H_2O]^{+}$	551.4(30.5)	551.4(29.6)	551.4(28.9)	551.4(42.9)	551.4(33.0)	551.4(6.5)	551.4(15.4)

^a m/z (relative abundance)

^b Bold-face indicates the most abundant ion of each analyte

^c Not detected

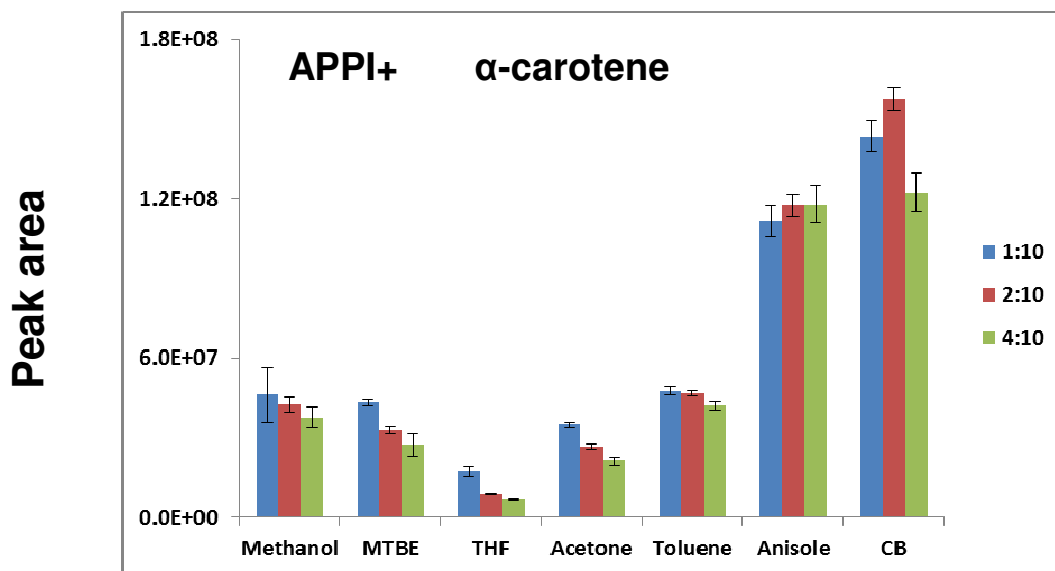
When dopants were added to the methanol solvent (except for anisole and chlorobenzene), carotenes formed protonated molecules as the base peaks of their positive ion APPI mass spectra (Table VIII). These spectra were similar to APCI mass spectra of carotenes.^[68] Although protonated molecules were abundant in the carotene mass spectra when anisole or chlorobenzene was used, these dopants facilitated the formation of radical cations so that the mass spectra resembled those obtained using positive ion electrospray or FAB.^[126, 142, 163]

As shown in Table VI, the IE values of carotenoids are much lower than those of anisole and chlorobenzene. After photoionization of anisole or chlorobenzene, ion-molecule charge-exchange reactions (Equation (8)) probably occurred to form molecular ions of carotenoids that had not already been ionized through direct photoionization. These dopant results are consistent with those of Kauppila *et al.*^[164] and Matějček^[146] for anisole and those of Robb *et al.*^[165] for chlorobenzene. However, higher percentages of protonated molecules were observed for the carotenes when chlorobenzene (86.8-97.9%) was the dopant compared with anisole (56.8-60.3%). The reason might be that chlorobenzene has lower proton affinity (753.1 kJ/mol) than does anisole (840.1 kJ/mol), while both are lower than the carotenes (PA = 925.0 kJ/mol for β -carotene; note that PA values of α -carotene and lycopene are not available in the literature).

Similarly, for lutein and zeaxanthin, radical cations at m/z 568 were also dominant as found during positive ion electrospray and FAB while anisole and chlorobenzene presented as dopants.^[126, 142, 163] Yet proton transfer process was preferred when other dopants were used. $[M+H-H_2O]^+$ at m/z 551 and $[M+H]^+$ at m/z 569 replaced radical

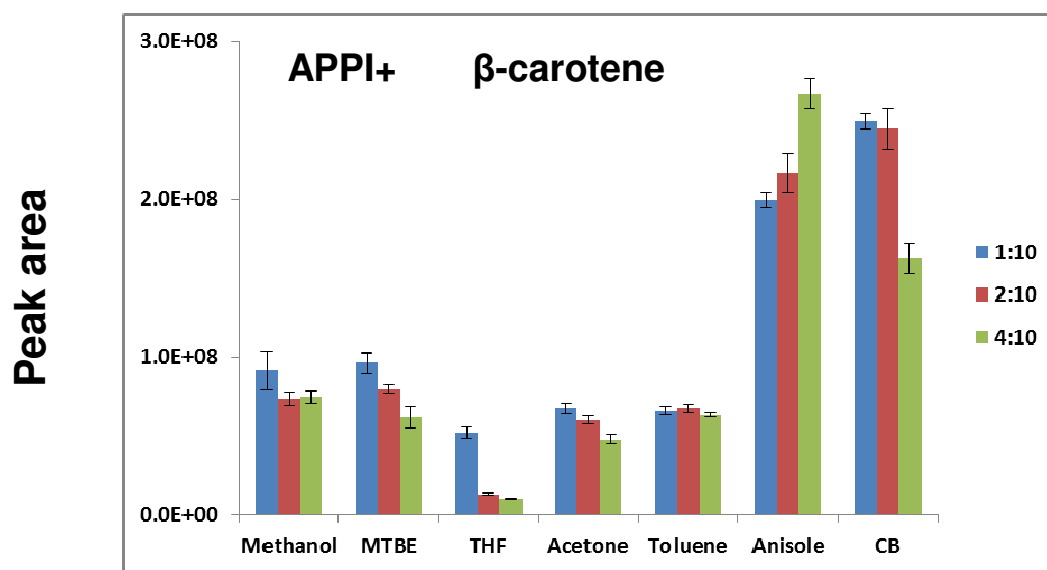
cations as the most abundant ions for lutein and zeaxanthin respectively which was identical to positive ion APCI.^[123]

During positive ion APPI, chlorobenzene, followed closely by anisole, were the most efficient dopants for lycopene, α -carotene, β -carotene, lutein, and zeaxanthin at nearly all three dopant addition ratios (Figures 35-39). The dopant chlorobenzene enhanced the peak areas of the most abundant analyte ion for each carotenoid 2-3 fold compared with the methanol solvent alone. In contrast, the dopants MTBE, acetone and toluene did not significantly enhance carotenoid ionization during positive ion APPI, which might be due to their much higher PA values compared with methanol.^[149] The addition of THF to methanol as a dopant was even less effective than methanol alone in the ionization of carotenes during positive ion APPI (Figures 35-37).



Dopants

Figure 35. Dopant effects on α -carotene ionization during positive ion APPI mass spectrometry. Key: blue (1:10), red (2:10), and green (4:10) represent 3 different dopant addition ratios: 20, 40, 80 $\mu\text{L}/\text{min}$ with a mobile phase flow rate of 200 $\mu\text{L}/\text{min}$.



Dopants

Figure 36. Dopant effects on β -carotene ionization during positive ion APPI mass spectrometry.

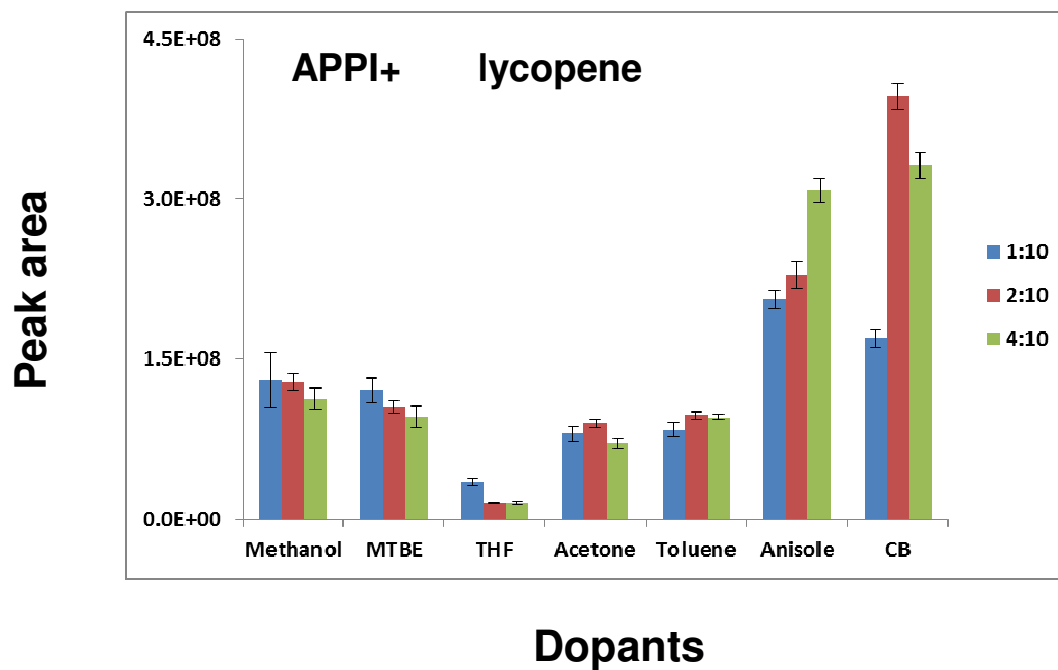


Figure 37. Dopant effects on lycopene ionization during positive ion APPI mass spectrometry.

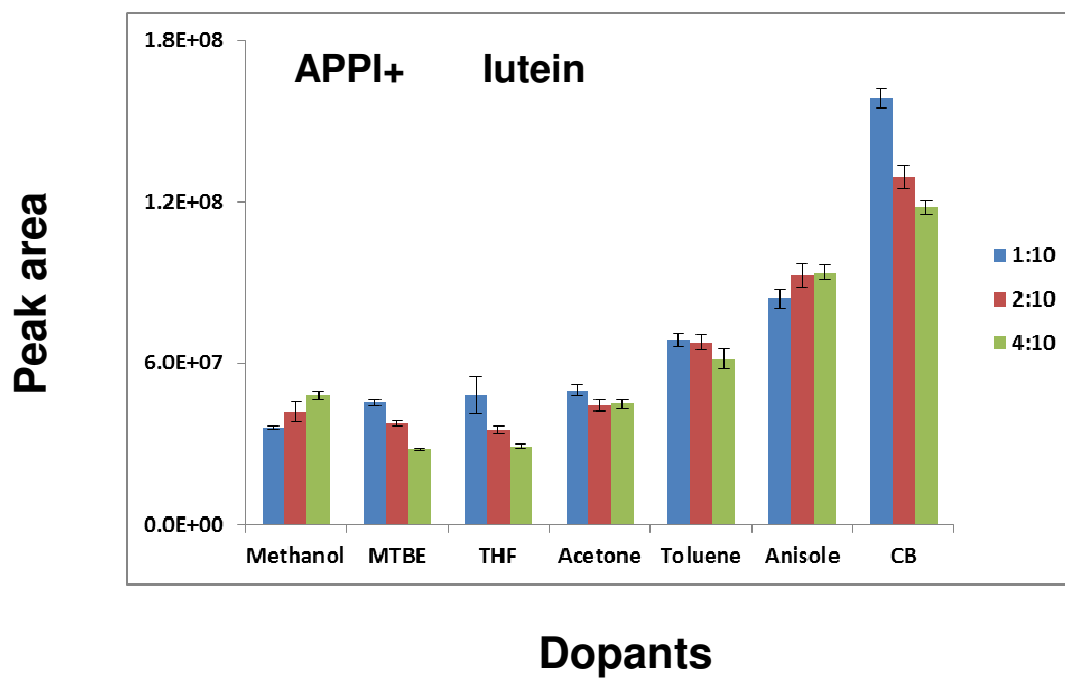


Figure 38. Dopant effects on lutein ionization during positive ion APPI mass spectrometry.

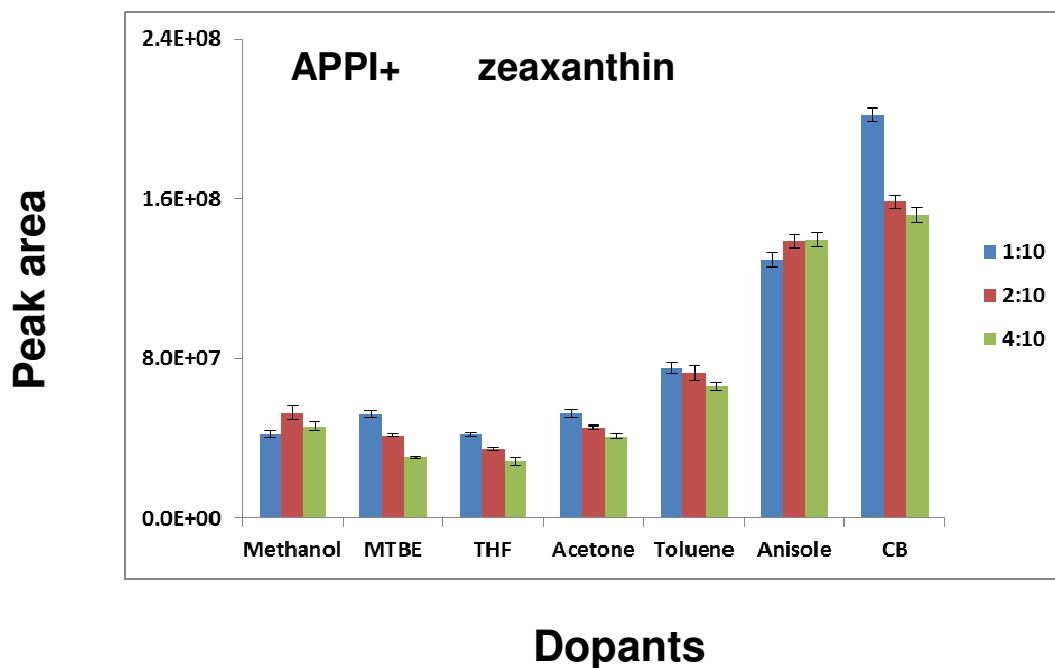


Figure 39. Dopant effects on zeaxanthin ionization during positive ion APPI mass spectrometry.

The poor performance of THF as a dopant for the non-polar carotenes was similar to that reported by Cai *et al.* for some non-polar drug candidates.^[96] Rivera *et al.* reported similar results for carotenoid ionization during positive ion APPI using the dopants chlorobenzene, anisole, toluene, and acetone.^[100] Note that Rivera and coworkers did not investigate negative ion APPI nor did they use MTBE as a dopant. However, their results that chlorobenzene outperformed anisole as a dopant for the positive ion APPI analysis of carotenes was consistent with the results reported here. Since Rivera *et al.* used different solvents and different instrumentation, it is not surprising that they reported some minor differences from our data such as finding that anisole was superior to chlorobenzene as a dopant for lutein analysis and that acetone was a better dopant for zeaxanthin. In summary,

our data and the literature are consistent in concluding that dopant-assisted APPI provides better sensitivity than direct APPI for the analysis of carotenoids.

4.3.2 Negative ion APPI MS

Except for the observation of deprotonated molecules of lutein and zeaxanthin at m/z 567 (Figure 40), none of the carotenes tested formed steady ions during negative ion APPI in methanol. With the addition of any dopant (Table IX), abundant $[M-H]^-$ ions were observed for all carotenes (Figure 41) and xanthophylls. Although the deprotonated molecules were always abundant when dopants were used, there were a few cases in which radical anions were the base peaks instead, such as in the negative ion APPI mass spectra of β -carotene and lycopene. Since the deprotonated carotenoids were not usually abundant in negative ion electrospray or APCI mass spectra,^[125] these new data add valuable information to what we reported previously on carotenoid ionization using negative ion electrospray, APCI, and FAB.^[124]

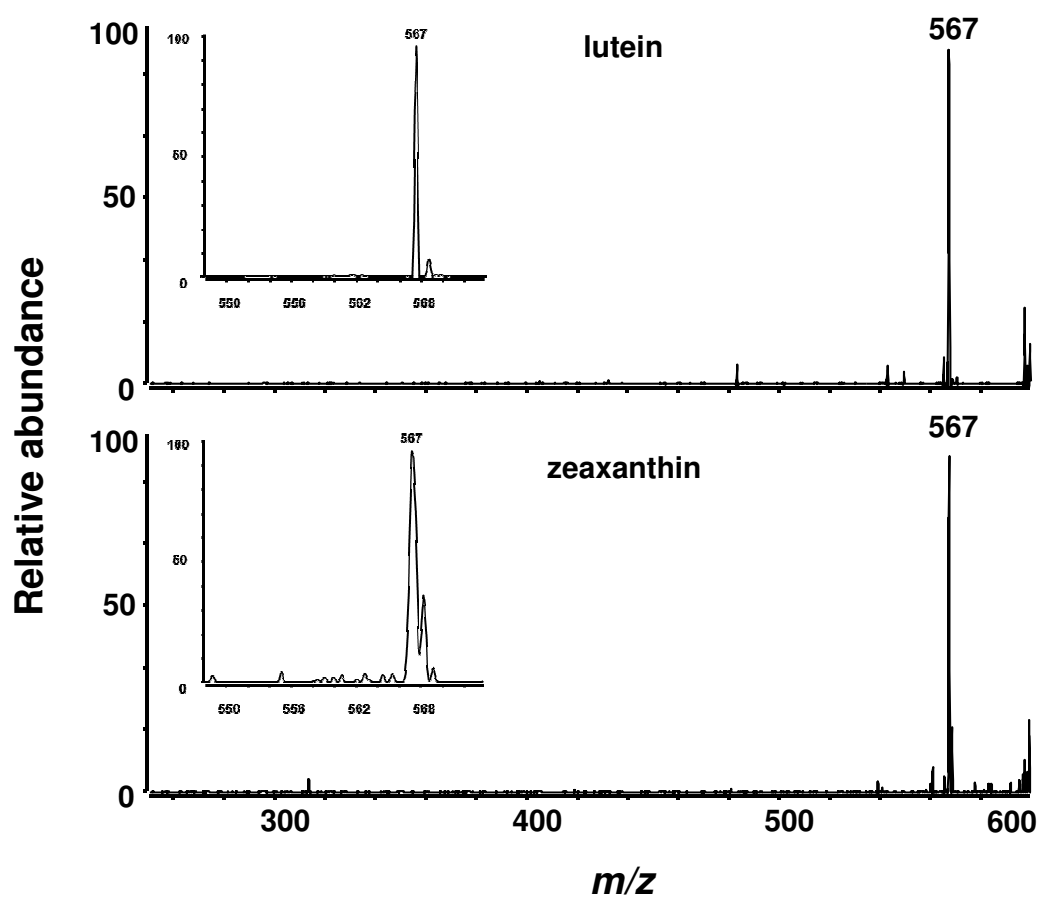


Figure 40. Negative ion APPI mass spectra of xanthophylls (no dapant)

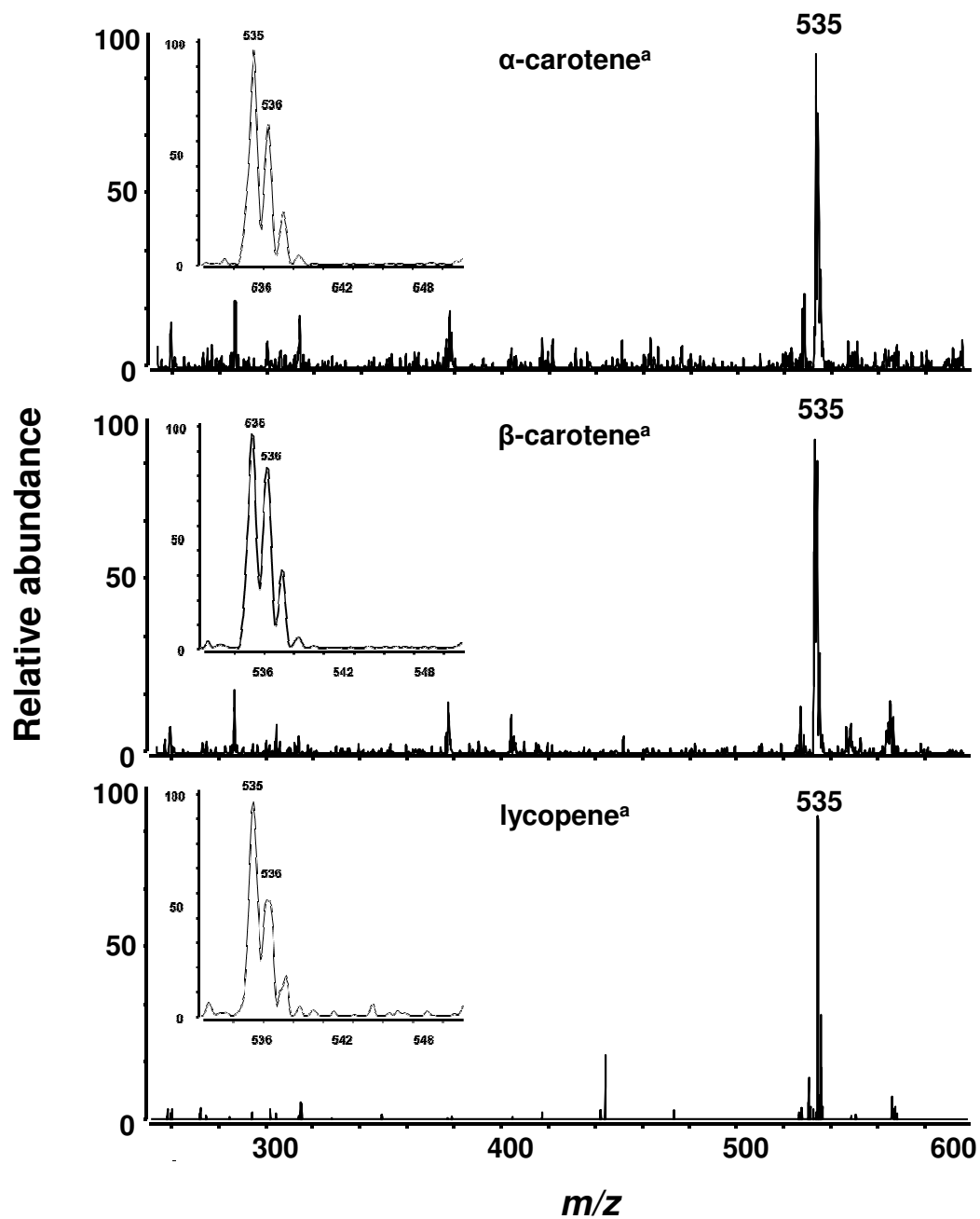


Figure 41. Negative ion APPI mass spectra of carotenoids

^a MTBE was used as the dopant since no steady signals were observed without a dopant.

TABLE IX
MAJOR IONS OBSERVED IN THE NEGATIVE APPI MASS SPECTRA OF INVESTIGATED CAROTENOIDS UNDER
DIFFERENT DOPANT CONDITIONS

Carotenoid	Formula	Ion	DOPANT						
			Methanol	MTBE	THF	Acetone	Toluene	Anisole	Chlorobenzene
α -carotene	$C_{40}H_{56}$	M^-	ND ^c	536.4(66.1) ^a	536.4(58.7)	536.4(98.9)	536.4(69.3)	536.4(92.5)	536.4(71.7)
		$[M-H]^-$	ND	535.4(100) ^b	535.4(100)	535.4(100)	535.4(100)	535.4(100)	535.4(100)
β -carotene	$C_{40}H_{56}$	M^-	ND	536.4(84.0)	536.4(76.2)	536.4(100)	536.4(77.9)	536.4(100)	536.4(74.8)
		$[M-H]^-$	ND	535.4(100)	535.4(100)	535.4(77.1)	535.4(100)	535.4(78.5)	535.4(100)
Lycopene	$C_{40}H_{56}$	M^-	ND	536.4(62.4)	536.4(75.8)	536.4(100)	536.4(72.6)	536.4(85.9)	536.4(97.9)
		$[M-H]^-$	ND	535.4(100)	535.4(100)	535.4(77.6)	535.4(100)	535.4(100)	535.4(100)
Lutein	$C_{40}H_{56}O_2$	M^-	ND	ND	ND	ND	ND	ND	ND
		$[M-H]^-$	567.4(100)	567.4(100)	567.4(100)	567.4(100)	567.4(100)	567.4(100)	567.4(100)
Zeaxanthin	$C_{40}H_{56}O_2$	M^-	ND	ND	ND	ND	ND	ND	ND
		$[M-H]^-$	567.4(100)	567.4(100)	567.4(100)	567.4(100)	567.4(100)	567.4(100)	567.4(100)

^a m/z (relative abundance)

^b Bold-face indicates the most abundant ion of each analyte

^c Not detected

During negative ion APPI in methanol containing no dopant, carotenes produced no stable signals and the xanthophylls formed deprotonated molecules as only low levels (Figures 42-46). However, every dopant at every ratio facilitated the formation of deprotonated carotenes and enhanced the formation of deprotonated xanthophylls. Among the 6 dopants investigated, MTBE produced the highest signals overall, but acetone showed comparable effects for the photoionization of lutein and zeaxanthin (Figures 45-46).

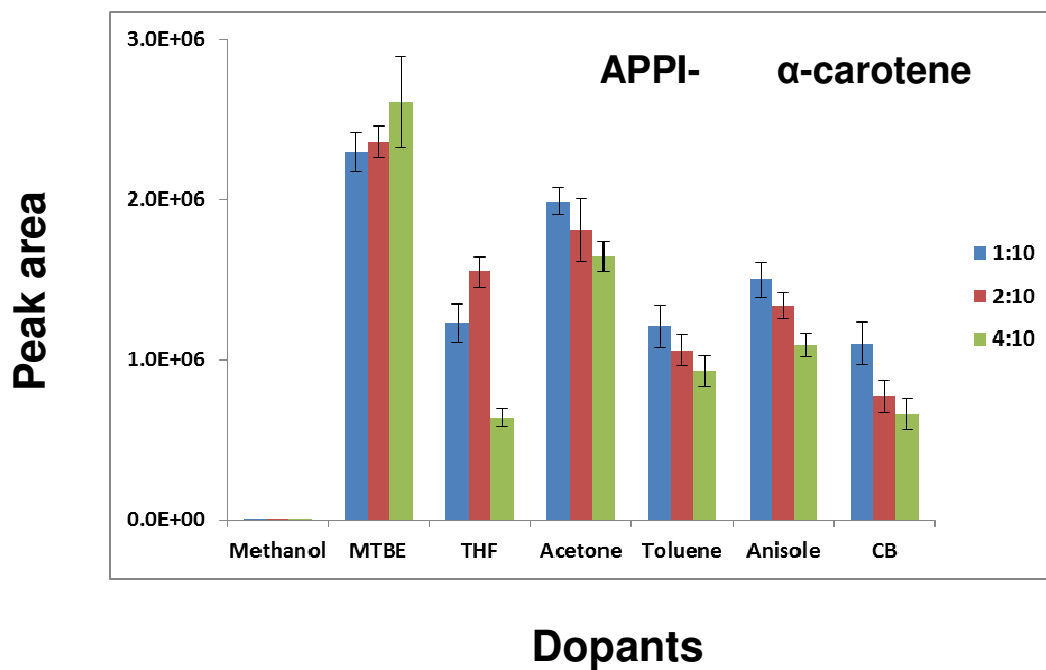


Figure 42. Dopant effects on α -carotene ionization during negative ion APPI mass spectrometry. The color key indicates ratios of dopant to the solvent methanol.

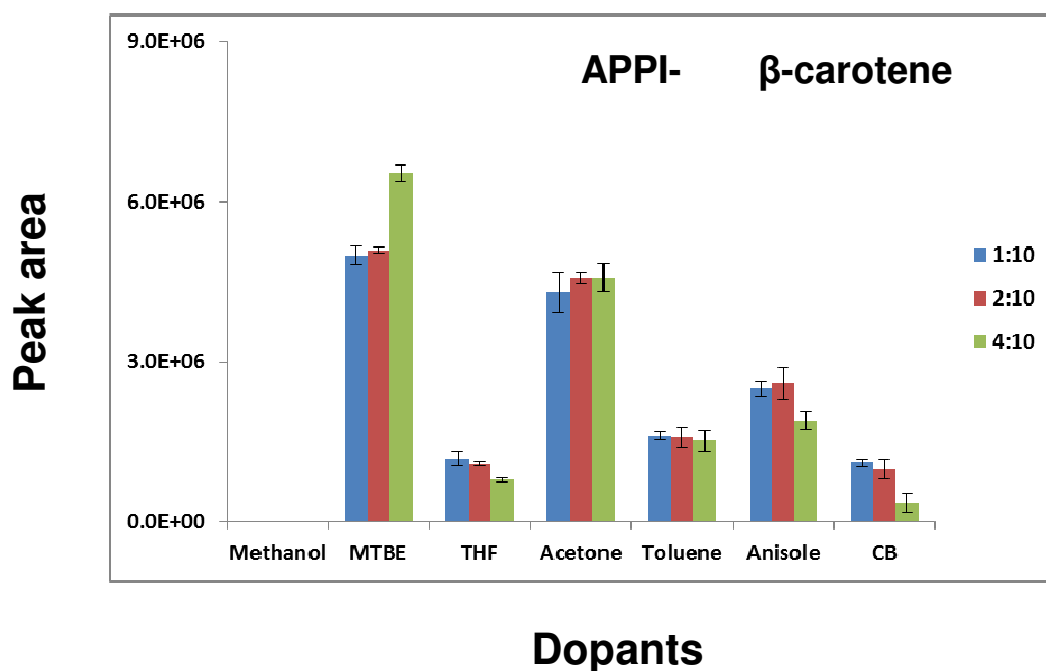


Figure 43. Dopant effects on β -carotene ionization during negative ion APPI mass spectrometry.

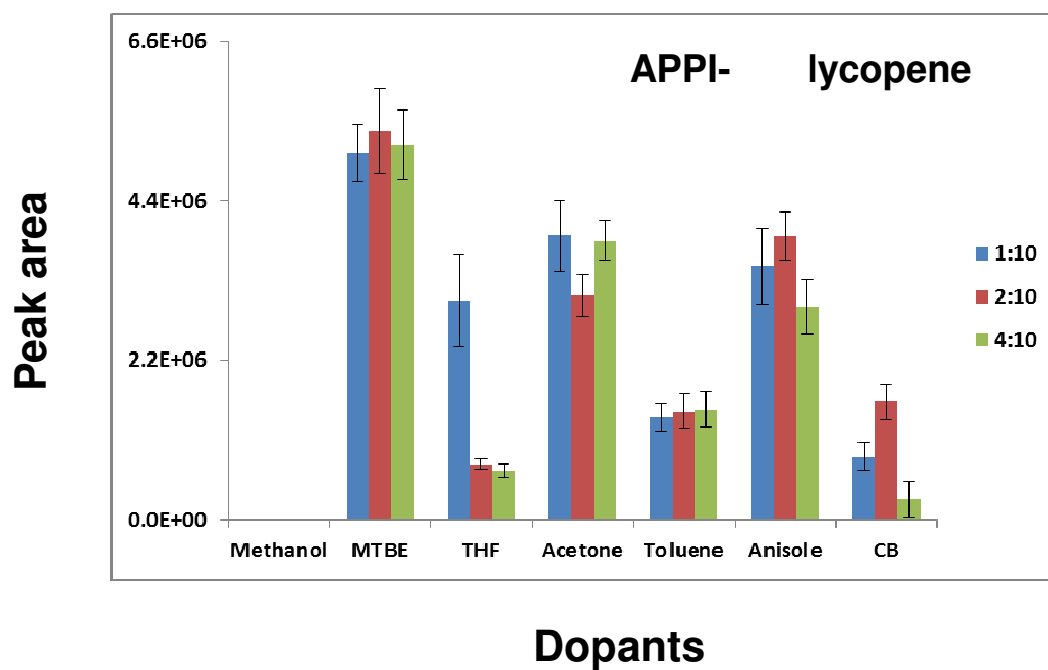


Figure 44. Dopant effects on lycopene ionization during negative ion APPI mass spectrometry.

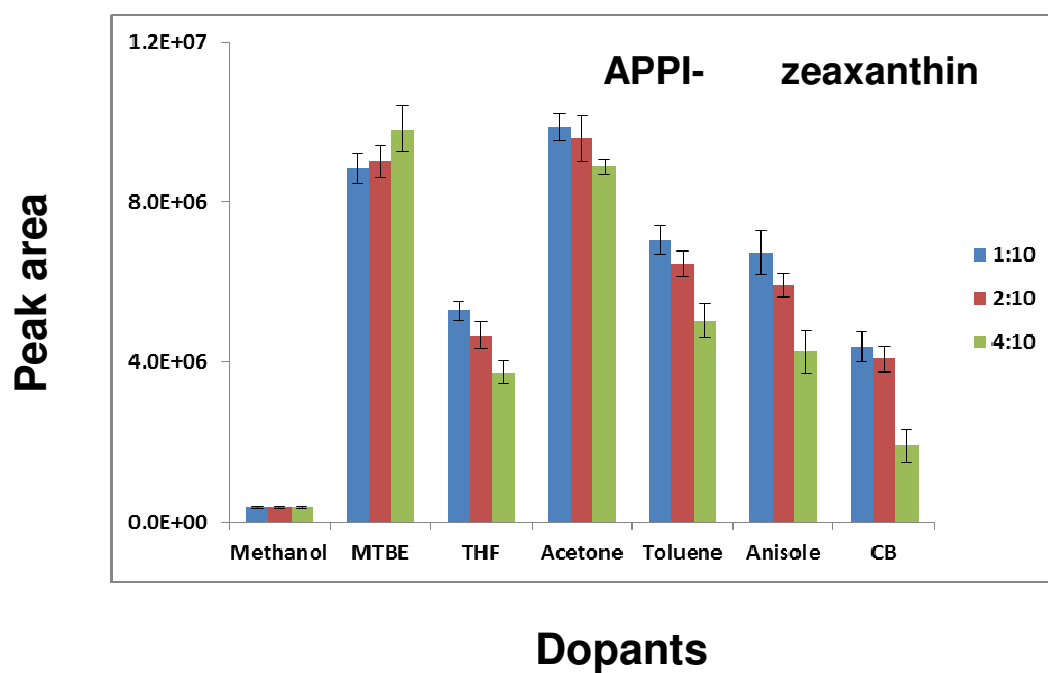


Figure 45. Dopant effects on lutein ionization during negative ion APPI mass spectrometry.

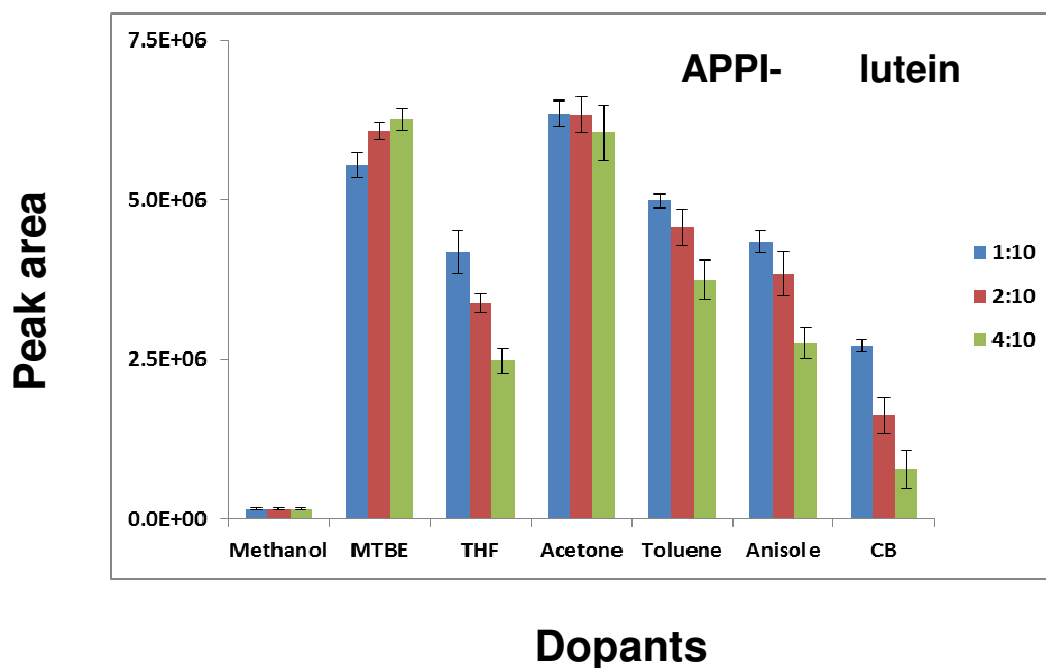


Figure 46. Dopant effects on zeaxanthin ionization during negative ion APPI mass spectrometry.

Three ratios of dopant-to-solvent were investigated for each carotenoid including 1:10, 2:10 and 4:10 (v/v). The results for both positive ion APPI and negative ion APPI are summarized in Figures 35-39 and 42-46. There were instances where each dopant ratio showed superior results for a particular dopant and a particular carotenoid. Since only minor differences were observed between the different dopant ratios that were evaluated, a dopant to eluent ratio of 1:10 appears to be a good starting point and is typical of ratios used in the literature.^[149] When measuring specific carotenoids using APPI mass spectrometry, optimization of dopant addition ratios should be carried out to achieve maximum signal-to-noise.^[162]

Comparing positive ion APPI using chlorobenzene as a dopant with negative ion APPI using MTBE as the dopant, only 1-2% as much signal was observed in negative ion mode. Significantly lower response during negative ion APPI does not appear to be limited to carotenoids, as similar results have been reported for avermectins^[166] and acylglycerol lipids.^[144, 145] However, even though lower MS signals were detected, the noise levels were also reduced during negative ion APPI using MTBE as the dopant. As shown in Table X, the same magnitude of signal to noise ratios were found in both ionization modes, with only up to 2.6-fold higher S/N ratio during positive ion APPI using chlorobenzene as the dopant for the analysis of lutein. The results suggest that negative ion APPI may still be used as an alternative approach to analyze samples suffered from positively charged interferences.

TABLE X
COMPARISON OF THE SIGNAL TO NOISE RATIO OF
CAROTENOID PEAKS BETWEEN POSITIVE AND NEGATIVE ION APPI

Carotenoid	Peak-to-peak signal to noise ratio ^a (mean \pm SD)	
	DOPANT, ion	
	Chlorobenzene, M ⁺	MTBE, [M-H] ⁻
α -carotene	275 \pm 31	152 \pm 9
β -carotene	137 \pm 19	98 \pm 3
Lycopene	152 \pm 23	130 \pm 12
Lutein	545 \pm 67	206 \pm 10
Zeaxanthin	657 \pm 84	351 \pm 21

^a Peak-to-peak signal to noise ratios calculated by 5 FIA replicates at a dopant-to-solvent ratio of 1:10 (v/v).

4.3.3 Negative ion APPI MS-MS

Positive ion APPI produced protonated molecules and molecular cations of carotenes and xanthophylls. However, these molecular ion species have been observed previously using electrospray, FAB and/or APCI.^[68, 123-125, 138, 142, 167] Unlike FAB and electrospray which produced no molecular ions species in negative ion mode, and unlike negative ion APCI which produced only M⁻ species, deprotonated molecules and sometimes molecular anions were observed during APPI with dopants. As the product ion tandem mass spectra of [M+H]⁺, M⁺, and M⁻ produced by α -carotene, β -carotene,

lycopene, lutein, and zeaxanthin during FAB and/or APCI have been interpreted previously by our laboratory,^[68, 123-125, 138, 142, 167] the unique product ion tandem mass spectra of the $[M-H]^-$ species are presented herein. Compared with carotene molecular ions formed during APCI, electrospray or FAB, deprotonated carotenoids produced simpler and less informative product ion tandem mass spectra.

4.3.3.1 Carotenes

During negative ion APPI with dopants, the isomeric carotenes α -carotene, β -carotene, and lycopene formed $[M-H]^-$ ions of m/z 535 instead of molecular anions. In the product ion tandem mass spectra of these $[M-H]^-$ ions, no significant differences were observed between α -carotene and β -carotene (Figure 47A and 47B). Both compounds formed fragment ions of m/z 243 and 429, which represented one double bond cleavage of the polyene chain, $[M-H-292]^-$ and loss of xylene, $[M-H-106]^-$ (Figure 47A and 47B). Compared with α -carotene and β -carotene, product ion tandem mass spectra of lycopene showed a distinguishing ion of m/z 397 corresponding to the elimination of two terminal isoprene groups (Figure 47C), which can be used to distinguish lycopene from α -carotene and β -carotene.

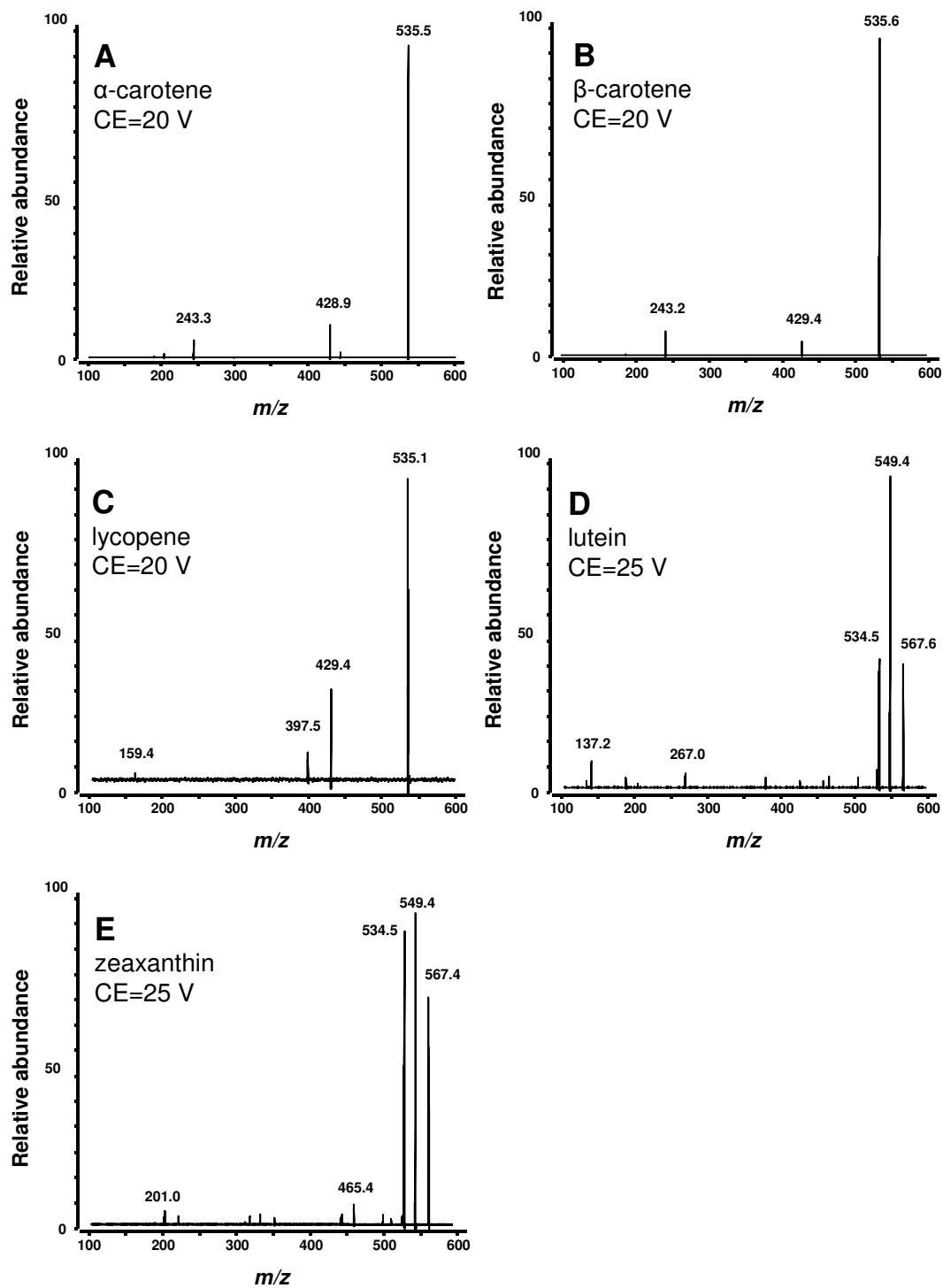


Figure 47. Negative ion APPI tandem mass spectra with CID of the deprotonated molecules of α -carotene (A), β -carotene (B), lycopene (C), lutein (D), and zeaxanthin (E).

Our previous investigation of the fragmentation pathways of carotene molecular anions during negative ion APCI indicated that structurally significant fragment ions were formed that could be used to distinguish all three isomeric carotenes α -carotene, β -carotene, and lycopene. For example, product ions of m/z 467 and 398 were characteristic of the acyclic terminal isoprene units of lycopene. Finally, α -carotene could be distinguished by the product ion of m/z 480 which was formed by retro-Diels-Alder fragmentation of the α -ionone ring.^[68]

4.3.3.2 Xanthophylls

During negative APPI, the product ion tandem mass spectra of lutein and zeaxanthin both showed product ions of m/z 549, $[M-H-H_2O]^-$ and m/z 534, $[M-H-H_2O-CH_3]^-$ (Figure 47D and 47E). However, no unique fragment ions were identified that could be used to distinguish between these isomeric xanthophylls. For comparison, lutein and zeaxanthin formed molecular anions during negative ion APCI and also fragmented to eliminate water or a molecule of water and a methyl radical. However, the radical anion of lutein also exhibited the unique fragment ions of m/z 429 and 512, corresponding to fragmentation within or adjacent to the α -ionone ring, respectively.^[68] These product ions were not observed in the corresponding APCI product ion tandem mass spectrum of zeaxanthin.

4.3.4 LC-APPI-MS-MS analysis of carotenoids

MTBE is an efficient organic modifier in the HPLC analysis of carotenoids and it has also showed noticeable dopant effect in this study. Therefore, LC-MS-MS analysis of a standard mixture of all-*trans*-lycopene, all-*trans*- β -carotene and all-*trans*-zeaxanthin

were carried out to demonstrate these advantages. As shown in Figure 48, the peak areas increased 2.2-fold for zeaxanthin, 2-fold for lycopene, 1.7-fold for β -carotene during positive ion APPI when compared with positive ion APCI. The SRM transition used to detect zeaxanthin was m/z 569 > 135 which corresponded to the dehydrated terminal ring with cleavage at the 7,8 carbon-carbon bond.^[68] The SRM transition selected to detect lycopene and β -carotene was m/z 537 > 121 due to higher abundance, which formed by a polyene chain cleavage. An example of positive ion APPI LC-MS-MS analysis of a human serum sample showing the detection of these carotenoids is shown in Figure 49.

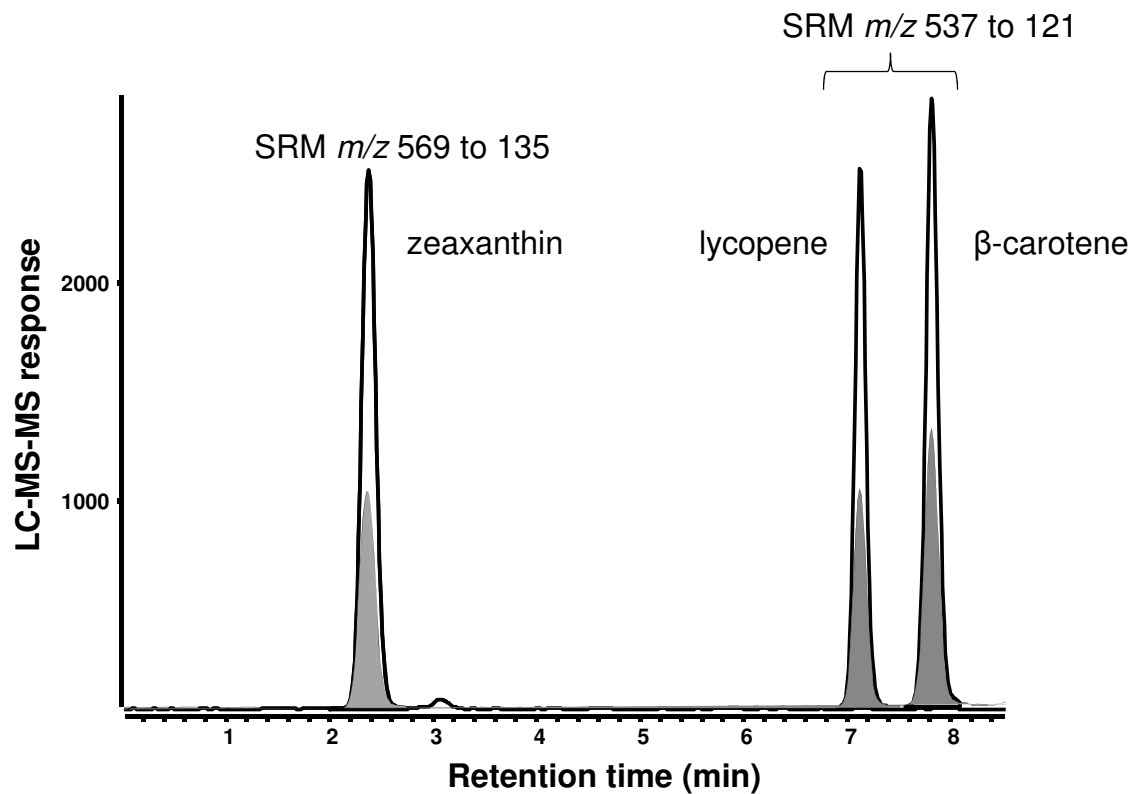


Figure 48. Positive ion APPI and APCI (filled traces with lower abundances) SRM chromatograms showing the detection of zeaxanthin (m/z 569 to 135), lycopene and β -carotene (m/z 537 to 121) in a standard mixture at 3 μ g/mL.

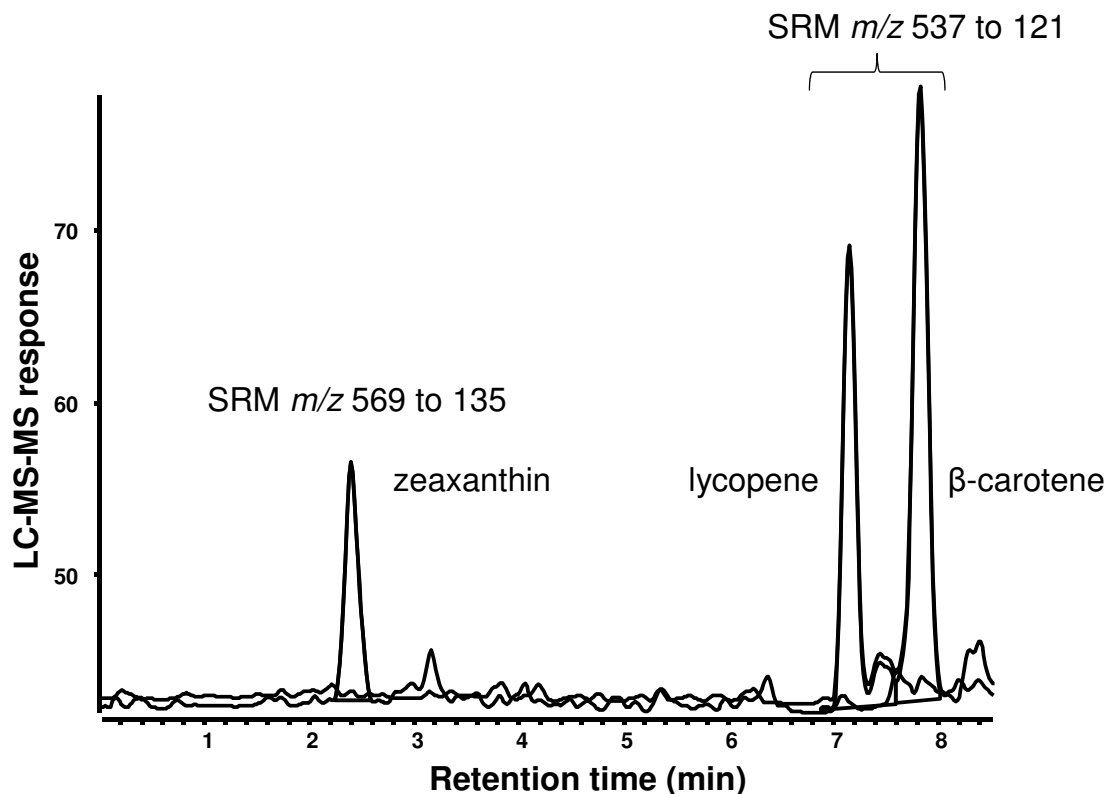


Figure 49. Positive ion APPI SRM chromatograms showing the detection of zeaxanthin (m/z 569 to 135, may also contain lutein), lycopene and β -carotene (m/z 537 to 121, may also contain α -carotene) in a human serum sample.

Since no product ion species were produced at high abundance during CID tandem mass spectrometry of zeaxanthin and β -carotene radical anions and deprotonated molecules, SRM transitions of m/z 567 > 567 vs m/z 568 > 568 and m/z 535 > 535 vs m/z 536 > 536 were used for the comparison of LC-MS-MS response during negative ion APPI and APCI of all three selected carotenoids. Compared with the observed peak areas during negative ion APCI, negative ion APPI showed 2.9-fold increase for zeaxanthin, 1.3-fold increase for lycopene, and 2.5-fold increase for β -carotene (Figure 50).

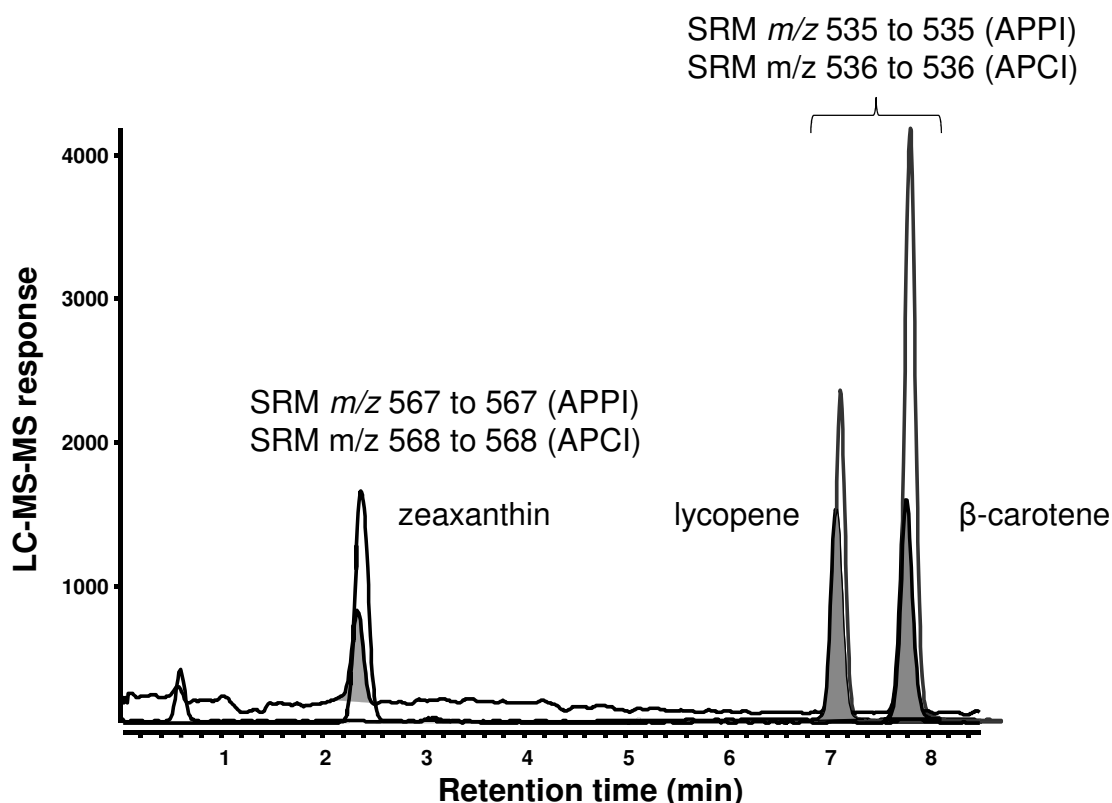


Figure 50. Negative ion APPI and APCI (filled traces with lower abundances) SRM chromatograms showing the detection of zeaxanthin (APPI: m/z 567 to 567; APCI: m/z 568 to 568), lycopene and β -carotene (APPI: m/z 535 to 535; APCI: m/z 536 to 536) in a standard mixture at $3\mu\text{g/mL}$.

In summary, similar or slightly better SRM responses were observed for zeaxanthin, lycopene and β -carotene when switched from APCI to APPI. In addition, the dopant effect of mobile phase constituent MTBE for carotenoids may also simplify the method transfer process from existing APCI based LC-MS assays.

4.4 Conclusions

While confirming previous studies on the use of dopants to enhance carotenoid ionization during positive ion APPI, we report the discovery that carotenoids can also be

ionized during negative ion APPI. The preferential formation of deprotonated molecules during negative ion APPI has not been reported using previous ionization techniques including FAB, electrospray or APCI. Unfortunately, the signal-to-noise of the deprotonated carotenoids was inferior to that obtained using positive ion APPI. Furthermore, fewer structurally significant fragment ions were observed in the product ion tandem mass spectra of carotenoids following negative ion APPI than have been reported using negative ion APCI. Therefore, negative ion APPI does not appear to be preferable to positive ion mode or to negative ion APCI for carotenoid analysis.

As reported previously for positive ion APPI of carotenoids, dopants were essential to enhance carotenoid ionization not only in positive ion mode but also during negative ion APPI. Without dopant addition, carotenes could not be ionized using the negative ion APPI, and xanthophyll signals were barely detectable. The dopants chlorobenzene and anisole were found to be the most effective for the ionization of carotenoids during positive ion APPI, and MTBE and acetone produced the most abundant carotenoid signals during negative ion APPI mass spectrometry.

During these studies, MTBE was evaluated as a new dopant for APPI and was found to provide the strongest signals of all dopants evaluated to date for negative ion APPI of carotenoids. As a frequently used mobile phase solvent or organic modifier for carotenoids HPLC, the utility of MTBE as a dopant during APPI is a useful discovery. The utility of MTBE as a dopant for APPI analysis of other classes of compounds might be worthy of future investigation.

No matter what dopants are used, the compositions of mobile phases, dopants, diluents, and their flow rates require optimization for carotenoid analysis. All these

parameters need to be fine-tuned in order to achieve the best sensitivity for a specific carotenoid. APPI is newer than electrospray or APCI, and ion source design continues to evolve.^[149] In the future, newer APPI sources might be redesigned to provide greater efficiency that enables the use of lower concentrations of dopant and improved limits of detection for carotenoids.^[168]

5. MAIN CONCLUSIONS AND FUTURE DIRECTIONS

Many natural occurring compounds, such as carotenoids, epigallocatechin gallate (EGCG), silibinin, genistein, vitamin D, and vitamin E, are under investigation as potential prostate cancer chemoprevention agents.^[28] Lycopene, a carotene and highly unsaturated long chain hydrocarbon, may serve as an effective ROS quencher in the human body after consumption and, since lycopene is concentrated in the human prostate, may reduce prostate cancer risk.^[33] According to the FDA^[104] and recent review articles,^[33, 169] only very limited evidence exists to support an association between lycopene consumption and prostate cancer prevention. Among published studies of prostate cancer chemoprevention by lycopene, most have been observational instead of interventional, and serum or tissue levels of lycopene were often not determined. Furthermore, the subjects enrolled in these studies were frequently suffering from prostate cancer or other prostatic diseases so that the results would need to be extrapolated to healthy men. Taken together, the majority of the published studies on lycopene and prostate cancer chemoprevention may be considered inconclusive, biased or even invalid.

In order to better address research questions regarding lycopene intervention and prostate cancer risk, we carried out a randomized placebo-controlled intervention trial evaluating the effects of lycopene supplementation on markers of oxidative stress in healthy men. A validated LC-MS-MS assay was used to accurately quantify serum levels of lycopene in each enrolled subject at 3 time points. Two additional validated LC-MS-MS assays were used to measure two systemic oxidative stress biomarkers of

study subjects before and after receiving lycopene supplementation or placebo. Prostate cancer screening biomarkers, PSA and free PSA in the serum, were to be determined by ELISA.

In the lycopene intervention study, a significant increase of serum levels of lycopene was observed following 21-day supplementation of either 30 or 60 mg/d lycopene. Doubling the lycopene intervention dosage did not change serum levels of lycopene dramatically. Although no significant changes were found for the levels of urinary 8-oxo-dG and 8-iso-PGF_{2α} in men randomized for intervention, a trend of reduced oxidative stress was observed in response to 60 mg/d lycopene dietary supplementation. Even though the dosage of lycopene was higher than in most previous studies, no pro-oxidant effects were observed. The trends of lower 8-oxo-dG and 8-iso-PGF_{2α} in urine from men receiving 60 mg/d lycopene might become significant if a larger number of subjects were to be evaluated. As new biomarkers of oxidative stress and prostate cancer risk become available, they should be evaluated in future clinical trials of lycopene at 60 mg/d as well as 30 mg/d.

Previously, we had observed a significant decrease of total PSA and no change in percent free PSA in serum of men receiving lycopene 30 mg/d for 21 days.^[42] However, the ELISA kits that were used for the 30 mg/d lycopene supplementation study are no longer available, and the current kits lack sufficient sensitivity for measuring PSA in serum from healthy men. Therefore, whether 60 mg/d lycopene supplementation produces similar or even stronger effects on total PSA and percent free PSA remains to be determined. We look forward to analyzing both PSA and free PSA levels in the future.

In our exploration of the utility of IM-MS and IM-MS-MS for carotenoid analysis, the separations of cis and all-trans isomers of lycopene, β -carotene, lutein, and zeaxanthin were accomplished using IMS with drift times from 1-4 ms.^[138] Although the cis and trans isomers could be resolved from each other, the various cis isomers produced a single, unresolved peak during IMS. After separation of the cis and all-trans carotenoid isomers using IMS, unique tandem mass spectra were obtained that may be used to distinguish them. However, cis/trans isomerization was found to occur in the ion source in a temperature dependent manner.

Although cis/trans isomerization could not be eliminated during electrospray, this temperature dependence suggests that softer ionization conditions can minimize cis/trans isomerization in the ion source. Therefore, a nanoelectrospray source operated at or below room temperature might be able to prevent or at least minimize isomerization thereby enabling the IM-MS-MS characterization and identification of geometric carotenoid isomers. This research has advanced carotenoid mass spectrometry toward the goal of separating and identifying carotenoids and their geometric isomers in a millisecond time scale instead of minute time scale of chromatography.

APPI is a relatively new ionization technique for carotenoid analysis. Unlike electrospray and APCI, APPI relies on carefully selected dopants to efficiently ionize carotenonids. During positive ion APPI, we confirmed literature reports that anisole and Chlorobenzene were superior dopants for carotenoid ionization. In this dissertation, the first negative ion APPI mass spectra of carotenoids were obtained. Not reported previously as a dopant for APPI, MTBE was identified among a set of candidate compounds as the most effective dopant for the formation of deprotonated carotenoids.

Although further investigation on the in-depth mechanisms of MTBE is required, it is likely that MTBE might facilitate the photoionization of analytes besides carotenoids due to its relatively low IE.

Deprotonated carotenoids were found to be the most abundant species in negative ion APPI, which is different from the molecular anions that are formed during negative ion APCI of carotenoids. Unfortunately, no unique fragment ions were observed during product ion tandem mass spectrometric analysis of the deprotonated carotenoids that might have provided structural information not otherwise available using negative ion APCI. Also, the development of more sensitive APPI ion sources and dopants will be needed before APPI LC-MS can compete with APCI LC-MS for carotenoid analysis.

CITED LITERATURE

1. Jemal, A.; Bray, F.; Center, M. M.; Ferlay, J.; Ward, E.; Forman, D.: Global cancer statistics, *CA-Cancer J. Clin.*, 61: 69-90, 2011.
2. Siegel, R.; Naishadham, D.; Jemal, A.: Cancer statistics, 2013, *CA-Cancer J. Clin.*, 63: 11-30, 2013.
3. Everson, K. M.; McQueen, C. E.: Lycopene for prevention and treatment of prostate cancer, *Am. J. Health Syst. Pharm.*, 61: 1562-1566, 2004.
4. Sood, A. K.; Kim, H.; Geradts, J.: PDEF in prostate cancer, *Prostate*, 72: 592-596, 2012.
5. American Cancer Society. Cancer Facts & Figures 2010. Atlanta: American Cancer Society; 2010.
6. Locke, J. A.; Guns, E. S.; Lubik, A. A.; Adomat, H. H.; Hendy, S. C.; Wood, C. A.; Ettinger, S. L.; Gleave, M. E.; Nelson, C. C.: Androgen levels increase by intratumoral De novo steroidogenesis during progression of castration-resistant prostate cancer, *Cancer Res.*, 68: 6407-6415, 2008.
7. Vis, A. N.; Schröder, F. H.: Key targets of hormonal treatment of prostate cancer. Part 1: the androgen receptor and steroidogenic pathways, *BJU Int.*, 104: 438-448, 2009.
8. Fang, L. C.; Merrick, G. S.; Wallner, K. E.: Androgen deprivation therapy: a survival benefit or detriment in men with high-risk prostate cancer?, *Oncology (Williston Park)*, 24: 790-796, 798, 2010.
9. Ramon, J. *Prostate Cancer*; Berlin Heidelberg: Springer-Verlag GmbH, 2007.
10. Knudsen, B. S.; Vasioukhin, V. In *Advances in Cancer Research, Vol 109*; VandeWoude, G. F., Klein, G., Eds., 2010; Vol. 109,1-50.
11. Agalliu, I.; Gern, R.; Leanza, S.; Burk, R. D.: Associations of high-grade prostate cancer with BRCA1 and BRCA2 founder mutations, *Clin. Cancer Res.*, 15: 1112-1120, 2009.
12. Foulkes, W. D.: Inherited susceptibility to common cancers, *New Engl. J. Med.*, 359: 2143-2153, 2008.
13. Del Chiaro, M.: Cancer risks in BRCA2 mutation carriers, *J. Natl. Cancer Inst.*, 91: 1310-1316, 1999.

14. Henderson, B. E.; Lee, N. H.; Seewaldt, V.; Shen, H.: The influence of race and ethnicity on the biology of cancer, *Nat. Rev. Cancer*, 12: 648-653, 2012.
15. Haiman, C. A.; Chen, G. K.; Blot, W. J.; Strom, S. S.; Berndt, S. I.; Kittles, R. A.; Rybicki, B. A.; Isaacs, W. B.; Ingles, S. A.; Stanford, J. L.: Genome-wide association study of prostate cancer in men of African ancestry identifies a susceptibility locus at 17q21, *Nat. Genet.*, 43: 570-573, 2011.
16. Yeager, M.; Orr, N.; Hayes, R. B.; Jacobs, K. B.; Kraft, P.; Wacholder, S.; Minichiello, M. J.; Fearnhead, P.; Yu, K.; Chatterjee, N.: Genome-wide association study of prostate cancer identifies a second risk locus at 8q24, *Nat. Genet.*, 39: 645-649, 2007.
17. Amundadottir, L. T.; Sulem, P.; Gudmundsson, J.; Helgason, A.; Baker, A.; Agnarsson, B. A.; Sigurdsson, A.; Benediktsdottir, K. R.; Cazier, J.-B.; Sainz, J.: A common variant associated with prostate cancer in European and African populations, *Nat. Genet.*, 38: 652-658, 2006.
18. Cancel-Tassin, G.; Cussenot, O.: Prostate cancer genetics, *Minerva Urol. Nefrol.*, 57: 289-300, 2005.
19. Erkkö, H.; Xia, B.; Nikkila, J.; Schleutker, J.; Syrjäkoski, K., et al.: A recurrent mutation in PALB2 in Finnish cancer families, *Nature*, 446: 316-319, 2007.
20. Muller, R.; Faria, E.; Carvalhal, G.; Reis, R.; Mauad, E.; Carvalho, A.; Freedland, S.: Association between family history of prostate cancer and positive biopsies in a Brazilian screening program, *World J. Urol.*: 1-6, 2012.
21. Stanford, J. L.; Ostrander, E. A.: Familial prostate cancer, *Epidemiol. Rev.*, 23: 19-23, 2001.
22. Carter, B. S.; Bova, G. S.; Beaty, T. H.; Steinberg, G. D.; Childs, B.; Isaacs, W. B.; Walsh, P. C.: Hereditary prostate cancer: epidemiologic and clinical features, *J. Urol.*, 150: 797-802, 1993.
23. Sporn, M. B.; Dunlop, N. M.; Newton, D. L.; Smith, J. M.: Prevention of chemical carcinogenesis by vitamin A and its synthetic analogs (retinoids), *Fed. Proc.*, 35: 1332-1338, 1976.
24. Qiu, X.; Yuan, Y.; Vaishnav, A.; Tessel, M. A.; Nonn, L.; van Breemen, R. B.: Effects of lycopene on protein expression in human primary prostatic epithelial cells, *Cancer Prev. Res.*, 6: 419-427, 2013.
25. Gerhauser, C.: Cancer chemoprevention and nutriepigenetics: state of the art and future challenges, *Top. Curr. Chem.*, 329: 73-132, 2013.

26. Klein, E. A.; Thompson, I. M.: Chemoprevention of prostate cancer: an updated view, *World J. Urol.*, 30: 189-194, 2012.
27. Mehta, R. G.; Murillo, G.; Naithani, R.; Peng, X.: Cancer chemoprevention by natural products: how far have we come?, *Pharm. Res.*, 27: 950-961, 2010.
28. Ozten-Kandas, N.; Bosland, M. C.: Chemoprevention of prostate cancer: Natural compounds, antiandrogens, and antioxidants - In vivo evidence, *J. Carcinog.*, 10: 27, 2011.
29. Sebastiano, C.; Vincenzo, F.; Tommaso, C.; Giuseppe, S.; Marco, R.; Ivana, C.; Giorgio, R.; Massimo, M.; Giuseppe, M.: Dietary patterns and prostatic diseases, *Front. Biosci. (Elite Ed)*, 4: 195-204, 2012.
30. Velicer, C.; Ulrich, C.: Vitamin and mineral supplement use among US adults after cancer diagnosis: a systematic review, *J. Clin. Oncol.*, 26: 665, 2008.
31. Khan, N.; Afaq, F.; Mukhtar, H.: Cancer chemoprevention through dietary antioxidants: progress and promise, *Antioxid. Redox Signal.*, 10: 475-510, 2008.
32. Bagchi, D.; Preuss, H. G. *Phytopharmaceuticals in cancer chemoprevention*; CRC Press: Boca Raton, Fla., 2005.
33. van Breemen, R. B.; Pajkovic, N.: Multitargeted therapy of cancer by lycopene, *Cancer Lett.*, 269: 339-351, 2008.
34. Tanaka, T.; Shnimizu, M.; Moriwaki, H.: Cancer chemoprevention by carotenoids, *Molecules*, 17: 3202-3242, 2012.
35. Gupta, P.; Bansal, M. P.; Koul, A.: Spectroscopic characterization of lycopene extract from *Lycopersicum esculentum* (tomato) and its evaluation as a chemopreventive agent against experimental hepatocarcinogenesis in mice, *Phytother. Res.*, 27: 448-456, 2013.
36. Di Mascio, P.; Kaiser, S.; Sies, H.: Lycopene as the most efficient biological carotenoid singlet oxygen quencher, *Arch. Biochem. Biophys.*, 274: 532-538, 1989.
37. Bohm, F.; Edge, R.; Truscott, G.: Interactions of dietary carotenoids with activated (singlet) oxygen and free radicals: potential effects for human health, *Mol. Nutr. Food Res.*, 56: 205-216, 2012.
38. Muzandu, K.; Ishizuka, M.; Sakamoto, K. Q.; Shaban, Z.; El Bohi, K.; Kazusaka, A.; Fujita, S.: Effect of lycopene and beta-carotene on peroxynitrite-mediated cellular modifications, *Toxicol. Appl. Pharmacol.*, 215: 330-340, 2006.

39. Muzandu, K.; El Bohi, K.; Shaban, Z.; Ishizuka, M.; Kazusaka, A.; Fujita, S.: Lycopene and beta-carotene ameliorate catechol estrogen-mediated DNA damage, *Jap. J. Vet. Res.*, 52: 173-184, 2005.
40. Park, Y. O.; Hwang, E. S.; Moon, T. W.: The effect of lycopene on cell growth and oxidative DNA damage of Hep3B human hepatoma cells, *BioFactors*, 23: 129-139, 2005.
41. Liu, A.; Pajkovic, N.; Pang, Y.; Zhu, D.; Calamini, B.; Mesecar, A. L.; van Breemen, R. B.: Absorption and subcellular localization of lycopene in human prostate cancer cells, *Mol. Cancer Ther.*, 5: 2879-2885, 2006.
42. Liu, A. 3364823, University of Illinois at Chicago, Health Sciences Center, United States -- Illinois, 2009.
43. Goo, Y. A.; Li, Z.; Pajkovic, N.; Shaffer, S.; Taylor, G.; Chen, J.; Campbell, D.; Arnstein, L.; Goodlett, D. R.; van Breemen, R. B.: Systematic investigation of lycopene effects in LNCaP cells by use of novel large-scale proteomic analysis software, *Proteomics Clin. Appl.*, 1: 513-523, 2007.
44. Giovannucci, E.: Tomatoes, tomato-based products, lycopene, and cancer: Review of the epidemiologic literature, *J. Natl. Cancer Inst.*, 91: 317-331, 1999.
45. Mills, P. K.; Beeson, W. L.; Phillips, R. L.; Fraser, G. E.: Cohort study of diet, lifestyle, and prostate-cancer in adventist men, *Cancer*, 64: 598-604, 1989.
46. Giovannucci, E.; Ascherio, A.; Rimm, E. B.; Stampfer, M. J.; Colditz, G. A.; Willett, W. C.: Intake of carotenoids and retinol in relation to risk of prostate-cancer, *J. Natl. Cancer Inst.*, 87: 1767-1776, 1995.
47. Gann, P. H.; Ma, J.; Giovannucci, E.; Willett, W.; Sacks, F. M.; Hennekens, C. H.; Stampfer, M. J.: Lower prostate cancer risk in men with elevated plasma lycopene levels: results of a prospective analysis, *Cancer Res.*, 59: 1225-1230, 1999.
48. Nomura, A. M.; Stemmermann, G. N.; Lee, J.; Craft, N. E.: Serum micronutrients and prostate cancer in Japanese Americans in Hawaii, *Cancer Epidemiol. Biomarkers Prev.*, 6: 487-491, 1997.
49. Hsing, A. W.; Comstock, G. W.; Abbey, H.; Polk, B. F.: Serologic precursors of cancer. Retinol, carotenoids, and tocopherol and risk of prostate cancer, *J. Natl. Cancer Inst.*, 82: 941-946, 1990.
50. Chen, L.; Stacewicz-Sapuntzakis, M.; Duncan, C.; Sharifi, R.; Ghosh, L.; van Breemen, R.; Ashton, D.; Bowen, P. E.: Oxidative DNA damage in prostate cancer patients consuming tomato sauce-based entrees as a whole-food intervention, *J. Natl. Cancer Inst.*, 93: 1872-1879, 2001.

51. Key, T. J.; Appleby, P. N.; Allen, N. E.; Travis, R. C.; Roddam, A. W., et al.: Plasma carotenoids, retinol, and tocopherols and the risk of prostate cancer in the European Prospective Investigation into Cancer and Nutrition study, *Am. J. Clin. Nutr.*, 86: 672-681, 2007.
52. van Breemen, R. B.; Sharifi, R.; Viana, M.; Pajkovic, N.; Zhu, D.; Yuan, L.; Yang, Y.; Bowen, P. E.; Stacewicz-Sapuntzakis, M.: Antioxidant effects of lycopene in African American men with prostate cancer or benign prostate hyperplasia: a randomized, controlled trial, *Cancer Prev. Res. (Phila)*, 4: 711-718, 2011.
53. Kristal, A. R.; Till, C.; Platz, E. A.; Song, X.; King, I. B.; Neuhausser, M. L.; Ambrosone, C. B.; Thompson, I. M.: Serum lycopene concentration and prostate cancer risk: results from the Prostate Cancer Prevention Trial, *Cancer Epidemiol. Biomarkers Prev.*, 20: 638-646, 2011.
54. Giovannucci, E.: Commentary: Serum lycopene and prostate cancer progression: a re-consideration of findings from the prostate cancer prevention trial, *Cancer Causes Control*, 22: 1055-1059, 2011.
55. Lee, G. L.; Dobi, A.; Srivastava, S.: Prostate cancer: diagnostic performance of the PCA3 urine test, *Nat. Rev. Urol.*, 8: 123-124, 2011.
56. Wang, M. C.; Valenzuela, L. A.; Murphy, G. P.; Chu, T. M.: Purification of a human prostate specific antigen, *Invest. Urol.*, 17: 159-163, 1979.
57. Bermudez-Tamayo, C.; Martin Martin, J. J.; Gonzalez Mdel, P.; Perez Romero, C.: Cost-effectiveness of percent free PSA for prostate cancer detection in men with a total PSA of 4-10 ng/ml, *Urol. Int.*, 79: 336-344, 2007.
58. Xie, C.; Wang, G.: Development of simultaneous detection of total prostate-specific antigen (tPSA) and free PSA with rapid bead-based immunoassay, *J. Clin. Lab. Anal.*, 25: 37-42, 2011.
59. Christensson, A.; Laurell, C.-B.; Lilja, H.: Enzymatic activity of prostate-specific antigen and its reactions with extracellular serine proteinase inhibitors, *Eur. J. Biochem.*, 194: 755-763, 1990.
60. Zhu, L.; Jäämaa, S.; af Hällström, T. M.; Laiho, M.; Sankila, A.; Nordling, S.; Stenman, U.-H.; Koistinen, H.: PSA forms complexes with α 1-antichymotrypsin in prostate, *Prostate*, 73: 219-226, 2013.
61. Filella, X.; Alcover, J.; Molina, R.; Rodriguez, A.; Carretero, P.; Ballesta, A. M.: Clinical evaluation of free PSA/total PSA (prostate-specific antigen) ratio in the diagnosis of prostate cancer, *Eur. J. Cancer*, 33: 1226-1229, 1997.

62. Meany, D. L.; Zhang, Z.; Sokoll, L. J.; Zhang, H.; Chan, D. W.: Glycoproteomics for prostate cancer detection: changes in serum PSA glycosylation patterns, *J. Proteome. Res.*, 8: 613-619, 2009.
63. Catalona Wj, P. A. W. S. K. M.; et al.: Use of the percentage of free prostate-specific antigen to enhance differentiation of prostate cancer from benign prostatic disease: a prospective multicenter clinical trial, *JAMA*, 279: 1542-1547, 1998.
64. Selvadurai, E. D.; Singhera, M.; Thomas, K.; Mohammed, K.; Woode-Amissah, R.; Horwich, A.; Huddart, R. A.; Dearnaley, D. P.; Parker, C. C.: Medium-term outcomes of active surveillance for localised prostate cancer, *Eur. Urol.*, xx: xxx-xxx, 2013.
65. Dunn, B. K.; Akpa, E.: Biomarkers as surrogate endpoints in cancer trials, *Semin. Oncol. Nurs.*, 28: 99-108, 2012.
66. MacKinnon, D. P.; Lockwood, C. M.; Brown, C. H.; Wang, W.; Hoffman, J. M.: The intermediate endpoint effect in logistic and probit regression, *Clin. Trials*, 4: 499-513, 2007.
67. Cazzonelli, C. I.: Carotenoids in nature: insights from plants and beyond, *Funct. Plant Biol.*, 38: 833-847, 2011.
68. van Breemen, R. B.; Dong, L.; Pajkovic, N. D.: Atmospheric pressure chemical ionization tandem mass spectrometry of carotenoids, *Int. J. Mass spectrom.*, 312: 163-172, 2012.
69. Tan, J. S. L.; Wang, J. J.; Flood, V.; Rochtchina, E.; Smith, W.; Mitchell, P.: Dietary antioxidants and the long-term incidence of age-related macular degeneration: the Blue Mountains Eye Study, *Ophthalmology*, 115: 334-341, 2008.
70. Erdman Jr., J. W.; Thatcher, A. J.; Hofmann, N. E.; Lederman, J. D.; Block, S. S.; Lee, C. M.; Mokady, S.: All-trans beta-carotene is absorbed preferentially to 9-cis beta-carotene, but the latter accumulates in the tissues of domestic ferrets (*Mustela putorius puro*), *J. Nutr.*, 128: 2009-2013, 1998.
71. Boileau, A. C.; Merchen, N. R.; Wasson, K.; Atkinson, C. A.; Erdman, J. W., Jr: *cis*-lycopene is more bioavailable than *trans*-lycopene in vitro and in vivo in lymph-cannulated ferrets, *J. Nutr.*, 129: 1176-1181, 1999.
72. Shi, J.: Lycopene in tomatoes: chemical and physical properties affected by food processing, *Crit. Rev. Biotechnol.*, 20: 293-334, 2000.
73. O'Neil, C.; Schwartz, S.: Chromatographic analysis of cis-trans carotenoid isomers, *J. Chromatogr.*, 624: 235-252, 1992.

74. Rivera, S. M.; Canela-Garayoa, R.: Analytical tools for the analysis of carotenoids in diverse materials, *J. Chromatogr. A*, 1224: 1-10, 2012.
75. Furr, H. C.: Analysis of retinoids and carotenoids: problems resolved and unsolved, *J. Nutr.*, 134: 281S-285, 2004.
76. van Breemen, R. B.; Xu, X.; Viana, M. A.; Chen, L.; Stacewicz-Sapuntzakis, M.; Duncan, C.; Bowen, P. E.; Sharifi, R.: Liquid chromatography-mass spectrometry of *cis*- and all-*trans*-lycopene in human serum and prostate tissue after dietary supplementation with tomato sauce, *J. Agric. Food Chem.*, 50: 2214-2219, 2002.
77. Brown, M. J.; Ferruzzi, M. G.; Nguyen, M. L.; Cooper, D. A.; Eldridge, A. L.; Schwartz, S. J.; White, W. S.: Carotenoid bioavailability is higher from salads ingested with full-fat than with fat-reduced salad dressings as measured with electrochemical detection, *Am. J. Clin. Nutr.*, 80: 396-403, 2004.
78. Ferruzzi, M. G.; Sander, L. C.; Rock, C. L.; Schwartz, S. J.: Carotenoid determination in biological microsamples using liquid chromatography with a coulometric electrochemical array detector, *Anal. Biochem.*, 256: 74-81, 1998.
79. Ferruzzi, M. G.; Nguyen, M. L.; Sander, L. C.; Rock, C. L.; Schwartz, S. J.: Analysis of lycopene geometrical isomers in biological microsamples by liquid chromatography with coulometric array detection, *J. Chromatogr. B Biomed. Sci. Appl.*, 760: 289-299, 2001.
80. Toth, K.; Stulik, K.; Kutner, W.; Feher, Z.; Lindner, E.: Electrochemical detection in liquid flow analytical techniques: characterization and classification, *Pure Appl. Chem.*, 76: 1119-1138, 2004.
81. Sander, L. C.; Sharpless, K. E.; Craft, N. E.; Wise, S. A.: Development of engineered stationary phases for the separation of carotenoid isomers, *Anal. Chem.*, 66: 1667-1674, 1994.
82. Sims, R. B.: Development of sipuleucel-T: autologous cellular immunotherapy for the treatment of metastatic castrate resistant prostate cancer, *Vaccine*, 30: 4394-4397, 2012.
83. Wittmer, D.; Chen, Y. H.; Luckenbill, B. K.; Hill, H. H.: Electrospray ionization ion mobility spectrometry, *Anal. Chem.*, 66: 2348-2355, 1994.
84. Eiceman, G. A.; Karpas, Z. *Ion mobility spectrometry*, 2nd ed.; CRC Press: Boca Raton, FL, 2005.
85. Fenn, L.; Kliman, M.; Mahsut, A.; Zhao, S.; McLean, J.: Characterizing ion mobility-mass spectrometry conformation space for the analysis of complex biological samples, *Anal. Bioanal. Chem.*, 394: 235-244, 2009.

86. Kane, M.; Folias, A.; Wang, C.; Napoli, J.: Quantitative profiling of endogenous retinoic acid in vivo and in vitro by tandem mass spectrometry, *Anal. Chem.*, 80: 1702-1708, 2008.
87. Pierson, N. A.; Chen, L.; Russell, D. H.; Clemmer, D. E.: cis–trans isomerizations of proline residues are key to bradykinin conformations, *J. Am. Chem. Soc.*, 135: 3186-3192, 2013.
88. Laphorn, C.; Pullen, F.; Chowdhry, B. Z.: Ion mobility spectrometry-mass spectrometry (IMS-MS) of small molecules: Separating and assigning structures to ions, *Mass Spectrom. Rev.*, 32: 43-71, 2013.
89. Pringle, S. D.; Giles, K.; Wildgoose, J. L.; Williams, J. P.; Slade, S. E.; Thalassinou, K.; Bateman, R. H.; Bowers, M. T.; Scrivens, J. H.: An investigation of the mobility separation of some peptide and protein ions using a new hybrid quadrupole/travelling wave IMS/oa-ToF instrument, *Int. J. Mass spectrom.*, 261: 1-12, 2007.
90. Fenn, L.; McLean, J.: Biomolecular structural separations by ion mobility–mass spectrometry, *Anal. Bioanal. Chem.*, 391: 905-909, 2008.
91. Robb, D. B.; Covey, T. R.; Bruins, A. P.: Atmospheric pressure photoionization: an ionization method for liquid chromatography-mass spectrometry, *Anal. Chem.*, 72: 3653-3659, 2000.
92. Syage, J. A.; Hanning-Lee, M. A.; Hanold, K. A.: A man-portable, photoionization time-of-flight mass spectrometer, *Field Anal. Chem. Tech.*, 4: 204-215, 2000.
93. Watson, J.; Sparkman, O. *Introduction to mass spectrometry: instrumentation, applications, and strategies for data interpretation*; John Wiley Chichester, 2007.
94. De Hoffmann, E.; Stroobant, V. *Mass spectrometry: principles and applications*; Wiley-Interscience, 2007.
95. Syage, J. A.; Short, L. C.; Cai, S. S.: APPI: the second source for LC-MS, *LC GC N. Am.*, 26: 286-291, 2008.
96. Cai, Y.; McConnell, O.; Bach, A. C., 2nd: Suitability of tetrahydrofuran as a dopant and the comparison to other existing dopants in dopant-assisted atmospheric pressure photoionization mass spectrometry in support of drug discovery, *Rapid Commun. Mass Spectrom.*, 23: 2283-2291, 2009.
97. Robb, D. B.; Blades, M. W.: State-of-the-art in atmospheric pressure photoionization for LC/MS, *Anal. Chim. Acta*, 627: 34-49, 2008.

98. Kauppila, T. J.; Kostiainen, R.; Bruins, A. P.: Anisole, a new dopant for atmospheric pressure photoionization mass spectrometry of low proton affinity, low ionization energy compounds, *Rapid Commun. Mass Spectrom.*, 18: 808-815, 2004.
99. Raffaelli, A.; Saba, A.: Atmospheric pressure photoionization mass spectrometry, *Mass Spectrom. Rev.*, 22: 318-331, 2003.
100. Rivera, S.; Vilaro, F.; Canela, R.: Determination of carotenoids by liquid chromatography/mass spectrometry: effect of several dopants, *Anal. Bioanal. Chem.*, 400: 1339-1346, 2011.
101. Syage, J. A.; Evans, M. D.; Hanold, K. A.: Photoionization mass spectrometry, *Am. Lab.*, 32: 24-29, 2000.
102. Robb, D. B.; Covey, T. R.; Bruins, A. P.: Atmospheric pressure photoionization: an ionization method for liquid chromatography-mass spectrometry, *Anal. Chem.*, 72: 3653-3659, 2000.
103. Vaikkinen, A.; Haapala, M.; Kersten, H.; Benter, T.; Kostiainen, R.; Kauppila, T. J.: Comparison of direct and alternating current vacuum ultraviolet lamps in atmospheric pressure photoionization, *Anal. Chem.*, 84: 1408-1415, 2012.
104. Kavanaugh, C. J.; Trumbo, P. R.; Ellwood, K. C.: The U.S. Food and Drug Administration's evidence-based review for qualified health claims: tomatoes, lycopene, and cancer, *J. Natl. Cancer Inst.*, 99: 1074-1085, 2007.
105. Fang, L.; Pajkovic, N.; Wang, Y.; Gu, C.; van Breemen, R. B.: Quantitative analysis of lycopene isomers in human plasma using high-performance liquid chromatography-tandem mass spectrometry, *Anal. Chem.*, 75: 812-817, 2003.
106. Dahl, J. H. 3446259, University of Illinois at Chicago, Health Sciences Center, United States -- Illinois, 2010.
107. Yuan, L. 3316568, University of Illinois at Chicago, Health Sciences Center, United States -- Illinois, 2008.
108. Tsikas, D.; Mitschke, A.; Gutzki, F.-M.; Meyer, H. H.; Frülich, J. C.: Gas chromatography-mass spectrometry of cis-9,10-epoxyoctadecanoic acid (cis-EODA): II. Quantitative determination of cis-EODA in human plasma, *J. Chromatogr. B*, 804: 403-412, 2004.
109. Kirby, R.; Challacombe, B.; Dasgupta, P.; Fitzpatrick, J. M.: Prostate cancer treatment: the times they are a' changin', *BJU Int.*, 110: 1408-1411, 2012.

110. Dahl, J. H.; van Breemen, R. B.: Rapid quantitative analysis of 8-iso-prostaglandin-F(2 α) using liquid chromatography-tandem mass spectrometry and comparison with an enzyme immunoassay method, *Anal. Biochem.*, 404: 211-216, 2010.
111. Johansen, J. E.; Eidem, A.; Liaaen-Jensen, S.: Mass spectrometry of carotenoids—in-chain fragmentations of deuterium labelled carotenoids, *Acta Chem. Scand. B*, 28: 385-392, 1974.
112. Kim, J. Y.; Paik, J. K.; Kim, O. Y.; Park, H. W.; Lee, J. H.; Jang, Y.: Effects of lycopene supplementation on oxidative stress and markers of endothelial function in healthy men, *Atherosclerosis*, 215: 189-195, 2011.
113. Clark, P. E.; Hall, M. C.; Borden, L. S.; Miller, A. A.; Hu, J. J.; Lee, W. R.; Stindt, D.; D'Agostino, R.; Lovato, J.; Harmon, M.; Torti, F. M.: Phase I-II prospective dose-escalating trial of lycopene in patients with biochemical relapse of prostate cancer after definitive local therapy, *Urology*, 67: 1257-1261, 2006.
114. Gustin, D. M.; Rodvold, K. A.; Sosman, J. A.; Diwadkar-Navsariwala, V.; Stacewicz-Sapuntzakis, M.; Viana, M.; Crowell, J. A.; Murray, J.; Tiller, P.; Bowen, P. E.: Single-dose pharmacokinetic study of lycopene delivered in a well-defined food-based lycopene delivery system (tomato paste-oil mixture) in healthy adult male subjects, *Cancer Epidemiol. Biomarkers Prev.*, 13: 850-860, 2004.
115. Stahl, W.; Sies, H.: Uptake of lycopene and its geometrical isomers is greater from heat-processed than from unprocessed tomato juice in humans, *J. Nutr.*, 122: 2161-2166, 1992.
116. Ross, A. B.; Vuong le, T.; Ruckle, J.; Synal, H. A.; Schulze-Konig, T., et al.: Lycopene bioavailability and metabolism in humans: an accelerator mass spectrometry study, *Am. J. Clin. Nutr.*, 93: 1263-1273, 2011.
117. Fritz, B. E.; Hauke, R. J.; Stickle, D. F.: New onset of heterophilic antibody interference in prostate-specific antigen measurement occurring during the period of post-prostatectomy prostate-specific antigen monitoring, *Ann. Clin. Biochem.*, 46: 253-256, 2009.
118. Sporn, M. B.; Clamon, G. H.; Dunlop, N. M.; Newton, D. L.; Smith, J. M.; Saffiotti, U.: Activity of vitamin A analogues in cell cultures of mouse epidermis and organ cultures of hamster trachea, *Nature*, 253: 47-50, 1975.
119. Malone, W.: Studies evaluating antioxidants and beta-carotene as chemopreventives, *Am. J. Clin. Nutr.*, 53: 305S-313, 1991.

120. Agarwal, S.; Rao, A. V.: Tomato lycopene and its role in human health and chronic diseases, *CMAJ*, 163: 739-744, 2000.
121. Milanowska, J.; Gruszecki, W. I.: Heat-induced and light-induced isomerization of the xanthophyll pigment zeaxanthin, *J. Photochem. Photobiol. B: Biol.*, 80: 178-186, 2005.
122. Furr, H. C.; Clifford, A. J.; Daniel Jones, A.; Lester, P. In *Methods in Enzymology*; Academic Press, 1992; Vol. 213, 281-290.
123. van Breemen, R. B.; Huang, C.-R.; Tan, Y.; Sander, L. C.; Schilling, A. B.: Liquid chromatography/mass spectrometry of carotenoids using atmospheric pressure chemical ionization, *J. Mass Spectrom.*, 31: 975-981, 1996.
124. van Breemen, R. B.: Innovations in carotenoid analysis using LC/MS, *Anal. Chem.*, 68: 299A-304A, 1996.
125. van Breemen, R. B.: Liquid chromatography/mass spectrometry of carotenoids, *Pure Appl. Chem.*, 69: 2061-2066, 1997.
126. van Breemen, R. B.: Electrospray liquid chromatography-mass spectrometry of carotenoids, *Anal. Chem.*, 67: 2004-2009, 1995.
127. Emenhiser, C.; Sander, L. C.; Schwartz, S. J.: Capability of a polymeric C30 stationary phase to resolve cis-trans carotenoid isomers in reversed-phase liquid chromatography, *J. Chromatogr. A*, 707: 205-216, 1995.
128. Yeum, K. J.; Booth, S. L.; Sadowski, J. A.; Liu, C.; Tang, G.; Krinsky, N. I.; Russell, R. M.: Human plasma carotenoid response to the ingestion of controlled diets high in fruits and vegetables, *Am. J. Clin. Nutr.*, 64: 594-602, 1996.
129. Lessin, W. J.; Schwartz, S. J.: Quantification of cis-trans isomers of provitamin A carotenoids in fresh and processed fruits and vegetables, *J. Agric. Food Chem.*, 45: 3728-3732, 1997.
130. Kimura, M.; Kobori, C. N.; Rodriguez-Amaya, D. B.; Nestel, P.: Screening and HPLC methods for carotenoids in sweetpotato, cassava and maize for plant breeding trials, *Food Chem.*, 100: 1734-1746, 2007.
131. Ichiyanagi, T.; Kashiwada, Y.; Shida, Y.; Ikeshiro, Y.; Kaneyuki, T.; Konishi, T.: Nasunin from eggplant consists of cis-trans isomers of delphinidin 3-[4-(p-coumaroyl)-l-rhamnosyl (1-6)glucopyranoside]-5-glucopyranoside, *J. Agric. Food Chem.*, 53: 9472-9477, 2005.
132. Gorman, G. S.; Coward, L.; Kerstner-Wood, C.; Cork, L.; Kapetanovic, I. M.; Brouillette, W. J.; Muccio, D. D.: In vitro metabolic characterization, phenotyping,

- and kinetic studies of 9cUAB30, a retinoid X receptor-specific retinoid, *Drug Metab. Dispos.*, 35: 1157-1164, 2007.
133. Camont, L.; Cottart, C.-H.; Rhayem, Y.; Nivet-Antoine, V.; Djelidi, R.; Collin, F.; Beaudeau, J.-L.; Bonnefont-Rousselot, D.: Simple spectrophotometric assessment of the trans-/cis-resveratrol ratio in aqueous solutions, *Anal. Chim. Acta*, 634: 121-128, 2009.
 134. Williams, J. P.; Bugarcic, T.; Habtemariam, A.; Giles, K.; Campuzano, I.; Rodger, P. M.; Sadler, P. J.: Isomer separation and gas-phase configurations of organoruthenium anticancer complexes: ion mobility mass spectrometry and modeling, *J. Am. Soc. Mass Spectrom.*, 20: 1119-1122, 2009.
 135. Henderson, S. C.; Li, J.; Counterman, A. E.; Clemmer, D. E.: Intrinsic size parameters for Val, Ile, Leu, Gln, Thr, Phe, and Trp residues from ion mobility measurements of polyamino acid ions, *J. Phys. Chem. B*, 103: 8780-8785, 1999.
 136. Updike, A. A.; Schwartz, S. J.: Thermal processing of vegetables increases cis isomers of lutein and zeaxanthin, *J. Agric. Food Chem.*, 51: 6184-6190, 2003.
 137. Li, X.-X.; Han, L.-J.: Iron(II)-induced isomerization of (all-E)-xanthophyll pigments lutein, zeaxanthin, and β cryptoxanthin in acetone, *Eur. Food Res. Technol.*, 227: 1307-1313, 2008.
 138. Dong, L.; Shion, H.; Davis, R. G.; Terry-Penak, B.; Castro-Perez, J.; van Breemen, R. B.: Collision cross-section determination and tandem mass spectrometric analysis of isomeric carotenoids using electrospray ion mobility time-of-flight mass spectrometry, *Anal. Chem.*, 2010.
 139. Guo, W.-H.; Tu, C.-Y.; Hu, C.-H.: cis-trans isomerizations of beta-carotene and lycopene: a theoretical study, *J. Phys. Chem. B*, 112: 12158-12167, 2008.
 140. Mesleh, M. F.; Hunter, J. M.; Shvartsburg, A. A.; Schatz, G. C.; Jarrold, M. F.: Structural information from ion mobility measurements: effects of the long-range potential, *J. Phys. Chem. A*, 101: 968-968, 1996.
 141. Tao, L.; Dahl, D. B.; Pérez, L. M.; Russell, D. H.: The contributions of molecular framework to IMS collision cross-sections of gas-phase peptide ions, *J. Am. Soc. Mass Spectrom.*, 20: 1593-1602, 2009.
 142. van Breemen, R. B.; Schmitz, H. H.; Schwartz, S. J.: Fast atom bombardment tandem mass spectrometry of carotenoids, *J. Agric. Food Chem.*, 43: 384-389, 1995.

143. Wang, Y.; Chang, W. Y.; Prins, G. S.; van Breemen, R. B.: Simultaneous determination of all-trans, 9-cis, 13-cis retinoic acid and retinol in rat prostate using liquid chromatography-mass spectrometry, *J. Mass Spectrom.*, 36: 882-888, 2001.
144. Cai, S. S.; Syage, J. A.: Comparison of atmospheric pressure photoionization, atmospheric pressure chemical ionization, and electrospray ionization mass spectrometry for analysis of lipids, *Anal. Chem.*, 78: 1191-1199, 2006.
145. Cai, S. S.; Syage, J. A.: Atmospheric pressure photoionization mass spectrometry for analysis of fatty acid and acylglycerol lipids, *J. Chromatogr. A*, 1110: 15-26, 2006.
146. Matejcek, D.: On-line two-dimensional liquid chromatography-tandem mass spectrometric determination of estrogens in sediments, *J. Chromatogr.*, 1218: 2292-2300, 2011.
147. Ghislain, T.; Faure, P.; Michels, R.: Detection and monitoring of PAH and oxy-PAHs by high resolution mass spectrometry: comparison of ESI, APCI and APPI source detection, *J. Am. Soc. Mass Spectrom.*, 23: 530-536, 2012.
148. Hanold, K. A.; Fischer, S. M.; Cormia, P. H.; Miller, C. E.; Syage, J. A.: Atmospheric pressure photoionization. 1. General properties for LC/MS, *Anal. Chem.*, 76: 2842-2851, 2004.
149. Robb, D. B.; Blades, M. W.: State-of-the-art in atmospheric pressure photoionization for LC/MS, *Anal. Chim. Acta.*, 627: 34-49, 2008.
150. Syage, J. A.: Mechanism of $[M + H]^+$ formation in photoionization mass spectrometry, *J. Am. Soc. Mass Spectrom.*, 15: 1521-1533, 2004.
151. Ahmed, A.; Choi, C. H.; Choi, M. C.; Kim, S.: Mechanisms behind the generation of protonated ions for polyaromatic hydrocarbons by atmospheric pressure photoionization, *Anal. Chem.*, 84: 1146-1151, 2012.
152. Ehrenhauser, F. S.; Wornat, M. J.; Valsaraj, K. T.; Rodriguez, P.: Design and evaluation of a dopant-delivery system for an orthogonal atmospheric-pressure photoionization source and its performance in the analysis of polycyclic aromatic hydrocarbons, *Rapid Commun. Mass Spectrom.*, 24: 1351-1357, 2010.
153. Marchi, I.; Rudaz, S.; Veuthey, J. L.: Atmospheric pressure photoionization for coupling liquid-chromatography to mass spectrometry: a review, *Talanta*, 78: 1-18, 2009.
154. Mairanovsky, V. G.; Engovatov, A. A.; Ioffe, N. T.; Samokhvalov, G. I.: Electron-donor and electron-acceptor properties of carotenoids: Electrochemical study of carotenes, *J. Electroanal. Chem. (Lausanne Switz)*, 66: 123-137, 1975.

155. Guaratini, T.; Vessecchi, R. L.; Lavarda, F. C.; Maia Campos, P. M.; Naal, Z.; Gates, P. J.; Lopes, N. P.: New chemical evidence for the ability to generate radical molecular ions of polyenes from ESI and HR-MALDI mass spectrometry, *Analyst*, 129: 1223-1226, 2004.
156. NIST: *NIST Chemistry Webbook*.<http://webbook.nist.gov/chemistry/>.
157. Guaratini, T.; Vessecchi, R.; Pinto, E.; Colepicolo, P.; Lopes, N. P.: Balance of xanthophylls molecular and protonated molecular ions in electrospray ionization, *J. Mass Spectrom.*, 40: 963-968, 2005.
158. Raffaelli, A.; Saba, A.: Atmospheric pressure photoionization mass spectrometry, *Mass Spectrom. Rev.*, 22: 318-331, 2003.
159. Borsdorf, H.; Rammler, A.: Continuous on-line determination of methyl tert-butyl ether in water samples using ion mobility spectrometry, *J. Chromatogr. A*, 1072: 45-54, 2005.
160. Marotta, E.; Seraglia, R.; Fabris, F.; Traldi, P.: Atmospheric pressure photoionization mechanisms - 1. The case of acetonitrile, *Int. J. Mass spectrom.*, 228: 841-849, 2003.
161. Short, L. C.; Cai, S.-S.; Syage, J. A.: APPI-MS: effects of mobile phases and VUV lamps on the detection of PAH compounds, *J. Am. Soc. Mass Spectrom.*, 18: 589-599, 2007.
162. Robb, D. B.; Blades, M. W.: Effects of solvent flow, dopant flow, and lamp current on dopant-assisted atmospheric pressure photoionization (DA-APPI) for LC-MS. Ionization via proton transfer, *J. Am. Soc. Mass Spectrom.*, 16: 1275-1290, 2005.
163. van Breemen, R. B.; Schmitz, H. H.; Schwartz, S. J.: Continuous-flow fast-atom-bombardment liquid chromatography/mass spectrometry of carotenoids, *Anal. Chem.*, 65: 965-969, 1993.
164. Kauppila, T. J.; Kostianen, R.; Bruins, A. P.: Anisole, a new dopant for atmospheric pressure photoionization mass spectrometry of low proton affinity, low ionization energy compounds, *Rapid Commun. Mass Spectrom.*, 18: 808-815, 2004.
165. Robb, D. B.; Smith, D. R.; Blades, M. W.: Investigation of substituted-benzene dopants for charge exchange ionization of nonpolar compounds by atmospheric pressure photoionization, *J. Am. Soc. Mass Spectrom.*, 19: 955-963, 2008.
166. Turnipseed, S. B.; Roybal, J. E.; Andersen, W. C.; Kuck, L. R.: Analysis of avermectin and moxidectin residues in milk by liquid chromatography-tandem

- mass spectrometry using an atmospheric pressure chemical ionization/atmospheric pressure photoionization source, *Anal. Chim. Acta.*, 529: 159-165, 2005.
167. van Breemen, R. B.: Electrospray liquid chromatography-mass spectrometry of carotenoids, *Anal. Chem.*, 67: 2004-2009, 2002.
 168. Tabrizchi, M.; Bahrami, H.: Improved design for the atmospheric pressure photoionization source, *Anal. Chem.*, 83: 9017-9023, 2011.
 169. Haseen, F.; Cantwell, M.; O'Sullivan, J.; Murray, L.: Is there a benefit from lycopene supplementation in men with prostate cancer? A systematic review, *Prostate Cancer Prostatic Dis.*, 12: 325-332, 2009.

VITA

NAME	Linlin Dong
EDUCATION	Ph.D., Pharmacognosy, College of Pharmacy, University of Illinois at Chicago, Chicago, Illinois, 2013 B.S. in Chemistry, Yunnan University, Kunming, China, 1996
RESEARCH EXPERIENCE	Department of Medicinal Chemistry and Pharmacognosy, University of Illinois at Chicago, Illinois: Research Assistant, 2006-2012
TEACHING EXPERIENCE	College of Pharmacy, University of Illinois at Chicago, Chicago, Illinois: Fundamentals of drug action III, 2006; Principles of drug action & therapeutics VII, 2007
WORKING EXPERIENCE	Department of Drug Metabolism & Preclinical Safety, Biogen Idec, Cambridge, Massachusetts: Summer Intern, 2012 Department of Analytical Sciences (GPO), Abbott Laboratories, North Chicago, Illinois, Summer Intern, 2011 Department of Drug Analysis (GPRD), Abbott Laboratories, Abbott Park, Illinois, Summer Intern, 2008 China Institute of Veterinary Drug Control, Beijing, China Group Leader, 2004-2006; Research Scientist, 1996-2003
HONORS	Charles L. Bell Award, College of Pharmacy, University of Illinois at Chicago, 2010 Rho Chi Honor Society
PROFESSIONAL MEMBERSHIP	American Society for Mass Spectrometry
PUBLICATIONS	Dong L , Mo S, van Breemen RB. Tandem mass spectrometric analysis of cis/trans isomers of lutein and zeaxanthin using ion mobility time-of-flight mass spectrometry (in preparation). Dong L , Mo S, Li Y, van Breemen RB. Atmospheric pressure photoionization mass spectrometry of carotenoids using methyl- <i>tert</i> -butyl ether as a dopant (in preparation).

Mo S, Calderón AI, Cao H, **Dong L**, Nikolic D, Yu R, Hurst JW, van Breemen RB. Screening of cyclooxygenase (COX) inhibitors in cocoa (*theobroma cacao*) using ultrafiltration mass spectrometry (in preparation).

Mo S, **Dong L**, Hurst JW, van Breemen RB (2013) Quantitative analysis of phytosterols in edible oils using APCI liquid chromatography-tandem mass spectrometry (accepted).

van Breemen RB, **Dong L**, Pajkovic ND (2012) Atmospheric pressure chemical ionization tandem mass spectrometry of carotenoids. *International Journal of Mass Spectrometry*, 312: 163-172

Dong L, Shion H, Davis RG, Terry-Penak B, Castro-Perez J, van Breemen RB (2010) Collision cross-section determination and tandem mass spectrometric analysis of isomeric carotenoids using electrospray ion mobility time-of-flight mass spectrometry. *Analytical Chemistry*, 82(21): 9014-9021

Liu Y, **Dong L**, Zhong F, Sun L, Jiang H, Zhao G, Meng Y(2006) Determination of nitrofurantoin metabolites in chicken muscle by high performance liquid chromatography-tandem mass spectrometry. *Chinese Journal of Veterinary Drug*, 40(9): 6-9

Dong L, Liu Y, Wang X, Zhong F, Peng L, Yue X, Gao L (2005) Determination of four fluoroquinolone residues in edible chicken tissues by reversed-phase high performance liquid chromatography. *Sepu*, 23(3): 285-288

Zhong F, Guo X, Huang Q, **Dong L**, Liu Y, Zhou Z, Zeng Y, Jin X, Lu F, Han Z (2005) Studies on the depletion of enrofloxacin residues in the porcine tissue. *Chinese Journal of Veterinary Drug*, 39(2): 6-9

Zhong F, **Dong L**, Wang X (2002) Study on the detection method of oxolinic acid and flumequine residues in fish tissues. *Chinese Journal of Veterinary Drug*, 36(11): 20-22

Zhong F, Wang X, **Dong L** (2002) Study on the detection method of oxolinic acid and flumequine residues in chicken tissues. *Chinese Journal of Veterinary Drug*, 36(9), 19-21, 2002

Dong L (2001) New tips on collecting blood from rabbit ears. *Animal Science & veterinary medicine*, 18(3): 27

Dong L, Jiang T, Gong R. (2000) Adjuvant activity of liposomes for NDV envelope proteins. *Chinese Journal of Veterinary Drug*, 34(4), 3-5

PRESENTATIONS

Dong L, Mo S, Davis RG, van Breemen RB. Tandem mass spectrometric analysis of cis/trans isomers of lutein and zeaxanthin using ion mobility time-of-flight mass spectrometry. 1110-4P. *Pittcon Conference & Expo*, Orlando, FL, Mar 2012

Dong L, Gong HH, Ling C, Blessing RA, Long M. Knowledge management through creation of an impurity mass spectral database. No.024. *Abbott Summer Intern Poster Session*, Abbott Park, IL, Jul 2011

Dong L, Shion HY, Davis RG, van Breemen RB. Analysis of cis/trans isomers of carotenoids using ion mobility time-of-flight mass spectrometry. TP 136. *The 59th ASMS conference*, Denver, CO, Jun 2011

Mo S, **Dong L**, Hurst JW, van Breemen RB. Quantitative analysis of phytosterols in cocoa and vegetable oils using liquid chromatography-tandem mass spectrometry. WP 147. *The 59th ASMS conference*, Denver, CO, Jun 2011

Wright B, Mo S, **Dong L**, Dahl J, Hurst JW, van Breemen RB. Quantitative analysis of epicatechin metabolites in human serum using UHPLC-MS-MS. WP 345. *The 59th ASMS conference*, Denver, CO, Jun 2011

Dong L, Shion HY, Davis RG, Terry-Penak B, van Breemen RB. Collision cross-section determination of isomeric carotenoids using electrospray ion mobility time-of-flight mass spectrometry. WP650. *The 58th ASMS conference*, Salt Lake City, UT, May 2010

Li Y, Vaishnav A, **Dong L**, Nonn L, van Breemen RB. Lycopene sub-cellular localization in primary prostate epithelial and stromal cells. WP 431. *The 58th ASMS conference*, Salt Lake City, UT, May 2010

Mo S, **Dong L**, Nikolic D, Hurst JW, van Breemen RB. Identification of cyclooxygenase-2 inhibitors in cocoa (*Theobroma cacao*) using ultrafiltration LC-MS. TP 312. *The 58th ASMS conference*, Salt Lake City, UT, May 2010

Wright B, Mo S, **Dong L**, Hurst JW, van Breemen RB. Pharmacokinetics of epicatechin in humans after ingestion of cocoa products. TP 318. *The 58th ASMS conference*, Salt Lake City, UT, May 2010

Dong L, Davis RG, van Breemen RB. Separation of isomeric carotenoids using ion mobility spectrometry-time-of-flight mass spectrometry. WP216. *The 57th ASMS Conference*, Philadelphia, PA, Jun 2009

Dong L, Nikolic D, Liang W, Banuvar S, Shulman L, Geller SE, Farnsworth NR, and van Breemen RB. Serum levels of isoflavones in women receiving a red clover dietary supplement. TP280. *The 56th ASMS Conference*, Denver, CO, Jun 2008

Liu A, **Dong L**, van Breemen RB. Effect of lycopene on plasma testosterone levels in men as a prostate cancer prevention agent. TP297. *The 56th ASMS Conference*, Denver, CO, Jun 2008

Dong L, Rodila R, Zhang J, Wu H. Exploration of bioanalytical quantitation of siRNA using LC-MS/MS. *Abbott Summer Intern Poster Session*, Abbott Park, IL, Jul 2008